Modeling underwater visual ability and varied color expression in the diamondback terrapin (*Malaclemys terrapin*) in relation to potential mate preference by females

A Thesis

Submitted to the Faculty

of

Drexel University

by

Abigail Elizabeth Dominy

in partial fulfillment of the

requirements for the degree

of

Doctor of Philosophy

April 2015

Dedication

When I heard the learn’d astronomer,

When the proofs, the figures, were ranged in columns before me,

When I was shown the charts and diagrams, to add, divide, and measure them,

When I sitting heard the astronomer where he lectured with much applause in the lecture-room,

How soon unaccountable I became tired and sick,

Till rising and gliding out I wander’d off by myself,

In the mystical moist night-air, and from time to time,

Look’d up in perfect silence at the stars.

- Walt Whitman (When I Heard the Learn’d Astronomer)

Acknowledgements

I would first like to thank my dissertation committee. Their support throughout my graduate career, and in some cases also my undergraduate career, has been instrumental in my development as a scientist. I am especially grateful for the persistent faith in my abilities, from the inception of my thesis during my senior year at Drexel to the final product presented here.

I remember clearly my first meeting with Dr. Harold Avery in 2005. I was a pre-junior (3rd year) at Drexel interviewing for my 2nd co-op. The co-op position was to be as a field assistant collecting freshwater turtles in and around the Philadelphia International Airport. I was interested in this position because it involved being outside and getting dirty. Considering my first co-op was monitoring clean room operations at a biopharmaceutical company, this is understandable. The fact that we would be catching and handling turtles was just a bonus. In any case, working on this co-op with Hal introduced me to the wonderful world of turtle ecology and biology, to which I have dedicated nearly the last 10 years of my life. After this co-op experience I continued to work with Hal on other projects, namely the terrapin project in Barnegat Bay. It was during this time that I became fascinated by the color variation found in terrapins, and with Hal's support, was able to conduct some preliminary investigations.

I met Dr. James Spotila early on in my undergraduate career. As a rising sophomore in a newly integrated Environmental Science program in the Biology department, Jim and I were matched as mentor and mentee. I would later take Jim's Tropical Ecology class in 2008 which included a field trip to Costa Rica where we

experienced the surreal nesting behavior of sea turtles on Playa Grande. Upon hearing the need for field assistants for the upcoming nesting season, I didn't hesitate to jump on board. During my time living and working in Playa Grande, I contemplated graduate school at Drexel with the idea that I would pursue my interest in terrapin coloration.

Dr. Susan Kilham and Dr. Walter Bien are both amazingly knowledgeable scientists. Their passionate enthusiasm for scientific discovery is infectious and having them on my committee was an honor. Sue, as the only female on my committee, was a great support as my committee chair; she never shied away from reigning in the other committee members. Walt always made sure that I knew what I was talking about, because honestly, sometimes I didn't! I can only hope to be as good when I get to that point in my career. With Dr. Daniel Marenda, anything seems possible. I thank him for pushing my assumptions and loaning me bench space, even during the chaos of moving to a new building. Last, but not least, Dr. Ellis Loew, as my external committee member from Cornell University, offered invaluable expertise in the complex and fascinating field of visual ecology. I truly could not have done this work without his support.

Data collection and analysis for my research was supported from many sources. Primarily, the Earthwatch Institute with funds awarded to Hal to conduct field work in Barnegat Bay. Research and stipend funding was also awarded to me by the William L. McLean III Fellowship for Ornithology and Environmental Science. This funding allowed me to visit Dartmouth College for a term to collaborate and work on developing my model. The Betz Chair of Environmental Science and the NASA: from earth to sky program under the direction of Jim provided auxiliary funding. Data were collected under wildlife collecting and holding permits issued by the State of New Jersey Division of Fish

and Wildlife, with special use permitting from the Forsythe National Wildlife Refuge. Data were collected in accordance with protocols issued by Drexel University's Institutional Animal Care and Use Committee. I would like to thank the numerous Earthwatch volunteers who helped with data collection.

My time at Drexel was greatly influenced and enriched by my fellow graduate students. My graduate labmates, in no particular order: Emily Basile, Claire Sheridan, Lori Lester, John Wnek, Julia Stone, Steve Pearson, Jules Winters, Aliki Panagopoulou, and Yu Xiang Fei. I would like to especially thank Claire for being my mentor and supporting my endeavors to continue her work on terrapin genetics; John for knowing so much about terrapins he is no doubt an honorary member of the species; Steve for taking care of my cat, and returning her ☺, but seriously you are an exemplary colleague and friend, and I will remember fondly our late night MATLAB collaborations; Jules for being a great friend, always thinking two steps ahead, and being the most effervescent person I have ever known.

My fellow ecology graduates, past and present, and in no particular order: LeeAnn Haaf, Dane Ward, Noga Neeman, Tom Radzio, Drew Cronin, Jake Owens, Kaitlin Baudier, Anna Jaworski, Kevin Smith, Erica Christensen, Brian Kelley, Elise Forbes, Lori Pester, Rachel Rutherford, Marilyn Sobel, Laurie Mauger, Ashley Lavender, Maria Berezin, Kurt Cheng, Stephen Mason, Karen Sullam, Nina Desianti, Shauna Henley, Narayan Wong, Samir Patel, Pat McLaughlin, Yi Hu, Drew Smith, Victoria Egerton, Julianne Koval, Jacquie Walters, and Andy Harrison. I would especially like to thank LeeAnn for being the best sounding board in both work and personal life, and for just being an awesome person; Dane, Noga and Kevin for being my drinking buddies and

commiserating over the trials and tribulations of graduate school; Erica, Brian, and Elise for being the best graduate field assistants a frazzled researcher could ask for.

This work could not have been done without the solid bedrock of undergraduate labor. In no particular order, the undergraduates who were fortunate enough to work with me on my research, or unfortunate, depending on how you look at it: Rickie Miglin, Kathy Tong, Lauren Donaghy, Anna Gourlay, Kevin Biallas, Chris Petito, Allison Tipton, Stefanie Farrell, Anika Vittands, Drew McQuade, Andy Rdesinski, Nirali Patel, Kayla Kelly, Kevin Peters, Lia Domico and many many more. If I've not mentioned you, it's because I have a horrible memory for names.

There are of course those people who don't fit into neat little categories, but nevertheless supported me as colleague and friend during my (long) tenure at Drexel: Jason Howard, Johnna Holding, Jenell Black, Shaya Honarvar, Dan Rostick, Kate Walsh, Piotr Lukasik, Tom Backof, Bibi Santidrian Tomillo, Gabriela Blanco, Maggie Cunningham, Sara Valentine, Pola Galie, and Pat Augustine.

Last but not least, I would like to thank my family. My parents, who have instilled in me the intense desire to perpetually ask why and learn more. They are themselves a wonder of persistence, both being the first generation to not just go to college, but achieve advanced degrees in science. My older brother Nate is also a model of success, being a professor of Anthropology at Dartmouth College. I always look forward to visiting Nate, his wife Erin and their beautiful children Eleanor and Emerson. They're already as smart as their parents; I can't wait to see who they grow up to be.

Table of Contents

List of Tables

List of Figures

Abstract

Modeling underwater visual ability and varied color expression in the diamondback terrapin (*Malaclemys terrapin*) in relation to potential mate preference by females

Abigail Elizabeth Dominy

Co-Supervisor: Harold W. Avery
Co-Supervisor: James R. Spotila

Color vision is utilized by animals to navigate the environment, distinguish between objects (e.g. prey and conspecifics), perceive differences in fitness between potential mates, as well as a number of other visual tasks. Color vision varies greatly among species and as a consequence a visual signal varies greatly in how it is perceived. The conditions of the environment additionally impact the ability of an animal to perceive the intrinsic value of a visual signal. The field of visual ecology has only recently received a great deal of attention due to technological advancements that allow objective measures of animal coloration. However, ease of organismal sampling has created a bias in the literature, with avian and mammalian taxa garnering greater attention than reptilian taxa. The estuarine diamondback terrapin (*Malaclemys terrapin*), hereafter called terrapin, is an aquatic turtle facing human-induced population declines. Population models and estimates of viability only hold under the assumption of random mating, which is often not the case. In this study I tested the hypothesis that female terrapins exhibit preferences for mates with color or color patterns that differ from the general population. I captured gravid females and males in Barnegat Bay, New Jersey as part of a long term population study conducted by my lab. To determine if non-random mating is occurring in the Barnegat Bay terrapin population, I conducted a paternity analysis on

hatchlings that were obtained from captured gravid females. I genotyped blood samples for six highly polymorphic microsatellite loci from all adult males and gravid females, and tissue samples from all hatchlings. To determine whether genotype-matched fathers exhibited color phenotypes different from the population, I implemented the three concepts of visual ecology: (1) measure physiological visual ability, (2) measure the visual target being perceived, and (3) measure the light environment in which the visual target is perceived. I found four distinct classes of photoreceptor cones in the terrapin and modeled their sensitivity in the UV, blue, green and red portions of the electromagnetic spectrum (~355-640 nm), conferring tetrachromatic visual ability. Terrapins exhibited unusual absorbance of light in the ocular media, resulting in unusual spectral tuning of photoreceptor sensitivities. I measured the light environment in the water column at the surface and at half-meter intervals below the surface. The downwelling irradiant light environment at the surface of the water column spectrally matched the visual sensitivity modeled here in the terrapin, resulting in optimal photon capture. I measured spectral reflectance of ten distinct color patches on the terrapin which also spectrally matched modeled sensitivities and surface downwelling light, resulting in optimal perception of conspecific coloration at the surface of the water column. Five color patches were measured on the skin and five on the shell. Skin color patches exhibited a clear UV and longwave components, while the shell only exhibited a longwave component. Hatchling paternity results suggested that females potentially preferred males with higher color contrast between the shell and the skin, as well as greater hue saturation of the shell. Although the number of genotype-matched fathers was low (N = 14), this study suggests that non-random mating may be occurring in the Barnegat Bay, NJ terrapin population.

CHAPTER 1: General Introduction

1.1 Visual ecology

Secondary sexual characteristics are a common phenomenon across the animal kingdom and are often cited to be a result of sexual selection leading to evolutionary changes (Emlen & Oring 1977; Schluter & McPhail 1992; Higashi, Takimoto & Yamamura 1999). In most examples, it is the male that exhibits bright colors, acoustic rhythms and/or intricate courting behavior. The diamondback terrapin (*Malaclemys terrapin*) exhibits sexual size dimorphism, with adult females being much larger than males (Hartsell 2001; Lee & Chew 2008), and highly variable color patterns shared by both sexes. The terrapin expresses extreme within-population variation, with skin color ranging from dark gray to light blue or green with spots, and shell colors from dark brown and yellow, to blue and green.

It has been long appreciated that color vision is one of the ways influencing how an organism perceives and interacts with its environment (Kelber, Vorobyev & Osorio 2003). The capacity to utilize wavelength-specific information from the environment requires the presence of at least two different chromatic channels and the neural mechanisms for interpreting differences in their outputs. Most mammals have the requisite two spectrally different channels (usually a short and medium; blue and green/yellow) and are called dichromats; but some primates have three channels with an additional long wavelength-sensitive channel and are called trichromats. Most diurnal reptiles, birds and some fishes can have more channels due to gene duplication or the addition of another channel in the ultraviolet (UV). In addition to rods supporting

scotopic vision, turtles have four spectral classes of cone, including UV, providing them with potential tetrachromatic vision (Loew & Govardovskii 2001; Honkavaara *et al.* 2002). In addition to cones, the turtle, and other diurnal reptiles and birds, have colored oil droplets associated with their cone cells which not only shape the spectral sensitivity of the photoreceptor but may also create a new chromatic channel (Loew & Govardovskii 2001).

Human color vision is based on retinal photoreceptors with peak spectral sensitivities (λ_{max}) in the yellow, green, and blue regions of the visible spectrum. Many species in the Teleostei, Aves, and Reptilia have a fourth retinal photoreceptor with a λ_{max} in the near UV region, conferring tetrachromatic vision. As a result, many anthropogenic assessments of animal coloration may have drawn faulty conclusions about their ecological significance due to our physiological inability to incorporate UV signals into our color vision system (Dominy & Lucas 2001; Eaton 2005; Hastad & Odeen 2008). These additional 'colors' that can be perceived may reveal additional or cryptic coloration upon which conspecific recognition and sexual selection occurs. In an attempt to perform unbiased and quantitative assessments of bird coloration, recent studies have used a reflectance spectroradiometer to measure avian coloration (Figuerola, Senar & Pascual 1999; Heindl & Winkler 2003). As a result, several studies have revealed formerly non-dichromatic species as dichromatic in the UV spectrum, such as in the blue tit (Andersson, Ornborg & Andersson 1998; Hunt *et al.* 1998; Hunt *et al.* 1999), discovered independently by two different research groups. In addition to baseline visual ability, visual perception may also be influenced by ambient light conditions and other environmental factors. Air pollution has been shown to direct the phenotype of the

peppered moth due to visual predation, but can these external factors also impact the direction of sexual selection?

Spectral reflectance measurements have been used for quantifying color in many studies (Endler & Thery 1996; Font, De Lanuza & Sampedro 2009; Rowe *et al.* 2009). Rowe *et al.* (2006) utilized reflectance spectra to assess the phenotypic plasticity of turtle carapace and skin color and how they change to match substrate coloration. The authors surmise that the ability to change coloration to blend in with the environment is an evolved trait that assists in predator-avoidance. Endler and Thery (1996) utilized reflectance spectra of birds to assess whether male birds required a specific quality of ambient light to perform the mating behavior known as lekking. They found that deforestation changed the ambient light quality and prevented these male birds from optimally displaying their colors. Font, De Lanuza and Sampedro (2009) found ocellated lizards performed mate selections based on different skin reflectance patterns in the ultraviolet spectrum, providing evidence for UV sensitive photoreceptors and mate selection based on coloration in reptiles. The diamondback terrapin may also have this additional UV channel (and tetrachromatic color vision) and perform mate selection based on color patterns that reflect within the UV-VIS spectrum. The boundary conditions for a color vision system can be determined by measuring the spectral sensitivity of individual photoreceptor cells using a technique such as microspectroradiometry (MSP). This technique can also measure the spectral properties of any inert color filters such as oil droplets. MSP has been successfully used for obtaining sensitivity spectra for retinal cones as well as absorbance spectra for retinal oil

droplets in the red-eared slider turtle (*Trachemys scripta*; Liebman and Granda (1971); Loew and Govardovskii (2001)).

Reputedly monochromatic bird taxa, such as the blue tit, were originally considered to be sexually indistinguishable based on human perceived coloration. However, with the advent of objective assessment using reflectance spectroradiometry and UV photography, new patterns were observed outside the human visual experience. The blue tit was found to be monochromatic in human perceived colors, but dichromatic with the addition of UV sensitivity (Hunt *et al.* 1998). It was found that 100 percent of the blue tits captured and sexed with DNA fingerprinting were correctly categorized based on reflectance spectra alone. Males expressed UV reflecting ornamentation while females did not. Thus, female blue tits are selecting for males with prominent or brighter UV ornamentation which may be a signal of some greater fitness (Hunt *et al.* 1998; Hunt *et al.* 1999). Andersson, Ornborg and Andersson (1998) further discuss the merit of UV signaling in the blue tit. Male tits attempting to court a female will use optimal backgrounds, microhabitat and time of day in order to optimally display their UV reflectance; UV reflectance contrasts very strongly against non-UV reflecting vegetation and morning light is rich in UV wavelengths. The authors also found that blue tits mated assortatively based on UV-reflecting ornamentation. Andersson & Amundsen (1997) found that female bluethroats were also selecting males based on UV ornamentation. They teased apart the effects of UV reflectance and brightness by using UV-absorbing and brightness reducing chemicals on male UV reflecting ornaments. Females clearly chose males that reflected UV, even when total brightness was controlled. The authors also found that there was a significant difference in UV reflectance between male age

classes, indicating a possible signal of reproductive readiness to females (Andersson & Amundsen 1997). Another previously assumed sexually monochromatic bird species is the blue-fronted Amazon parrot. Santos, Elward and Lumeij (2006), just as in the previous studies described above, were able to correctly predict the sex of each parrot by measuring plumage reflectance in the UV spectrum. In addition to reclassifying this species as dichromatic, the authors were able to determine the optimum body regions to measure for cryptic UV signals and also the most reliable incidence-angle to capture these reflected shortwave colors (Santos, Elward & Lumeij 2006).

Eaton and Lanyon (2003) surveyed over 300 bird species covering over 100 families of birds. They found that all families contained species that reflect significantly in the UV spectrum among feathers reflecting in the visible spectrum. The authors strongly suggest that due to the prevalence of apparently hidden UV signaling across bird families, any ecological study of bird populations should take into account the broader 'chromatic' world of birds, which seems to rely on UV reflection just as much as reflection in the wavelength range available to humans (Eaton & Lanyon 2003). Figuerola, Senar and Pascual (1999) and Eaton (2005) reviewed assessments of bird coloration and advancements in the field from subjective qualification. While the use of Munsell color codes had a relatively high reproducibility, they are still biased to human perceived colors. The use of a reflectance spectroradiometer (or colorimeter) allows assessment of bird coloration in respect to the visual ability of the intended receiver, which may be more or less than what humans are capable of seeing. Most (if not all) bird species are capable of perceiving short UV or violet wavelengths, and have potential for tetrachromacy. Most bird species also display and perform courtship behaviors that

strongly involve UV signals on various body regions. These facts should be reason enough to make it a necessity to use a reflectance spectroradiometer for any study of color relating to non-human ecology.

Given the rather recent discovery that many formerly assumed monochromatic species are in fact dichromatic in the UV spectrum, we may be facing a larger problem of biodiversity loss than previously estimated. It is important to again emphasize the need to assess an animal's behavior from the view point of how those behaviors are perceived by the intended viewer. Making assumptions and conclusions about an animal's behavior based on how humans perceive the signal or action, only results in biased and incomplete science. With the discovery that birds have potential tetrachromatic vision, there has been a flurry of research into the visual ability of other related taxa and potential sexual selection. Recent research has revealed a similar balance between natural and sexual selection in dichromatic reptile species (Stuart-Fox & Ord 2004; Font, De Lanuza & Sampedro 2009). While extensive research has delved into the mechanisms of sexual selection in avian taxa, we know very little about the mechanisms in reptilian taxa. Only very recently was it discovered that cryptic dichromatism exists outside of bird taxa, e.g. the ocellated lizard (Font, De Lanuza & Sampedro 2009).

1.2 Visual ability in vertebrates

The vertebrate retina is comprised of photoreceptor cells feeding into a network of neuronal cells responsible for the encoding and preprocessing of photoreceptor outputs. Underlying the photoreceptor cell layer, and often interdigitated with it is a supportive

epithelial layer, the retinal pigment epithelium. Vertebrate photoreceptors are divided into two morphological and physiological classes: rods and cones. Rods primarily function at low-light, scotopic levels, while cones function in daylight or high-light environments and subserve high acuity and color vision. When a photoreceptor is activated by photon absorption, both rods and cones relay the resulting signal first to bipolar and horizontal cells that feed these signals to amacrine and ganglion cells. The axons of retinal ganglion cells course over the inner surface of the retina converging at the optic disc where they form the optic nerve that carries the signal to higher centers (Kroeger & Katzir 2006).

Photoreceptor cells are divided into inner and outer segments. The inner segment contains the nucleus and other organelles as well as the previously mentioned oil droplets in diurnal birds and most diurnal reptiles. The outer segment consists of stacks of membranes laying perpendicular to the direction of photon flux. These membranes contain the visual pigment. The visual pigment molecule consists of a transmembrane protein, the opsin, and a bound molecule of vitamin A aldehyde, the chromophore, in the 11-cis configuration. Absorption of a photon causes a change from the cis to the all-trans isomer of the chromophore. This change activates a second messenger cascade ultimately resulting in membrane potential changes of the photoreceptor that is transmitted to the rest of the ascending neuronal pathway (Partridge & Cummings 1999).

The absorption characteristics of a visual pigment including its quantum efficiency and spectral range is determined by both the amino acid sequence of the opsin and the form of vitamin A/retinal used as the chromophore. Rhodopsins are visual pigments that use vitamin A1 (A1) and porphyropsins are visual pigments using vitamin A2 (A2). Almost all terrestrial vertebrates and marine teleosts have rhodopsins; while

freshwater fish, the aquatic phase of most amphibians and some reptiles, use A2 or a mixture of A1 and A2 (Lythgoe 1979). Since all visual pigments of a given chromophore class have similar shape, a single metric, the wavelength of maximal absorbance or λ_{max} can be used to define a given pigment. As mentioned above the λ_{max} can be 'tuned' by modifying either the amino acid sequence of the opsin, or the chromophore used. For a given opsin, the substitution of A2 as the chromophore shifts the total absorbance spectrum towards the red. For vertebrates, the range of λ_{maxes} ranges from about 355 nm in the near UV to 640 nm in the near infrared (IR) (Cronin *et al.* 2014).

1.3 Model organism background

The diamondback terrapin is an aquatic turtle with a large geographic distribution in coastal estuaries ranging from Cape Cod, Massachusetts to Corpus Christi, Texas (Schoepff 1792; Gray 1844). Diamondback terrapins were heavily exploited for commercial soup stock from the late 1800s to the 1920s but eventually became too scarce for profitable harvest and fell out of favor as a desirable food item in the 1930s (Hay 1892; Hay 1904; Coker 1906; Babcock 1926; McCauley 1945; Finneran 1948; Carr 1952). Historical and current anthropogenic factors—over-harvesting, shoreline development, vehicular mortality, boat traffic, loss of natal nesting sites, and unintentional trapping in crab pots (Bishop 1983; Roosenburg *et al.* 1997)—appear to have caused population declines of this once common species.

Human population densities are highest along the eastern coast of the United States, especially in the northeast (Culliton 1998). The state of New Jersey has the highest human population density of any other state in the union with approximately

1200 people per square mile (US Census Bureau 2009). Most of New Jersey's population is concentrated along coastal habitats. These facts lead to diminished environmental quality and fragmented habitats utilized by native wildlife (Butler et al. 2006, Culliton 1998). As a result, the northern diamondback terrapin population is currently under consideration by the state of New Jersey as a species of special concern (NJDEP 2008), due to threats of habitat loss and increased motor vehicle mortality. Management action may be necessary to prevent the negative impacts of inbreeding depression, which is commonly the result of habitat loss and fragmentation in many turtle species (Gray 1995, Lewis et al. 2004, Sheridan 2010). Understanding changes in animal behavior in relation to mating strategies that might affect reproductive success is an important component of the long-term population study being conducted by our research group.

Sheridan (2010) demonstrated that skewed sex ratios resulting from vehicular mortality have significant impacts on the terrapin mating system in Barnegat Bay, NJ, the study site for my research. Multiple paternity, in which multiple fathers contribute to a clutch, is significantly lower in areas with high road mortality of nesting females, which may be indicative of non-random mating patterns in which individual females have mating preferences (Sheridan 2010). If there is indeed non-random mating, then on what basis are females choosing mates? Does sexual selection play a role in the morphological diversity observed in the diamondback terrapin population in Barnegat Bay, NJ?

As with many turtle species in the Emydidae, the terrapin is sexually dimorphic in size with females attaining sizes three times larger than males. Sexual dimorphism is widespread in the animal kingdom and is often cited as a consequence of sexual selection (Emlen and Oring 1977, Schluter and McPhail 1992, Gray 2006). When sexual selection

occurs in a population, it is often female preference for males that express a preferred trait or suite of traits. Terrapins exhibit a high degree of variation in colors and patterns; **however there is no apparent dichromatism between the sexes.** This is most likely due to the fact that terrapins, like most reptiles, lack sex chromosomes and as a result have no sex-linked genes. Sex is determined by the temperature of the nest during incubation. There is then the possibility that sexually selected traits could be expressed in all offspring, whether male or female, resulting in cryptic sexual selection.

This study will determine whether color variation could be maintained in the terrapin through sexual selection in the Barnegat Bay estuary. My research on color variation will elucidate the behavioral ecology of the northern diamondback terrapin in a model estuarine ecosystem affected by anthropogenic impacts. My findings will contribute to an effective conservation plan for Barnegat Bay and elsewhere, using the diamondback terrapin as a model estuarine vertebrate.

Major research questions

Does intraspecific color variation in the diamondback terrapin play a role in female mate preference? How do terrapins visually perceive each other in their environment? Does the terrapin have a visual system similar to the closely-related freshwater red-eared slider turtle (*Trachemys scripta elegans*)?

CHAPTER 2: Modeling underwater irradiance with photoreceptor sensitivity in the estuarine diamondback terrapin (*Malaclemys terrapin*)

Abstract

To model physiological visual ability against measured ambient irradiance spectra I obtained the absorbance spectra of the ocular media (i.e. lens, cornea), oil droplets and visual pigments in retinal photoreceptors of the estuarine diamondback terrapin (*Malaclemys terrapin*). The oil droplets and ocular media act together with the visual pigments to determine the ultimate spectral sensitivity of the individual photoreceptors. Terrapins have the potential for a tetrachromatic visual system like the red-eared slider (*Trachemys scripta elegans*), a closely related freshwater turtle. However, the estuarine terrapin is markedly different in ocular media and subsequent visual pigment absorbance. I identified four visual pigments by microspectroradiometry (MSP) in the single cones with λ_{max} = 370 nm (UV sensitive), 457 nm (blue sensitive), 527 nm (green sensitive), and 615 nm (red sensitive). The ocular media measured in avian and other reptile species, including the red-eared slider, generally transmit light equally between 400 and 700 nm. However, the ocular media (lens, cornea, vitreous fluid) measured in the terrapin absorbed maximally at 505 nm, causing the ocular media to act unusually as both a short-pass and long-pass filter of light before it reached photoreceptors behind the retinal epithelium. This preretinal filtering resulted in alteration of photoreceptor cell spectral sensitivity producing four spectral channels with λ_{max} (the wavelength of maximum absorbance) at 356 nm (UV sensitive), 427 nm (blue sensitive), 572 nm (green sensitive), and 630 nm (red sensitive). Measured ambient irradiance spectra, just below the surface of the water column, had a minimum of irradiance around 500 nm in the blue-green

region. This resulted in relatively low photon capture probability by photoreceptors in the blue-green region. Given that the closely related red-eared slider turtle does not have the same ocular media absorbance as measured in the diamondback terrapin, I hypothesize that the terrapin 'color space' is a result of adaptation to the light environment that occurs in dynamic estuarine ecosystems. The filtering effects of the ocular media represent an evolutionary adaptation by the terrapin to match maximal light availability in their underwater habitat. This has implications for conspecific recognition and prey detection.

Introduction

Human color vision is primarily limited by the spectral sensitivities of retinal cone photoreceptors in the 'blue', 'green' and 'yellow-red' wavebands of the electromagnetic spectrum (i.e. ~400 to 700 nm), conferring trichromatic color vision (Bowmaker & Dartnall 1980; Jacobs 2009). However, solar radiation as short as 300 nm (ultra-violet) and as long as 800 nm (infrared) has the potential to produce the photochemical reactions that would be perceived as light in vertebrates. Vertebrates as a whole have four classes of cone photoreceptors characterized by wavelength spectral sensitivities (λ_{max}) as follows for A1 chromophore usage: 500-570 nm for longwave-sensitive (LWS), 480-530 nm for middlewave-sensitive (MWS), 400-470 nm for shortwave-sensitive type 2 (SWS2), and 355-445 nm for shortwave-sensitive type 1 (SWS1). The total wavelength range used by humans for color vision and the shape of our perceptual color space can be explained by invoking the ecology of our mammalian progenitors; nocturnal dichromats whose limited color vision became maladaptive with the move to diurnality and modified by evolution over time (Walls 1942; Heesy & Hall 2010). Improved trichromatic visual

ability likely evolved in our direct ancestors when they adopted diurnal habits (Jacobs 2009) and possibly also linked to frugivory and folivory (Dominy & Lucas 2001). As a consequence of largely avoiding an adaptive nocturnal stage, species in older lineages such as the classes Aves and Reptilia, and infraclass Teleostei, have a fourth retinal cone photoreceptor with a spectral sensitivity λ_{max} in the ultra-violet (300-400 nm) region (Losey *et al.* 1999; Loew & Govardovskii 2001; Ventura *et al.* 2001; Hunt *et al.* 2009). This potential for tetrachromatic visual ability reflects their long term evolution in diurnal habitats.

Visual pigments, located in the outer segment of the photoreceptor cell, are composed of an opsin protein and a bound aldehyde of vitamin A, either A1 or A2—the chromophore. The absorption of a photon causes a cis-trans isomerization of the chromophore that activates a second-messenger system leading to a membrane potential change. It is these receptor potentials that represent the input to the visual system and ultimately to the perceptual representation of the visual space experienced by an observer (Archer 1999; Rao & Ballard 1999).

Rod photoreceptors are specialized for dim-light 'scotopic vision' and provide only luminosity (i.e. brightness) information about the environment (Walls 1942). For terrestrial vertebrates, rod photoreceptors are maximally sensitive in the blue-green region of the spectrum around 500 nm. For aquatic vertebrates, rod photoreceptors are maximally sensitive to the dominant waveband of light available (Partridge & Cummings 1999). As a general rule, diurnal organisms have, in addition to rod photoreceptors, at least two types of cone photoreceptors that are maximally sensitive to different spectral regions making color vision possible. Their differential stimulation and subsequent

analysis allow for wavelength (i.e. color, hue) discrimination (Daw 1973). The ability to visually distinguish a color pattern or the color of an object as distinct from background may be ecologically important for detection of potential mates, prey, and avoidance of predators (Couldridge & Alexander 2002; Heindl & Winkler 2003; Stevens 2007).

Two photoreceptors having different spectral sensitivities are the minimum requirement for a color discrimination system (Bowmaker & Hunt 1999). Organisms that are 'dichromats' have limited hue discrimination. The average human is trichromatic with three inputs defining a color space. Organisms with the potential for tetrachromatic visual ability typically have four distinct classes of cone photoreceptors with λ_{maxes} in the UV or violet, blue, green and yellow-red wavebands (~355-640 nm). Thus, the general rule is the greater the number of unique spectral channels, the greater the range of hue discrimination, assuming that the necessary neuronal networks are present (Archer 1999). In addition to visual pigments, the colored oil droplets, commonly found in reptiles, birds and some fish, serve as optical filters that shift the absorbance maximum and narrow the bandwidth of the receptor's spectral sensitivity (Stavenga & Wilts 2014). This filtering and the resulting sensitivity change further improve color discrimination and enforce color constancy in dynamic light environments (Bowmaker 1980; Kelber, Vorobyev & Osorio 2003; Vorobyev 2003).

I measured the spectral absorbance of the visual pigments, oil droplets and ocular media of the diamondback terrapin (*Malaclemys terrapin*), a diurnal turtle that lives exclusively in coastal saltmarsh and mangrove habitats along the Eastern and Gulf coasts of the United States. Heterogeneous, and often eutrophic, these coastal environments are dynamic with frequent changes in the color characteristics of light in the water column

(Kennish *et al.* 2007). Given that terrapins are closely related to the potentially tetrachromatic red-eared slider turtle (both in family Emydidae), and it has been found that shallow-water light dynamics may have driven or enforced tetrachromacy in shallow-water fish (Sabbah *et al.* 2013), I hypothesized that the terrapin would have tetrachromatic vision adjusted to the unique spectral characteristic of light it experiences in its shallow estuarine environment.

Given our inability to name colors at wavelengths below ~400nm, it is necessary to model visual capability in animals that have the potential for UVS tetrachromatic vision, in order to interpret behavioral responses to visual tasks such as predation and mate choice. Thus, I developed a visual model to assess the visual capability of terrapins. The underlying assumptions in the visual model presented here were adapted from well-developed avian models (Hart & Hunt 2007), that have been well tested (Partridge 1989; Hart 2001; Stoddard & Prum 2008). Given the strong parallels that have been drawn between avian and reptilian visual systems (Vorobyev 2003), I hypothesize that the models designed for the assessment of avian visual tasks are largely applicable to the assessment of reptilian visual tasks. To date, there has been no attempt to build a model for a reptilian visual system using measured ambient light data. Incorporating measured ambient light into a visual model elucidates the evolutionary impact of different light regimes.

The inputs to the model developed in this study took into account the spectral absorbance of visual pigments, filtering by associated oil droplets, and light transmission through the ocular media, e.g. lens, cornea, and vitreous fluid (Hart & Vorobyev 2005). Presumed spectral sensitivity and the construction of a color space is determined by the

integrated product of the receptor's spectral sensitivity with measured ambient irradiance spectra. Given that terrapins are highly aquatic (Bels, Davenport & Renous 1998; Brennessel 2006), I measured underwater irradiance from various depths in the water column to model predicted visual sensitivity.

The underwater visual environment is complex and depends on many factors including total depth that affects the spectral irradiance due to absorption and scatter, biological productivity that adds 'filters' such as chlorophyll, and abiotic forces such as wind and tide (Lythgoe 1985). Water color can range from clear blue in deep ocean water to green and orange-brown in shallow coastal estuaries. Clear water is most transparent to short wavelengths, with shorter and longer wavelengths being scattered and absorbed, respectively (Loew & Lythgoe 1978; Ackleson 2003). In biologically active waters such as estuaries with high productivity, water color is dictated by the absorbance of shortwave light by CDOM (colored dissolved organic matter) and *Gelbstoffe* (yellow substances), and absorbance of longwave orange-red light by water, typically leaving middlewave light dictating background spacelight (Lythgoe 1979). The background spacelight influences the ability to distinguish the reflected color of objects (e.g. food, potential mates, etc.) in the water column (Partridge & Cummings 1999).

As morphologically similar species, the estuarine terrapin and the freshwater red-eared slider turtle occupy similar aquatic niches in their respective ecosystems. Examining the differences between the visual systems of these similar species allows us to quantify the environmental impact on visual abilities between freshwater and estuarine ecosystems.

Methods

Photoreceptor sensitivity model

I studied two adult female terrapins that sustained mortal injuries from vehicular impact. The individuals were dark-adapted and euthanized as per protocols established by the Wetlands Institute in Stone Harbor, NJ. Upon expiration, the eyes were enucleated and transported in light-tight containers to Cornell University. Retinal preparations were made under dim red and infrared light following the technique of Loew and Govardovskii (2001). I measured separately the absorbance of each photoreceptor outer segment containing the visual pigment, each photoreceptor inner segment containing the associated oil droplet, and the ocular media.

Using Microsoft Excel® and MATLAB® software, I Gaussian-smoothed absorbance spectra and normalized them to one at their maxima. I used the A2-porphyropsin templates created by Govardovskii *et al.* (2000) and references therein to create fitted template sensitivity curves (S (λ)) for each photoreceptor visual pigment (Fig. 2.3A). Visual inspection of each averaged absorbance spectrum was used to estimate the initial λ_{max} for each photoreceptor type i (where i = 1, 2 ... n). All other parameters in these equations were borrowed from Govardovskii *et al.* (2000). The visual pigment template is composed of the linear combination of two curves, designated as the α- and β-bands ($S_i = S_{i,\alpha} + S_{i,\beta}$). The α-band for each template was calculated using equations 1 and 2; the β-band was calculated using equations 3 and 4. After the summation of the α- and β-bands for each template, the initial λ_{max} was then adjusted to improve goodness of fit to the measured spectrum (Table 2.1; Fig. 2.3A).

The α-band visual pigment template, proposed by Govardovskii *et al.* (2000), takes on the functional form:

$$S_{i,\alpha}(\lambda) = \frac{1}{\exp[A(a-x)] + \exp[B(b-x)] + \exp[C(c-x)] + D} \quad \text{Eq 2.1}$$

where

$$\begin{aligned} A &= 62.7 + 1.834 \cdot \exp[(\lambda_{\max} - 625)/54.2], \\ a &= 0.875 + 0.0268 \cdot \exp[(\lambda_{\max} - 665)/40.7], \\ B &= 20.85,\ b = 0.9101,\ C = -10.37,\ c = 1.1123,\ D = 0.5343,\ x = (\lambda_{\max}/\lambda). \end{aligned} \quad \text{Eq 2.2}$$

The β-bands for the blue, green and red visual pigment templates were determined by:

$$S_{i,\beta}(\lambda) = A_{\beta} \cdot \exp\{-[(\lambda - \lambda_{m\beta})/b]^2\} \quad \text{Eq 2.3}$$

where

$$\begin{aligned} A_{\beta} &= 0.37, \\ \lambda_{m\beta} &= 216.7 + 0.287 \cdot \lambda_{\max}, \\ b &= 317 - 1.149 \cdot \lambda_{\max} + 0.00124 \cdot \lambda_{\max}^{\ 2}. \end{aligned} \quad \text{Eq 2.4}$$

I Gaussian-smoothed and normalized the absorbance spectra for each oil droplet to one at their maxima (Fig. 2.3B). Due to light leakage and scatter of the highly refractile oil droplets, a true measure of absolute absorbance is almost impossible using standard microspectroradiometer (MSP) techniques. Instead, parameters of the rapidly decreasing long-wave arm were used to characterize the filter properties. These parameters were determined by fitting a trend line to the absorbance data between 30 and 70%, which was roughly ± 10 nm of 50% absorbance (Lipetz 1984; Hart & Vorobyev 2005). Using the equation of the trend line, I calculated the wavelength points at which

there was 50% absorbance ($\lambda_{0.5}$), and 100% absorbance (λ_{cut}) for each oil droplet type (Table 2.1).

Oil droplet transmission templates ($T_{OD}(\lambda)$) were determined from one minus the absorbance spectra for each oil droplet type. The R-type oil droplet was associated with the red-sensitive visual pigment, the Y-type oil droplet was associated with the green sensitive, the C-type oil droplet was associated with the blue sensitive, and the T-type oil droplet was associated with the UV-sensitive visual pigment as observed using MSP. Following Hart and Vorobyev (2005), the transmission spectrum of each type of oil droplet was modeled as:

$$T_{i,OD}(\lambda) = \exp[-2.93 \cdot \exp[-2.89 \cdot B_{mid} \cdot (\lambda - \lambda_{cut})]] \quad \text{Eq 2.5}$$

where the slope of the transmittance was determined by

$$B_{mid} = \frac{0.5}{(\lambda_{0.5} - \lambda_{cut})}. \quad \text{Eq 2.6}$$

The T-type oil droplet associated with the UV-sensitive visual pigment was assumed to have a transmittance =1.0 from 300-700 nm, given that no significant absorbance was measured from this colorless oil droplet.

To model the distinctive ocular media transmission ($T_{OM}(\lambda)$) of the terrapin, I utilized the parameters of the oil droplet template proposed by Hart and Vorobyev (2005). Trend lines were fitted to both the short- and long-wave arms of the Gaussian-smoothed average spectrum and created the following ocular media transmission template:

$$T_{OM}(\lambda) = \exp[-2.93 \cdot \exp[-2.89 \cdot B_{mid\,1}(\lambda - \lambda_{cut\,1})]] + \exp[-2.93 \cdot \exp[-2.89 \cdot B_{mid\,2}(\lambda - \lambda_{cut\,2})]] \quad \text{Eq 2.7}$$

where the numerical subscripts represented the slopes and intercepts of the long (1) and short (2) wavelength slopes of the measured ocular media absorbance spectrum.

I modeled probable photon capture (C (λ)), from the ocular media transmittance, the oil droplet transmittance, and the associated visual pigment absorbance (Fig. 2.4A). Following Endler and Mielke (2005), I calculated wavelength specific capture probability for each cone photoreceptor type *i*:

$$C_i(\lambda) = 9.52x10^{-14} T_{OM}(\lambda) T_{i,OD}(\lambda)(1 - 10^{-0.225 Si(\lambda)}). \quad \text{Eq 2.8}$$

Probable photon capture by each photoreceptor type *i* can also be modeled by simply taking the product integral of the visual pigment absorbance, and ocular media and oil droplet transmissions:

$$C_i(\lambda) = S_i(\lambda) T_{OM}(\lambda) T_{i,OD}(\lambda). \quad \text{Eq 2.9}$$

The integrated probable photon capture, Q_i (λ), in a given light environment with spectrum I (λ) for cone photoreceptor type *i*, can then be calculated as:

$$Q_i = \int_{300}^{700} I(\lambda) C_i(\lambda) d\lambda. \quad \text{Eq 2.10}$$

Irradiance Spectroradiometry

I measured irradiance spectra from 30 different locations using an Ocean Optics USB2000 spectroradiometer and 5 m long, 600 µm diameter UV/SR fiber-optic cable with cosine corrector (Ocean Optics, Dunedin, FL, USA). Downwelling irradiance spectra is light available to an observer looking up at any depth in the water column. Surface upwelling irradiance is light available to an observer looking down into the water column from the surface. Downwelling measurements were taken from just below the surface and at half-meter intervals into the water column. Upwelling measurements were taken at the surface and normalized to surface downwelling from the same site. Irradiance spectra were averaged for each depth, converted from W $m^{-2}µm^{-1}$ to photons $m^{-2}s^{-1}nm^{-1}$, and normalized to the sum of one under the curve (Fig. 2.5A). Measurements were taken at various locations, weather conditions and times of day within and around Edwin B. Forsythe National Wildlife Refuge in Barnegat Bay, New Jersey USA, centered at 39.739984 latitude and -74.174139 longitude. The Refuge primarily protects saltmarsh habitats along the southern New Jersey coast line which serves as crucial habitat for many vulnerable species.

Results

Photoreceptor Sensitivity Model

Spectral absorbance properties of rod and cone visual pigments, cone oil droplets, and the ocular media were measured and recorded from the retinae of two specimens. The presence of five spectrally distinct visual pigments support a UVS tetrachromatic

visual system with four distinct classes of single cone photoreceptors and one type of rod photoreceptor, all best fit by a pure vitamin A2 template (Table 2.1; Fig. 2.3A).

The T-type oil droplets associated with UV-sensitive (SWS1) cones transmitted light between 300-700 nm and did not appear to function as a cut-off filter. In contrast, it is generally expected that cone oil droplets function as microlenses and long-pass filters of light before absorbance by the photoreceptor visual pigment (Stavenga & Wilts 2014). The optical properties of the other three cone oil droplets, which did act as long-pass filters, are reported in Table 2.1.

The ocular media, composed of the lens, cornea, and vitreous fluid, absorbed maximally at 505 nm, yet transmitted well below 400 nm and above 546 nm. Thus, the ocular media acted as both a *short-pass* and long-pass filter (Fig. 2.3C). After accounting for the effects of oil droplet and ocular media absorbance, the spectral sensitivity of each photoreceptor shifted as follows: UV-sensitive (SWS1) from 370 to 356 nm, blue-sensitive (SWS2) from 457 to 427 nm, green-sensitive (MWS) from 527 to 572 nm, and red-sensitive (LWS) from 615 to 630 nm (Fig. 2.4B). The terrapin's SWS1 and SWS2 sensitivities were shifted towards shorter wavelengths and the MWS and LWS sensitivities were shifted towards longer wavelengths. Additionally, the SWS2 sensitivity developed a smaller peak within the green region due to the maximal absorbance of the ocular media within the blue-green region (Fig. 2.4B).

Photoreceptor sensitivity model with irradiance

Ambient irradiance spectra were measured during the field season in 2011 and averaged across 30 sites at several depths (up to three meters below the surface) in the water column in Barnegat Bay, NJ. These measurements demonstrated unequal light availability across terrapin-visible wavelengths as well as unequal light attenuation with depth, resulting in unequal photon capture by the spectrally distinct photoreceptors (Fig. 2.5A). Ambient downwelling irradiance at the surface of the water column demonstrated greater photon capture probability by the SWS1 and SWS2 cones than the MWS and LWS cones. As light passed through the water column to 0.5 m depth, UV wavelengths were lost to scattering, causing nearly complete loss of photon capture probability by the SWS1 cone. The remaining three cones, SWS2, MWS and LWS were roughly equal in photon capture probability at 0.5 m depth. However, farther down the water column at 1.0 m below the surface, the SWS2 cone had less photon capture probability than the MWS and LWS cones. Ambient upwelling irradiance spectra at the surface demonstrated maximal photon capture probability by the MWS cone, with slightly less photon capture probability by the LWS cone and considerably less photon capture probability by the SWS2 cone.

Discussion

The four visual pigments identified in the diamondback terrapin support the assumption of a tetrachromatic color space with color discrimination in the UV, blue, green and red portions of the electromagnetic spectrum. The diamondback terrapin and

many freshwater turtle species have A2-porphoropsin based visual pigments, supporting the idea that the terrapin most likely evolved in a freshwater environment; sea turtles having A1-rhodopsin based visual pigments (Liebman & Granda 1971). The spectral range and visual pigment absorbance of the terrapin was similar to that of the red-eared slider (Loew & Govardovskii 2001; Vorobyev 2003), however the ocular media absorbance was markedly different, greatly altering probable photon capture. This difference is likely attributed to physiological adaptation of these two different species to the characteristic light regimes that distinguish freshwater and estuarine underwater habitats.

Most avian visual models use a template for ocular media transmission that assumes nearly complete transmission of light between 300-700 nm (Endler & Mielke 2005). I found a marked deviation from this assumption having directly measured the absorbance of the ocular media in the terrapin. The ocular media absorbed maximally at 505 nm, yet transmitted well below 400 nm and above 546 nm. Thus, the ocular media acted as a short-pass and long-pass filter. Consequently, the terrapin's SWS1 and SWS2 sensitivities were shifted towards shorter wavelengths and the MWS and LWS sensitivities were shifted towards longer wavelength.

Wavelength-specific absorbance by the ocular media and oil droplets enhance color discrimination by reducing overlap in spectral sensitivities among the different classes of cone photoreceptors (Vorobyev 2003; Stavenga & Wilts 2014). This absorbance by oil droplets and ocular media allows the observer to perceive and differentiate between more hues in a given wavelength range than they could otherwise. However, it is important to note that this improved color discrimination is only effective

in photopic environments with an abundance of light, as optical filtering by these mechanisms reduces overall photon capture (Vorobyev 2003). Given that terrapins rely on solar radiation for metabolism and have no ability to retain heat—heliothermic poikilotherms (Brennessel 2006)—nocturnal activity is likely limited in this species, especially due to lack of effective photon capture by photoreceptors in low light.

The visual environment of Barnegat Bay is typical of an estuary. Pure water is most transparent to blue light at wavelengths between 450 and 480 nm. That is why in the ocean the light at depths of 60-100 m is limited to the green and blue portions of the spectrum. In the Barnegat Bay estuary, green phytoplankton, yellow products from the decay of terrestrial and marine vegetation (CDOM and *Gelbstoff*e), and sands and silts in suspension modify ambient sunlight through absorption and scatter, with shorter wavelengths being attenuated more than long wavelengths (Jerlov & Nielsen 1974; Kennish *et al.* 2007).

Estuaries are dynamic light environments that change with solar angle, tidal flow, rainfall and biological productivity. Tetrachromatic visual ability with oil droplets and ocular media filtering in the terrapin potentially allow it to optimally perceive chromatic signals in its underwater light environment. Color vision plays an important role in conspecific recognition (Couldridge & Alexander 2002) and prey recognition (Stevens 2007). Color discrimination is critical in identifying color patterns on conspecifics and relatively cryptic prey such as slow moving snails, and potentially cryptic blue crabs which may have spectral matching between reflected color and background spacelight.

Ambient underwater irradiance measured at my study site in Barnegat Bay, NJ demonstrated a characteristic spectral shape at each depth in the water column (Fig. 2.5A). Downwelling irradiance spectra revealed unequal light availability; there was relatively less light available in the blue-green region of the spectrum. Additionally, a steep loss of UV wavelengths with increasing depth resulted in unequal attenuation of light. Surface upwelling irradiance revealed the availability of only long-wavelength light in the green and red portions of the spectrum (Fig. 2.5A). This is consistent with the fact that only in pure, clear water will the blue-green colors persist over longer wavelength green and red colors. The horizontal spacelight, although not directly measured, is assumed to be similar to the upwelling spectral irradiance. Thus, the apparent contrast, both brightness and hue, of visual targets will be different depending on direction of observation (Loew & Zhang 2006). Spectral reflectance measured on the terrapin matches well with the terrapin photoreceptor sensitivities modeled here. In other words, terrapins can potentially perceive the colors that they express (Chapter 3).

The maximal receptor sensitivities modeled in the terrapin demonstrate a sensitivity gap in the blue-green region of the spectrum, consistent with the relatively less abundant blue-green photons in downwelling light. This striking similarity may be the result of evolutionary adaptation to wavelength-specific light availability in the estuarine environment. Visual ecologists have long focused on the molecular structure and absorbance of visual pigments as the primary adaptive mechanism that responds to changes in ambient light conditions. In this study, absorbance by the ocular media appears to have primarily contributed to adaptive vision in the terrapin, causing divergent maximal sensitivities that markedly differ from the closely related red-eared slider.

This evolutionary adaptation has implications for color signal reception. UV signals quickly become undetectable with increasing observer distance from the UV reflecting target and the surface of the water column. The rapid attenuation of UV irradiance with increasing depth would suggest that UV signals are more conspicuous to an observer near the surface. This could be a form of cryptic signaling that allows terrapins to appear conspicuous to conspecifics in close proximity while remaining inconspicuous to distant predators. Most mammalian predators are naturally blind to UV signals (Heesy & Hall 2010), and tetrachromatic avian predators would have difficulty targeting prey that can dive below the surface (Stevens 2007). This would be especially important to hatchling and juvenile terrapins most at risk to predation (Witherington & Salmon 1992).

The visual system of the terrapin makes it well adapted to function in the dynamic light environment of estuaries along the Eastern and Gulf coasts of the United States. Given that the closely related red-eared slider does not have the same ocular media absorbance as measured in the terrapin in this study (Loew & Govardovskii 2001; Vorobyev 2003), it appears that the terrapin visual system has adapted to the unique light environment that occurs in dynamic, biologically active estuarine ecosystems. The terrapin is the only non-sea turtle that occupies estuaries. Whether this visual adaptation is applicable to a wider range of estuarine animals, or specific only to the terrapin is unknown and more comparative data are needed to clarify this observation. In addition to its visual adaptation the diamondback terrapin also has the ability to osmoregulate by means of lachrymal salt glands. These collective adaptations have allowed the terrapin to exploit a vast ecosystem with little to no competition from other turtles.

Table 2.1: Microspectroradiometric (MSP) measurements and sensitivity models. (A) Visual pigment (VP) absorbance measured in each of the five photoreceptor types: the four cone types SWS1, SWS2, MWS, LWS and one rod type; (B1) Oil droplet (OD) absorbance measured in each of the four cone types: T-, C-, Y- and R-types. Little to no absorbance found in the T-type oil droplet associated with the SWS1 visual pigment; (B2) Ocular media (OM) transmission measured through the optical structures: lens, cornea and vitreous fluid; (C) Mathematical models of visual sensitivity. Accounting for only OD filtering, visual sensitivities shifted toward longer wavelengths in all but the SWS1 cone. Accounting for both OD and OM filtering, visual sensitivities shifted toward shorter wavelengths in the SWS1 and SWS2 cones, and longer wavelengths in the MWS and LWS cones.

A. Visual pigment (VP)		**SWS1**	**SWS2**	**MWS**	**LWS**	**Rod**
Mean λ_{max} ± s.e.m (nm)		370.1 ± 3.19	456.9 ± 5.12	527.1 ± 1.15	615.2 ± 2.93	513.0 ± 2.89
	N =	8	7	10	14	11
B1. Oil droplets (OD)		**T- type**	**C-type**	**Y-type**	**R-type**	
Mean λ_{cut} (nm)			395.8	521.4	577.6	
Mean $\lambda_{0.5}$ (nm)			415.2	543.6	598.0	
Bmid			0.026	0.023	0.025	
	N =		15	30	25	
B2. Ocular media (OM)		**Short λ**	**Long λ**	**λ_{max} (nm)**		
Mean λ_{cut} (nm)		468.3	525.3	505		
Mean $\lambda_{0.5}$ (nm)		399.8	546.1			
Bmid		-0.007	0.024			
	N =	5				
C. Modeled sensitivities		**SWS1**	**SWS2**	**MWS**	**LWS**	**Rod**
VP x OD	λ_{max} (nm)	370	458	560	627	n/a
Eq. 2.8	λ_{max} (nm)	356	427	572	630	550*
Eq. 2.9	λ_{max} (nm)	358	426	569	626	549*
*VP x OM only (no OD present)						

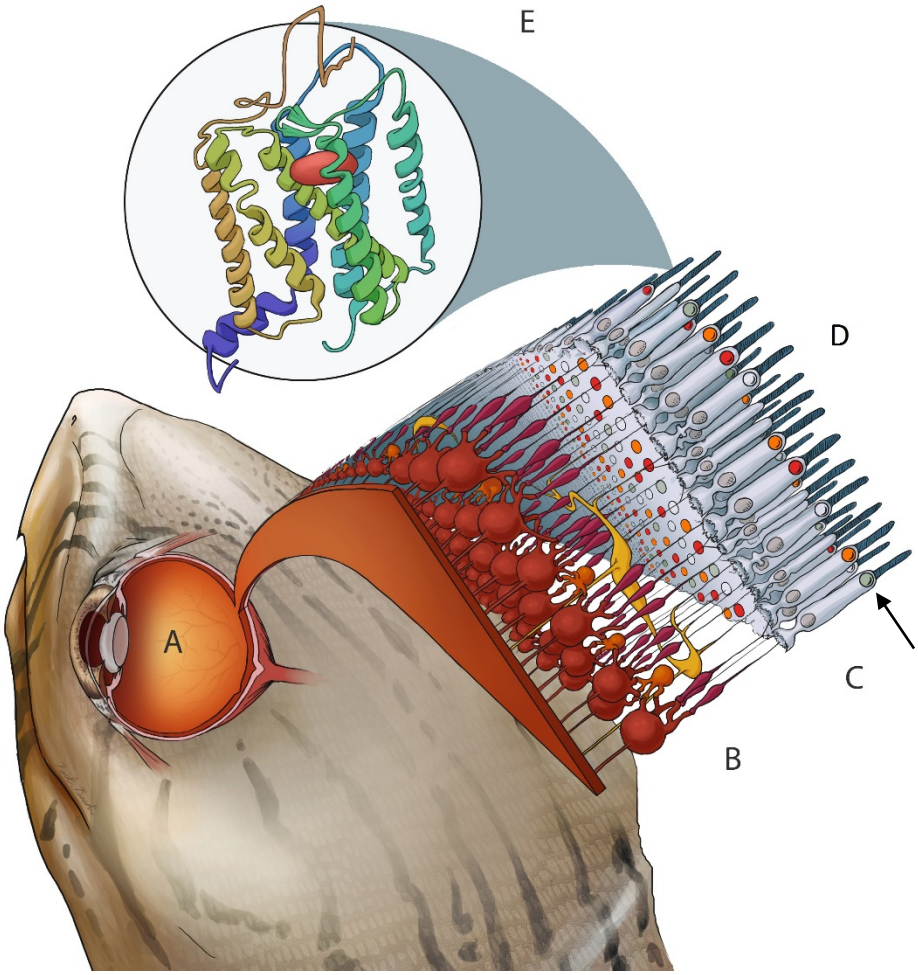

Figure 2.1: Light path and physiological features incorporated into the terrapin visual model. Illustration by Kaitlin Baudier. (A) ocular media: lens, cornea, vitreous fluid, etc; (B) neuronal cells; (C) Rod and cone photoreceptors; only the cones contain oil droplets indicated by the arrow. Oil droplets are contained within the inner segment of the cone photoreceptors; anterior to the visual pigments; (D) Visual pigments located in the outer segment of the rod and cone photoreceptors absorb the photons and activate a second messenger system that ultimately alters the membrane potential of the photoreceptor cell; (E) Molecular stucture of a visual pigment. This is a transmembrane molecule in the family of G-protein coupled receptors. In this case the chromophore (the red ovoid in the figure) can be considered the ligand. The molecular structure of the chromophore and opsin protein together with largely unknown interactions with membrane lipids determine the spectral position of the absorbance spectrum.

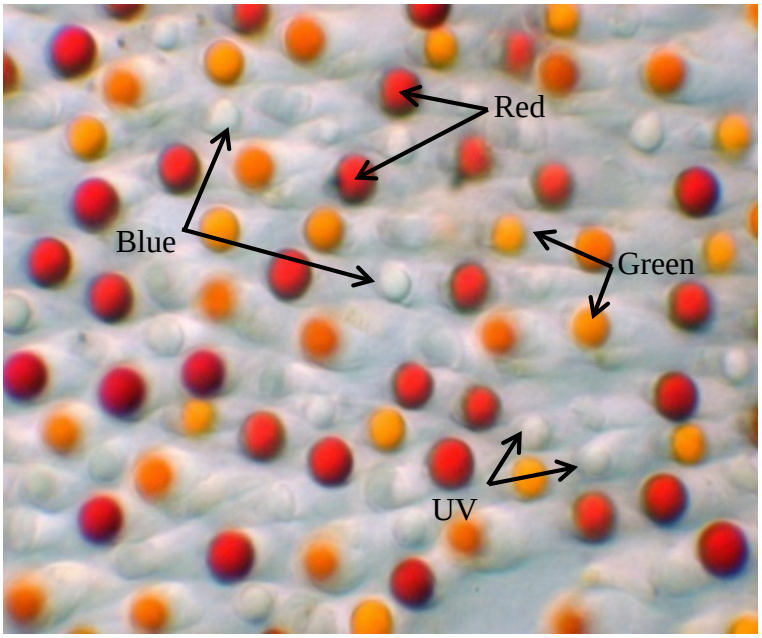

Figure 2.2: Photomicrograph of the terrapin's photoreceptors showing the presence of colored oil droplets in the photoreceptor inner segments. Image was taken as part of this study using the MSP instrument located at Cornell University. Arrows and labels indicate each of the four classes of single cone photoreceptors responsible for tetrachromatic color discrimination in the terrapin. The UV-sensitive cones contain the T-type oil droplet (colorless), blue-sensitive cones contain the C-type oil droplet (light blue), green-sensitive cones contain the Y-type oil droplet (yellow-orange), and red-sensitive cones contain the R-type oil droplet (red). Oil droplets are 4-6 μm in diameter.

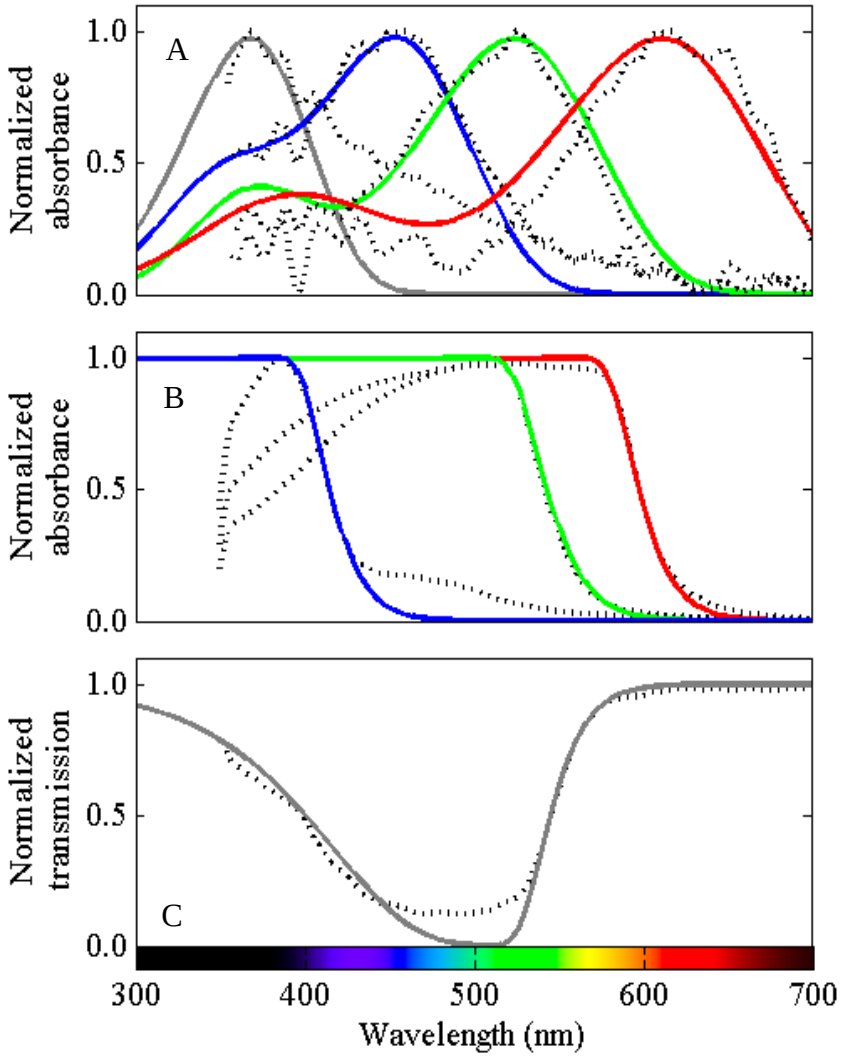

Figure 2.3: Photoreceptor sensitivity model. (A) Gaussian smoothed visual pigment absorbance spectra (dotted lines) with fitted visual pigment templates (solid lines) as modeled by equations 2.1-2.4. The β-band was not modeled for the UV-sensitive visual pigment due to aberrant measurements by the MSP at these wavelengths. Line colors correspond to visual pigment sensitivity; (B) Smoothed oil droplet absorbance spectra (dotted lines) with fitted oil droplet absorbance templates (solid lines) as modeled by equations 2.5 and 2.6. Line colors correspond to the associated visual pigment sensitivity. The inverse of these absorbance templates were used to model transmission of light through the oil droplet. (C) Smoothed ocular media transmission spectra (dotted line) with template (gray line) as modeled by equation 2.7.

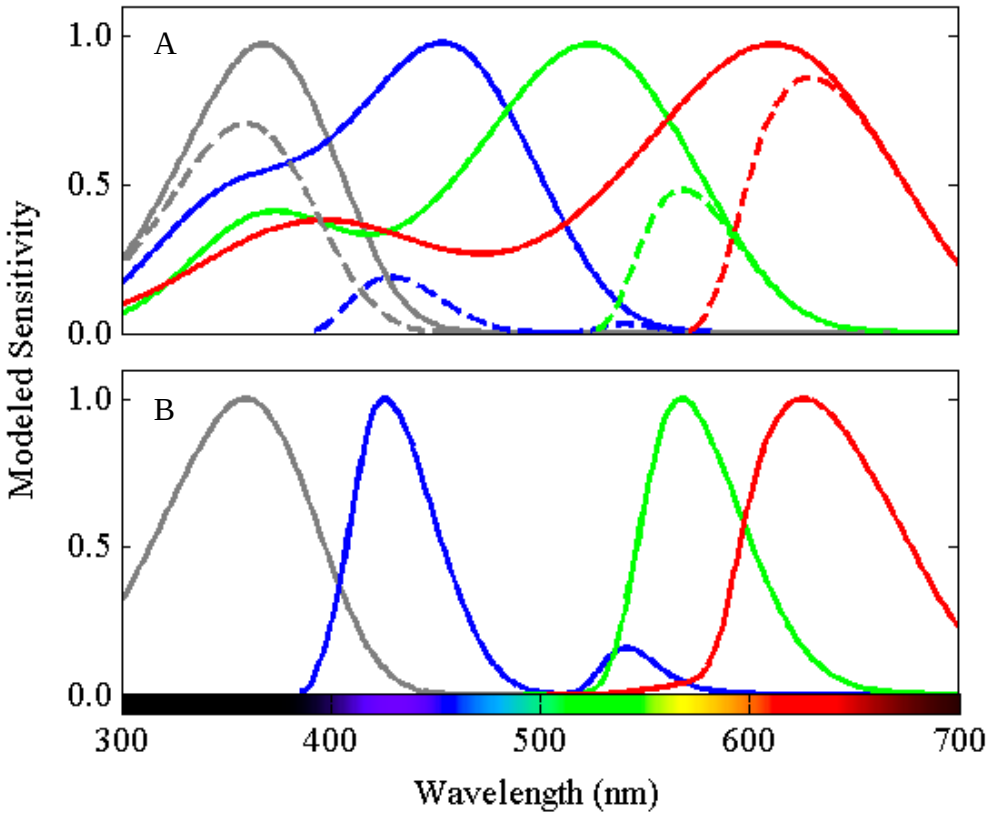

Figure 2.4: Modeled physiological vision sensitivity. (A) Visual pigment sensitivity templates (solid lines) with modeled receptor spectral sensitivities accounting for oil droplet and ocular media transmittances (dashed lines); (B) modeled receptor spectral sensitivities normalized to one at their maxima as calculated by equation 2.8, and similar results can be obtained from equation 2.9. All sensitivities are in inverse quantum units.

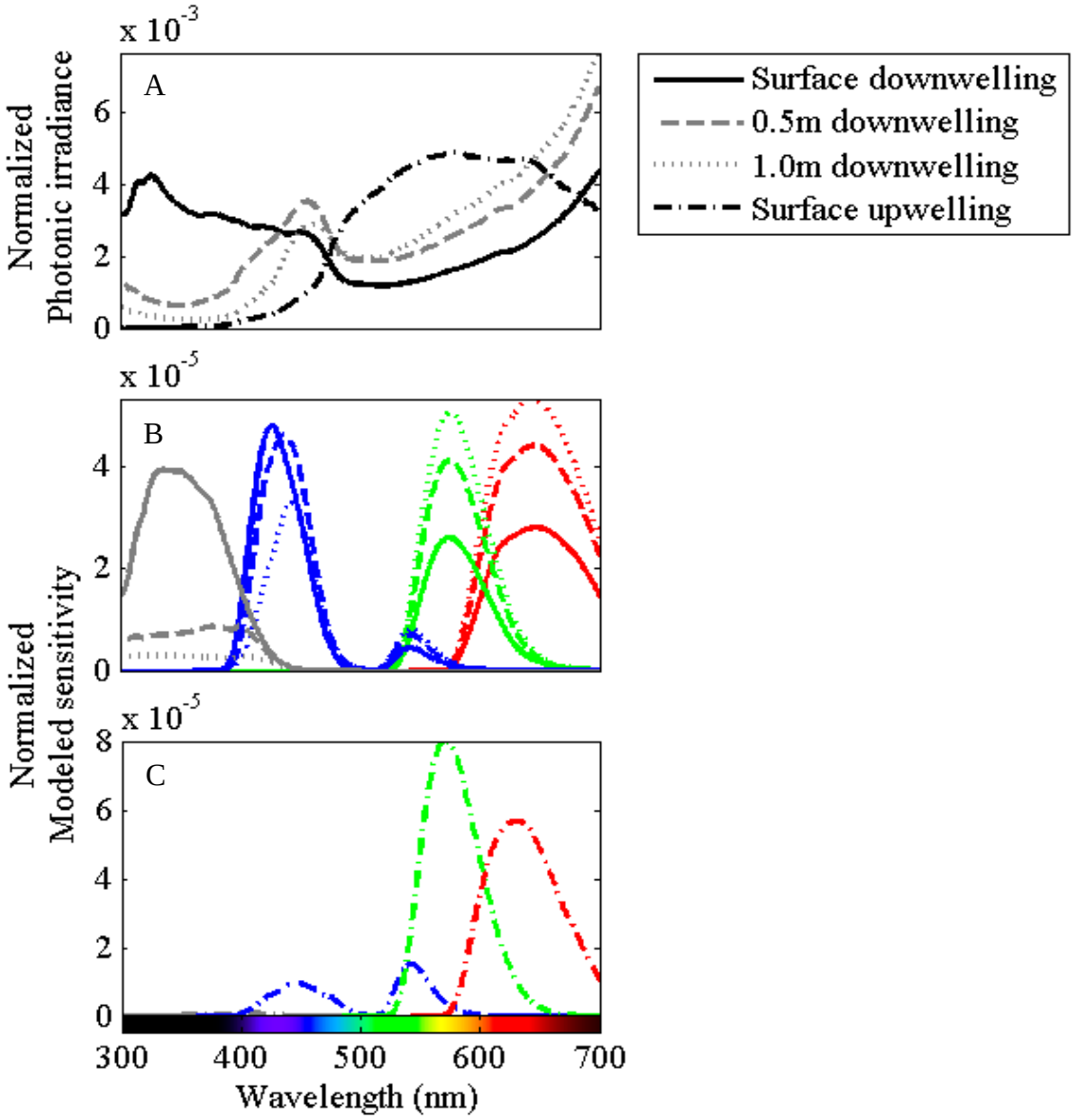

Figure 2.5: Photoreceptor sensitivity model with ambient irradiance. (A) Gaussian smoothed underwater irradiance measured at just below the surface and 0.5 m intervals into the water column. Irradiance was measured in W $m^{-2}\mu m^{-1}$ and converted to photons $m^{-2}s^{-1}nm^{-1}$; spectra were normalized to the sum of one under the curve. (B) Modeled receptor sensitivity for each measure of downwelling irradiance. (C) Modeled receptor sensitivity for surface upwelling irradiance.

CHAPTER 3: Modeling varied skin and shell colors as potential visual signals in the diamondback terrapin (*Malaclemys terrapin*)

Abstract

The diamondback terrapin (*Malaclemys terrapin*), an aquatic estuarine turtle, is well known for its within-population skin and shell color variation, especially along the Eastern coast of the United States. However, the few attempts to elucidate this phenomenon used subjective assessments based on human color vision. Objective measures of turtle coloration using reflectance spectroradiometry have only recently entered the literature, and haven't yet ventured to incorporate the visual system or spectral irradiance of the environment into a holistic model. By incorporating the terrapin visual system, and reflectance and irradiance spectroradiometry into a color vision model, I evaluated terrapin color patches in the proper context. There were two discrete groups of color patches. Color patches on the skin contained distinct UV and green-red reflectance components with a bimodal spectral shape, while shell color patches contained only a green-red color component with unimodal spectral shape, creating the potential for within-turtle color contrast. The UV-rich surface downwelling irradiance measured at my study site in Barnegat Bay, New Jersey optimized within-turtle contrast and differences within color patches, increasing detection of both chromatic and brightness differences between individuals over the full spectrum model. However, these differences were quickly lost with depth in the water column, suggesting that diving by the terrapin may be a simple strategy to reduce predation risk by tetrachromatic predators. In addition, counter-shading coloration on the carapace and plastron likely assist in camouflage against UV-blind mammalian predators (e.g. river otters, foxes). I conclude

from these observations that terrapins likely have both behavioral and physical adaptations to predation pressures to counteract conspicuous color signals that may be used by females in mate selection.

Introduction

Animal coloration often plays an important role in inter- and intra-specific communication, especially as a signal of quality in mate selection (Zahavi 1975; Andersson 1986; Andersson, Ornborg & Andersson 1998; Johnsen *et al.* 2003). These color signals have evolved to be optimally perceived by the visual system of the intended observer; i.e. color signals expressed by an animal with a tetrachromatic visual system (~300-700 nm) may be imperceptible to animals with a trichromatic or dichromatic visual system (Yokoyama & Yokoyama 1996; Siddiqi *et al.* 2004; Osorio & Vorobyev 2008). It is thus imperative to consider the visual system of the intended observer when assessing the adaptive significance of animal color patterns. Previous studies on terrapin coloration used only subjective and qualitative assessments based on the human trichromatic visual system (Hartsell 2001; Lee & Chew 2008). In this study of color variation in the diamondback terrapin (*Malaclemys terrapin*), I incorporated the tetrachromatic visual system of the terrapin, as modeled in Chapter 2, to assess the role of color in terrapin biology.

The literature on non-mammalian vertebrate color expression is focused largely on avian and teleost taxa (Marshall *et al.* 2003; Endler & Mielke 2005). Of the studies that involve reptiles, most focus on lizards (Fleishman, Loew & Whiting 2011). The

taxonomic bias in animal coloration studies presents a large gap in knowledge of reptile coloration, especially for turtles. The handful of studies on turtle coloration have found significant differences in sex or immune response with color patch size, spectral shape, or brightness, suggesting that color is a sexually selected trait (Bulte *et al.* 2013; Ibanez *et al.* 2013). Differences in spectral shape were attributed to different degrees of hue saturation, with preferred mates and those with greater immune function having greater hue saturation. These color differences are found on or near the head region, suggesting a face-to-face color signal assessment. Although Loew and Govardovskii (2001) and Ventura *et al.* (2001) found the freshwater red-eared slider turtle (*Trachemys scripta*) has the ability to detect ultraviolet signals (UV: ~300-400 nm), most turtle coloration studies report relatively little to no reflectance in the UV. Notable exceptions are the studies by Ibanez *et al.* (2014) and Wang *et al.* (2013) in which a UV component, though not spectrally dominant, was found in the yellow chin stripes and postorbital red patches of the red-eared slider. The presence of significant UV reflectance expressed by terrapins, as reported in this study, sets them apart from previous turtle spectral reflectance studies.

Animal coloration that is used in intra-specific communication often meets counter-balancing selection pressure from predation. A color signal that is perceived by both conspecifics and predators tends to be limited to a breeding season or otherwise concealed outside of courtship behaviors (e.g. the feather display of birds or dewlap of lizards). Another strategy is to express color that is outside the visual ability of the predator, thus allowing cryptic yet conspicuous signaling between conspecifics. The presence of UV-signals in the terrapin could be an evolutionary strategy to avoid predation by UV-blind mammalian predators (e.g. river otters, foxes).

Light entering the eye (radiance spectrum) is the product of ambient light conditions (scalar spectral irradiance) and the spectral reflectance of the target stimulus. The effectiveness of a signal to a conspecific and its conspicuousness to a predator is therefore dependent in part on environmental factors such as weather and habitat type. For example, male blue tits select backgrounds, such as highly contrasting non-UV-reflecting vegetation, and time of day, such as early morning when ambient light is rich in UV, to optimize the intensity of the UV signal directed toward female receivers (Andersson, Ornborg & Andersson 1998). The spectral properties of ambient light are affected by weather conditions and time of day as well as anthropogenic modifications to the environment. Endler and Thery (1996) created a visual model that incorporated bird coloration, visual ability, and ambient light to assess whether male birds required a specific quality of ambient light to perform the mating behavior known as lekking. The authors found that deforestation changed the ambient light in such a way that it prevented male birds from displaying their colors optimally. In aquatic systems, ambient irradiance can be significantly attenuated due to many factors, including total suspended solids, turbidity, and biological productivity. Thus, UV reflectance could be, alternatively or additionally, an evolutionary adaptation to complex underwater light regimes, in which tetrachromatic visual ability increases the ability to detect and reconstruct underwater color signals (Sabbah *et al.* 2013). Like deforestation, ambient light in the water of an estuary can be altered due to human activity such as boating and nutrient runoff, which can increase turbidity in the water column and consequently change light dynamics (Kennish *et al.* 2007).

In this study, I measured terrapin color variation and conspicuousness (i.e. contrast) in relation to potential tetrachromatic color vision system and spectral irradiance environment. I quantified the contrast of terrapin color signals to conspecifics and conspicuousness to predators by incorporating the three components necessary for constructing a color vision model: visual pigment absorbance, reflectance spectroradiometry of relevant visual targets and irradiance spectroradiometry of the environment in which the visual task is being performed. Varied measurements among the latter two components were considered when assessing the degree of color signal effectiveness and conspicuousness. Lastly, I discuss the possible ecological and evolutionary causes of the highly variable skin and shell color patterns found in the diamondback terrapin.

Methods

Terrapin capture

I conducted fieldwork in Edwin B. Forsythe National Wildlife Refuge in Barnegat Bay, New Jersey USA. The Refuge primarily protects saltmarsh habitats along the southern New Jersey coast, which serves as crucial habitat for many vulnerable species. Our laboratory captured, marked and recaptured terrapins during the summer season from 2006 to 2014 as part of a long-term population study (Sheridan *et al.* 2010). I used terrapins captured between 2010 and 2012 in this study. Methods of capture included passive aquatic traps, such as hoop and fyke nets, as well as active dip-netting and hand capture. I placed captured terrapins in canvas bags and brought them to our field station

in Waretown, NJ for processing. Each individual received a unique notch code and large females were additionally injected with passive integrated transponders (PIT tags). I recorded dimensional measurements (e.g. straight carapace length, width and height), physical characteristics and reflectance spectra from each individual.

Irradiance spectroradiometry

I measured irradiance spectra from 30 different locations using an Ocean Optics USB2000 spectroradiometer and 5 m long, 600 µm diameter UV/SR fiber-optic cable with cosine corrector (Ocean Optics, Dunedin, FL, USA). Downwelling irradiance spectra is light available to an observer looking up at a given depth in the water column. Surface upwelling irradiance is light available to an observer looking down into the water column from the surface. Downwelling measurements were taken from just below the surface and at half-meter intervals into the water column. Upwelling measurements were taken at the surface and normalized to surface downwelling from the same site. Irradiance spectra were averaged for each depth, converted from W $m^{-2}µm^{-1}$ to photons $m^{-2}s^{-1}nm^{-1}$, and normalized to the sum of one under the curve. Measurements were taken at various locations, weather conditions and times of day within our study site.

Reflectance spectroradiometry

I measured and recorded almost 10,000 reflectance spectra, $R(\lambda)$, from 760 individual captured terrapins using the Ocean Optics Jaz-PX spectrometer with full-

spectrum xenon light source and bifurcated fiber optic cable QR400-7-UV (Dunedin, FL, USA). To reduce specular glare, a probe tip sleeve angled at 45 degrees and 2mm distance from the reflecting surface was fitted to the fiber optic cable (Endler 1990). The Jaz spectrometer connected via USB to a notebook computer in which Ocean Optics SpectraSuite software recorded each reflectance measurement. Before each set of measurements, I calibrated the spectrometer using a dark non-reflecting fabric, and the Ocean Optics WS-1 Diffuse Reflectance Standard that reflected equally from 250-1500nm. I sampled between 10 and 20 specific color patches on each terrapin, depending on variation, and recorded representative spectra from each color patch (Fig. 3.1). I Gaussian smoothed and zero-line corrected all reflectance spectra (i.e. any negative values resulting from noise at low reflectance values were set to zero).

All spectra measured on a single individual became a unique spectral profile for that individual. All grouped color patches across individuals became a mean spectral profile for the terrapin population. After determining the mean spectrum of each color patch, I compared spectral shapes before and after normalization. Normalization to the integer of one controlled for brightness and allowed an independent assessment of spectral shape. Normalization to the maxima of one controlled for multi-modality in spectral shape. I performed principal component analysis (PCA) on each version of the mean spectra to determine absolute differences between the mean spectra of each color patch by reducing a large number of correlated variables (each wavelength measurement) into two orthogonal variables that describe the fundamental differences between mean spectra. Since PCA on spectral data breakdown differences in spectral shape, I indirectly

determined relative differences in hue, chroma (hue saturation) and brightness based on the spread of the principal components.

For each reflectance spectrum, I determined the value of maximal percent reflectance, or color intensity, and its corresponding wavelength. Plotting each value pair gave a general sense of all possible colors expressed by each color patch. I determined the frequency of all wavelength maxima and plotted against terrapin photoreceptor sensitivities, demonstrating degree of spectral matching between terrapin color expression and their color vision. I then plotted wavelength frequencies by color patch demonstrating within-patch differences in color intensity frequency.

Terrapin color model

To determine the ability of the terrapin to detect color contrast between a conspecific in its natural environment, I modeled the following parameters: spectral cone sensitivity that accounts for visual pigment absorption, ocular media and oil droplet transmission, $C_i(\lambda)$; the effect of the ambient spectral irradiance, $I(\lambda)$ (both described in Chapter 2); and normalized spectral reflectance from an anatomical color patch on the terrapin that functions as the visual target $R(\lambda)$. I used the MATLAB program TetraColorSpace.m provided by Stoddard and Prum (2008) to calculate and obtain the following color metrics.

The probability of photon capture for a given cone photoreceptor type *i* was calculated as (Endler & Mielke 2005):

$$Q_i = \int_{300}^{700} R(\lambda)I(\lambda)C_i(\lambda)d\lambda, \qquad \text{Eq 3.1}$$

then corrected for color constancy using the von Kries transformation (Vorobyev et al. 2001):

$$q_i = \frac{\int_{300}^{700} R(\lambda)I(\lambda)C_i(\lambda)d\lambda}{\int_{300}^{700} I(\lambda)C_i(\lambda)d\lambda}. \qquad \text{Eq 3.2}$$

The q_i values were normalized to the integral of one to calculate the relative photon capture for each cone photoreceptor (Endler & Mielke 2005):

$$u = \frac{q_1}{\sum q_i},\ s = \frac{q_2}{\sum q_i},\ m = \frac{q_3}{\sum q_i},\ l = \frac{q_4}{\sum q_i}, \qquad \text{Eq 3.3}$$

then transformed into Cartesian coordinates to create a point in the three-dimensional tetrahedral color space (Endler & Mielke 2005):

$$x = \frac{1-2s-m-u}{2}\sqrt{\frac{3}{2}},\ y = \frac{-1+3m+u}{2\sqrt{2}},\ z = u - \frac{1}{4}. \qquad \text{Eq 3.4}$$

The *x*, *y* and *z* Cartesian coordinates were converted into spherical coordinates θ, Φ, and *r* which function to define hue and saturation (for further discussion see Stoddard and Prum (2008)). Saturation (*r*) is the distance from the achromatic origin in tetrahedral color space. Thus, colors of the same hue but different saturation reside on the same line at varied distances from the origin (Fig. 3.7). The relative stimulus value for each cone

photoreceptor for a given hue varies as a function of chroma, i.e. the greater the hue saturation in a given direction, the greater the cone stimulus in that direction. However, due to geometric inequalities between the spherical coordinate system and tetrahedral color space, the achieved chroma ($r_A = r/r_{max}$) was calculated for each color stimulus (Stoddard & Prum 2008).

The average volume of color space occupied by each color patch was calculated from the minimum convex polygon created by the *x*, *y* and *z* coordinates plotted in tetrahedral color space. The distance, or color span, between two color stimuli in tetrahedral color space, also known as the Euclidean distance, was calculated to determine the extent of chromatic contrast between two stimuli (*a* and *b*). Following Endler and Mielke (2005), the Euclidean distance based on color space was calculated as:

$$D_{ab} = \sqrt{(x_a - x_b)^2 + (y_a - y_b)^2 + (z_a - z_b)^2}, \qquad \text{Eq 3.5}$$

where *x*, *y* and *z* are the Cartesian coordinates in tetrahedral color space.

Results

Reflectance spectroradiometry

I selected 10 color patches on the terrapin that represented the variation between and among individuals (Figs. 3.1 and 3.2); 5 skin patches: chin skin, tympanum, forelimb, hindlimb and head dark spots; and 5 shell patches: top head, plastron light, plastron dark, edges and carapace. The mean spectra of each color patch had one of two spectral shapes (Fig. 3.3). The skin color patches had a bimodal shape with a maximal

peak in both the UV and green-red spectral regions. The shell color patches had only one peak in the green-red spectral region. Generally, skin color patches were brighter than shell color patches, except for the plastron color patches which had greater brightness than most skin color patches. The normalized color patches controlled for brightness, allowing for direct comparison of spectral shapes (Figs. 3.3B and 3.3C). Here, the skin patches were more similar to each other than to any of the shell patches, but some within-patch-type differences were visible. Both the edges and plastron light patches were offset towards longer wavelengths compared to the other shell color patches. The skin patches normalized to the maxima of one demonstrated differences in UV reflectance, possibly indicating several classes of UV reflectance.

Principal component analysis (PCA) of the raw and normalized mean color patches further revealed similarities and dissimilarities between the color patches (Fig. 3.4). The PCA of the raw color patch spectra showed a slight separation of skin and shell color patches due to the differences in spectral shape. Brightness, however, was clearly a strong factor, with the brightest color patch, the chin skin, falling far from the other skin color patches. Normalized color patches that controlled for brightness revealed a very different spread of the principal components. Spectral shape, which indirectly informed me on hue and chroma, became the primary difference between color patches. For both normalizations, PC1 showed differences in modality and hue between the color patches, with the bimodal UV-containing color patches falling to the left of zero and unimodal non-UV reflecting patches falling to the right of zero. PC2 showed differences in spectral evenness or chroma (purity of color). Color patches falling below zero were more even and less pure and those falling above zero were less even and more pure of color.

Mean spectral shapes of each color patch revealed differences between patches, however there was great variation within patches that revealed additional patterns. Taking peak percent reflectance and its corresponding wavelength (hue) of each color patch measurement revealed several details (Fig. 3.5A). First, it was a confirmation that peak reflectance measurements in the UV were only found on the skin color patches, which were also primarily the brightest. Second, two groups fell out in the green-red spectral region. To clarify the potential cause, I reduced the data into a frequency histogram and overlaid the spectral sensitivities of terrapin photoreceptors (Fig 3.5B). The cone spectral sensitivities (λ_{max}) used here were those modeled in Chapter 2: 356 nm (UV-sensitive SWS1), 427 nm (blue-sensitive SWS2), 572 (green-sensitive MWS) and 630 nm (red-sensitive LWS). Terrapin color patches were maximally bright in their own visual system, causing a separation of peak reflectance in the green-red region to cluster more toward the green or red regions matching the green and red photoreceptor sensitivities. Interestingly, no colors were maximally bright in the blue region. To summarize the differences in color patch spectra, I re-plotted the frequency of peak reflectance measurements for each color patch (Fig. 3.6). The frequency of individual skin color patches were approximately normally distributed within the three spectral groups: UV, green and red. The shell color patches were also approximately normally distributed within the green and red spectral groups. Frequency bars that did not cluster near a spectral group were most likely the result of low reflectance values that produced arbitrary hues.

Terrapin color model

Differences between color patches can change due to receiver bias and ambient irradiant conditions. I first tested the effect of terrapin photoreceptor sensitivities on color patch differences by creating the tetrahedral color space model described by Eqs 3.1-3.5. Each color patch was modeled and plotted separately in a three dimensional tetrahedron created by the tetrahedral color space (Figs. 3.7 and 3.8). The skin color patches generally clustered toward the UV hue and origin of the color space, and the shell color patches generally clustered toward the green and red hues and the floor of the color space. All color patches plotted together showed the relative clustering of the different color patches and the boundaries within which terrapin colors occurred (Fig. 3.9A). The few points that fell outside the cluster were most likely measurements of unusual spectral shape or low reflectance that yielded unrealistic color space coordinates. The color space coordinates of the mean color patches were plotted together to show the relative three dimensional positions of each mean color patch (Fig. 3.9B). The skin color patches clustered centrally toward the UV hue while the shell color patches clustered below the origin and toward the green and red hues.

Downwelling irradiance was measured just below the surface, and at half- and one-meter depths in the water column. Surface upwelling irradiance, which is the result of filtering and scatter within the water column as well as downwelling light reflecting off the bottom substrate, was also measured. The radiance spectrum was the modeled color signal available to a receiver and the result of multiplying the spectral integrals of irradiance and reflectance. Differences between color patches changed due to the different effects that a single light spectrum had on different color spectra (Fig. 3.10).

The calculated radiance spectra, which can also be considered probable photon capture, demonstrated a quick loss of UV signals below the surface (Fig. 3.10, column 2). Color differences decreased with depth to the point where only radiance in the green-red spectrum was available to a receiver. Adding terrapin spectral sensitivities to the radiance model yielded similar results but with narrower peaks that increased hue saturation (color purity), potentially lending to greater perceived color contrast (Fig. 3.10, column 3). The narrowing of the radiance spectrum can be attributed to the ocular media absorbance that was modeled into terrapin spectral sensitivity in Chapter 2. Principal component analysis of the radiance spectra (Fig. 3.10, column 5) demonstrated decreasing differences between the spectral shapes of color patches. The surface upwelling light environment demonstrated no difference between color patches. The reduction in spectral shape translated to a reduction in the ability to visually discriminate between color patches, especially if an observer is looking up at a conspecific that is illuminated by upwelling irradiant light.

The chroma, color span and volume of space occupied by each color patch in tetrahedral color space either changed or stayed the same, depending on depth, after incorporating the effects of spectral irradiance (Fig. 3.11). The gray lines and dots indicate full spectrum or no spectral irradiance was used in the model. Any points above the gray line suggest that those spectral irradiances increased that metric more than full spectrum light; any points below the gray line suggest that those spectral irradiances decreased that metric. The surface downwelling spectral irradiance increased within-patch color differences, increasing the ability to differentiate between individuals. Irradiance below the surface and upwelling at the surface decreased within-patch color

differences, decreasing the ability to differentiate the same color patch between individuals. Within-turtle color patches also changed with irradiant environment. The available light changed the spectral shape of reflected color, thus altering the perceived differences between any two color patches on an individual. These pairwise differences tended to decrease with increasing depth and light attenuation (Fig. 3.12). Similar to the within-patch color contrast results, within-turtle color contrast was greater in surface downwelling light compared to the full spectrum model.

Discussion

The diamondback terrapin expresses a high degree of within-population color pattern variation, with spectral reflectance ranging between 300-700 nm. This phenotypic variability is unmatched, or at least unmeasured, in any other interbreeding turtle population (Fig. 3.2). All color patches in the terrapin are available for visual assessment, unlike in many bird species where color patches can be hidden under wings or tail feathers, or lizard species where colorful dewlaps can be folded away (Macedonia, Echternacht & Walguarnery 2003). In lieu of concealment, terrapins can dive down into the water column to control and reduce conspicuousness, much like birds who display in forest shade or open canopy (Endler 1983; Endler 1990; Endler & Thery 1996). Terrapins are most conspicuous—have the greatest color contrast—in surface downwelling light environments where the spectral bandwidth is the greatest (Fig. 3.11 and 3.12). As a result, terrapins benefit from displaying to conspecifics at the surface of the water column that optimizes color patch differences within and between turtles. Indeed, reports of mating aggregations typically describe a large group of males and females ‘frothing’ with

activity at the surface. These reports also suggest that males arrive before the females to find optimal displaying conditions, much like male birds in lekking species (Estep 2005; Brennessel 2006). Displaying at the surface, however, also increases conspicuousness to UV-sensitive tetrachromatic avian predators. In response to this predation pressure, terrapins need only to dive a short distance (<1 m) down into the water column where conspicuousness, or high color contrast, is reduced due to both spectral and brightness attenuation. In addition to behavioral avoidance, the shell color patches suggest a counter-shading color pattern to further deter predation at the surface and on land by UV-blind mammalian predators (e.g. river otters, foxes). The duller carapace is cryptic against surface upwelling light, and the brighter plastron color patches reduce the shading effect of surface downwelling light (Ruxton, Speed & Kelly 2004). Lastly, the diversity of color and color patterning in terrapins possibly limits characteristic recognition by predators. These physical and behavioral counter measures to predation pressure allows the terrapin to express conspicuous color patterns to conspecifics.

The within-turtle color patch contrast was broadly found between skin and shell color patches, with skin color patches having a significant UV reflectance component. This UV reflectance, and as a result skin-shell contrast, was enhanced by surface downwelling spectral irradiance (Fig. 3.10). Skin-shell color patch contrast was further enhanced by accounting for terrapin photoreceptor sensitivities as modeled in Chapter 2. The separation of the short-wavelength sensitive cones (UV and blue) from the long-wavelength sensitive cones (green and red) by unusual absorbance of the ocular media, increased color discrimination by increasing hue saturation, or color purity (narrower radiance peaks). The proximity of the green and red cone sensitivities increased detection

and discrimination of the duller color patches on the shell, possibly adjusting for the much brighter skin color patches detected by the UV-sensitive cone. The presence of a significant UV signal along with UV-sensitivity are correlated with the visual environment (Tovee 1995; Losey *et al.* 1999). Bright daylight and clear, blue skies are rich in UV radiation, creating conditions in which UV signals have high detectability against non-UV-reflecting backgrounds (e.g. submerged aquatic vegetation in shallow estuaries and underwater background spacelight). In addition to the significant within-turtle contrast created by the UV signal, the proximity of the red and green cone sensitivities allows for fine scale discrimination of color patch hues in the green-red spectral region.

The presence of significant UV reflectance on terrapin skin suggests the possibility of sexual selection in my study population. The intensity and chromaticity of UV reflecting color is sometimes the sole trait that females evaluate during mate choice experiments with fish (Endler 1983; Smith *et al.* 2002) and in birds (Andersson, Ornborg & Andersson 1998; Hunt *et al.* 1999). Additionally, the high level of variation of color and color patterns in the terrapin may be maintained in the population due to context-dependent sexual selection. In other words, varying levels of terrapin brightness or conspicuousness may result from differential female preference based on particular ambient light conditions. For example, on a particularly bright and clear day where UV radiation is at its greatest, a female may be receptive to a relatively UV-dull individual because he is just as bright as a bright individual on a cloudy day. This phenomenon is related to color constancy, a cognitive function involved in object recognition where the color of an object is perceived to stay the same in changing illumination (e.g. patchy

cloudiness or wave action; Osorio and Vorobyev (2005)). However, two different objects under different illumination regimes can be difficult to compare, especially with distance, and especially underwater (Vorobyev *et al.* 2001). In addition, the parameters used in conspecific recognition may be more relaxed in the terrapin due to nearly exclusive use of estuarine ecosystems by small-bodied turtles, making the risk of hybridization very low. The wide-ranging colors found on the terrapin are most likely maintained in the population due to all, or a combination of, several factors: ease of behavioral predator avoidance, context-dependent sexual selection, and non-stringent conspecific recognition. Visual predator avoidance behavior can be exhibited by the terrapin in the form of diving below the surface of the water column; context-dependent sexual selection can be exhibited when season, time of day, weather and depth potentially affect mate preferences; and non-stringent recognition can be exhibited when broad color markers are used in identification of potential mates. In conclusion, the terrapin has likely adapted skin pigmentation that reflects maximally within the terrapin's color vision system. This vision system is supported by a visual cortex in the brain that shares similar structural homology and neural connections with that of the neocortex found in mammals (Hall *et al.* 1977), allowing visualization of terrapin colors by the terrapin.

The clear lack of any maximal color reflectance in the blue region of the modeled terrapin visual system suggests the possibility that terrapins can easily distinguish between blue crabs and conspecifics. Atlantic blue crabs (*Callinectes sapidus*), as their name suggests, are known for a distinct blue hue, as well as being fast swimmers in the water column. Since terrapins are known to eat blue crabs, I posit that terrapins have the ability to quickly discern between blue crabs as a food item and conspecifics.

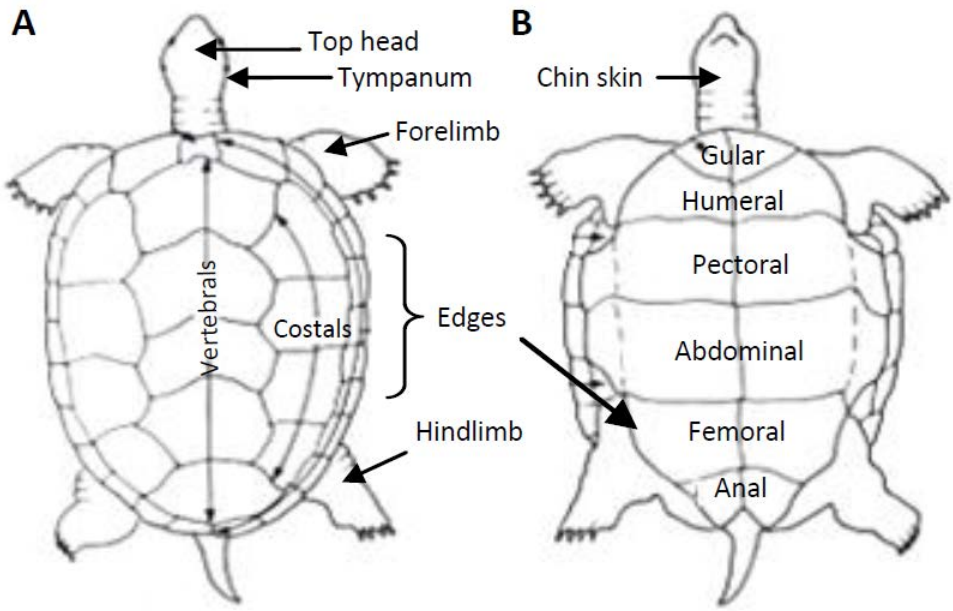

Figure 3.1: Schematic of terrapin anatomical regions on the dorsal (A) and ventral (B) surfaces where reflectance spectra were measured. Combined vertebral and costal color patch measurements make up the carapace color patch. Combined gular, humeral, pectoral, abdominal, femoral and anal scute color patch measurements made up the plastron light and plastron dark color patches. Measurements on the bridges and along the edge of the plastron made up the edges color patch.

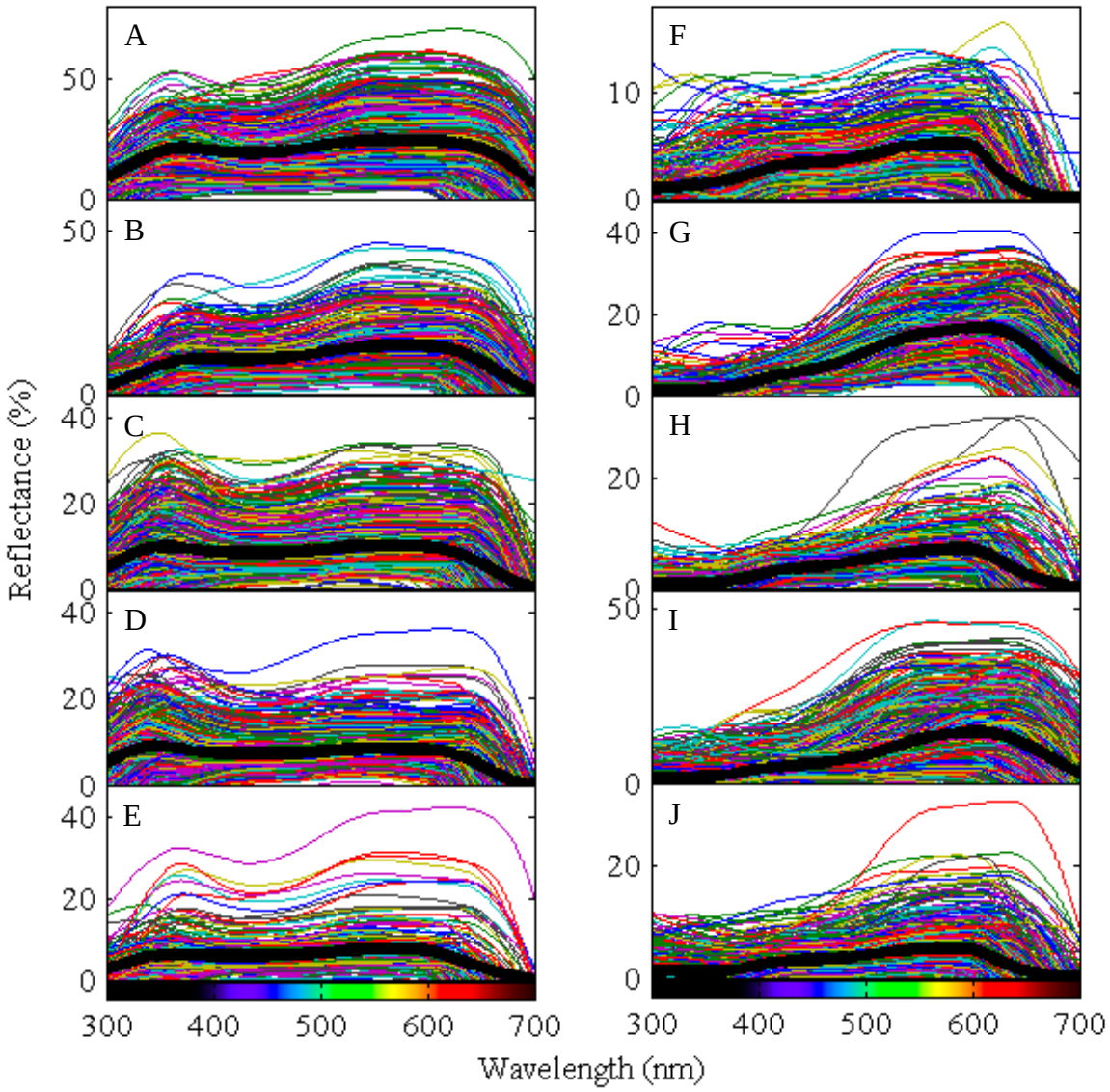

Figure 3.2: Gaussian smoothed reflectance spectra from ten (10) color patches on the terrapin. (A) Chin skin (n = 506). (B) Tympanum (n = 485). (C) Forelimb (n = 781). (D) Hindlimb (n = 735). (E) Head dark spots (n = 200). (F) Top head (n = 507). (G) Plastron light (n = 622). (H) Plastron dark (n = 393). (I) Shell edges (n = 1243). (J) Carapace (n = 926). Mean spectrum denoted by bold black line.

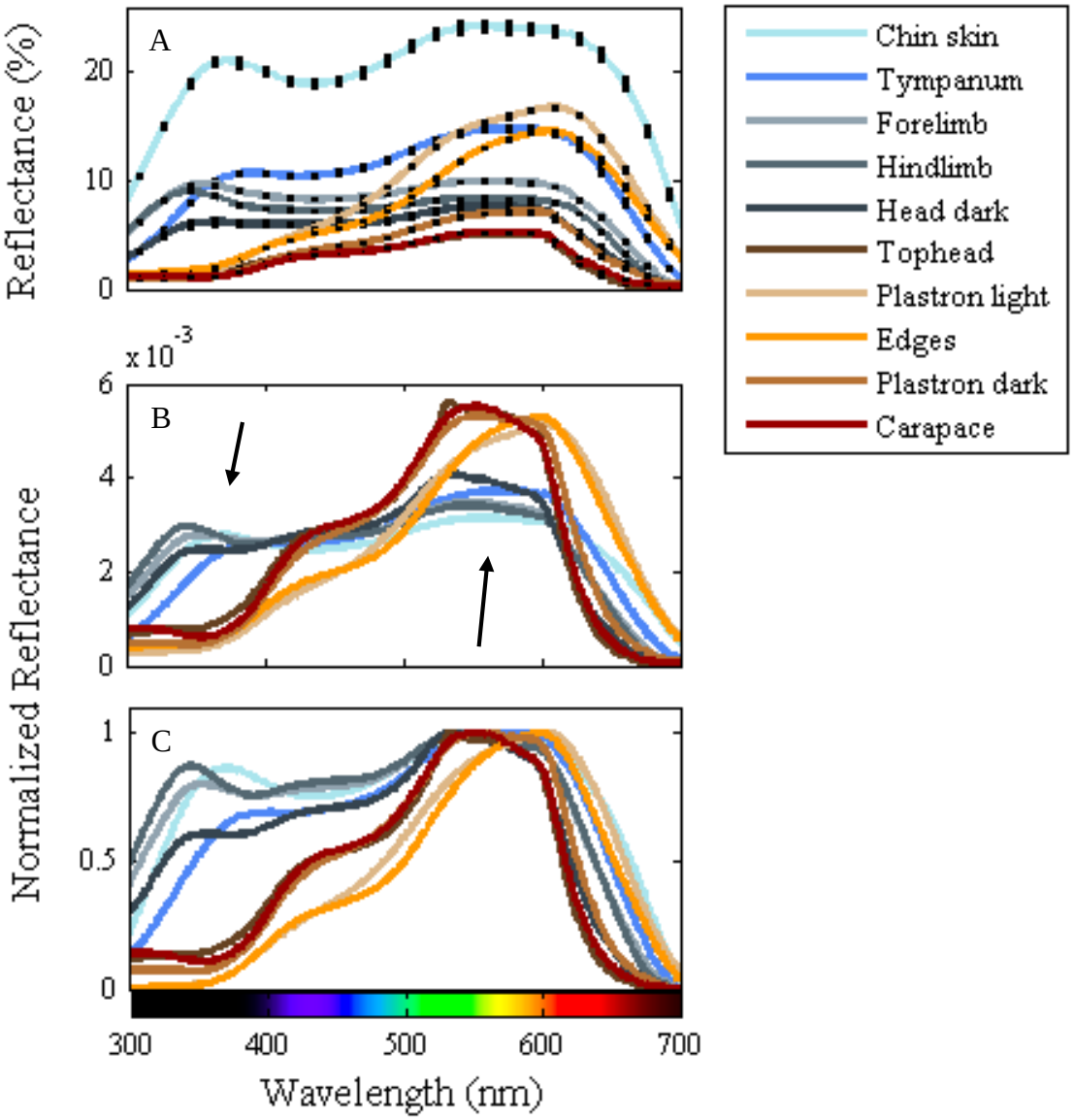

Figure 3.3: Reflectance spectra from ten (10) anatomical sampling patches on the terrapin. (A) Gaussian smoothed mean color measurements. Black bars are +/- one standard error of the mean (SEM). (B) Gaussian smoothed color measurements, normalized to the sum of one under the curve. Normalization to the sum of one controls for differences in brightness (percent reflectance). Arrow indicate the differences in spectral shape fall in the UV and long-wave portions of the spectrum. (C) Gaussian smoothed color measurements, normalized to one at the maximal reflectance value. Normalization to one controls for multi-modality in spectral shape, demonstrating true differences in spectral shape.

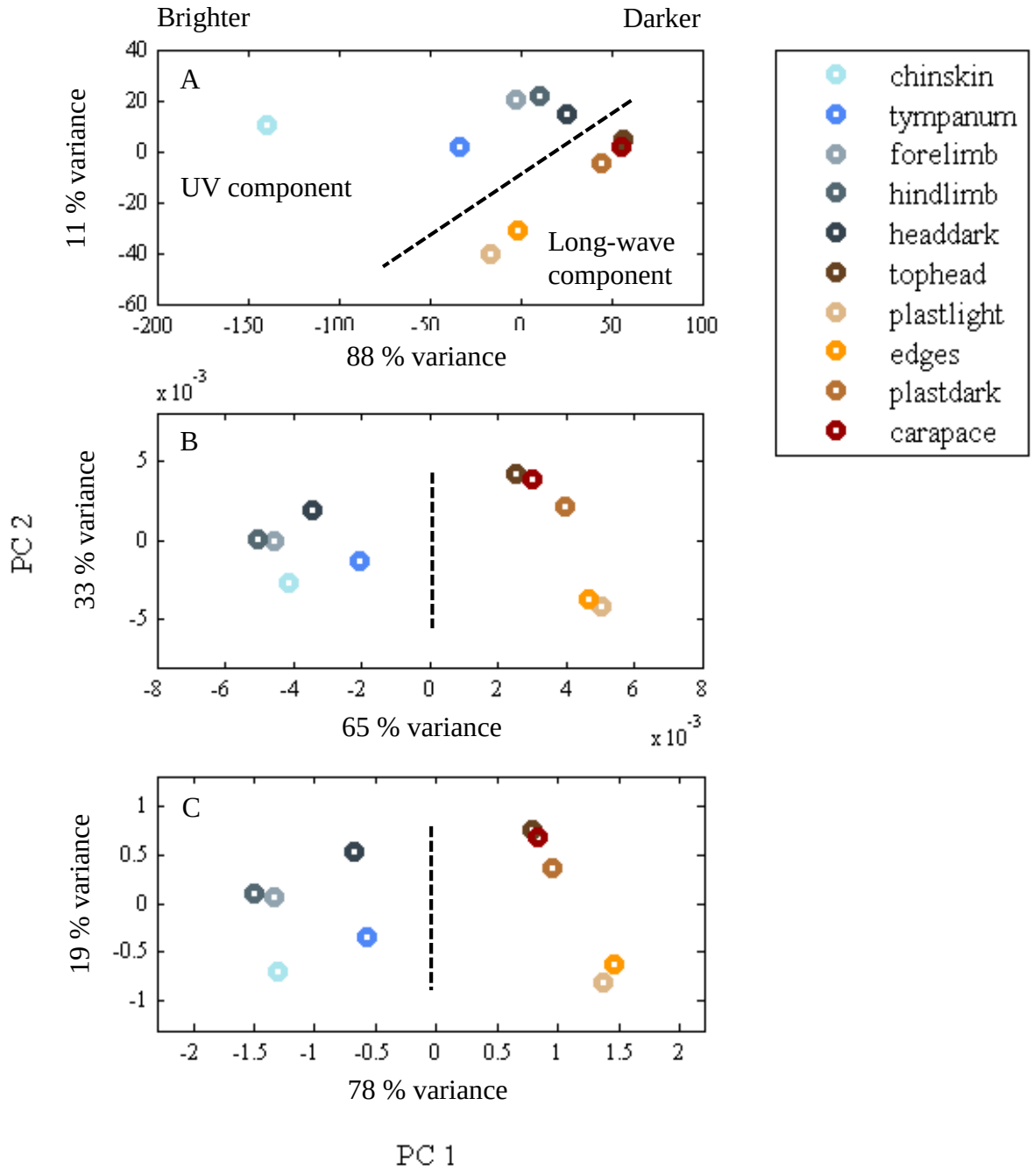

Figure 3.4: Principal component analysis (PCA) of mean reflectance spectra from ten (10) color patches on the terrapin. (A) PCA of Gaussian smoothed reflectance spectra. (B) PCA of Gaussian smoothed reflectance spectra normalized to the sum of one. Demonstrates color patch differences in spectral shapes while controlling for brightness. (C) PCA of Gaussian smoothed reflectance spectra normalized to one at the maximal wavelength value. Demonstrates color patch differences in spectral shapes while controlling for both brightness and multi-modality of hue.

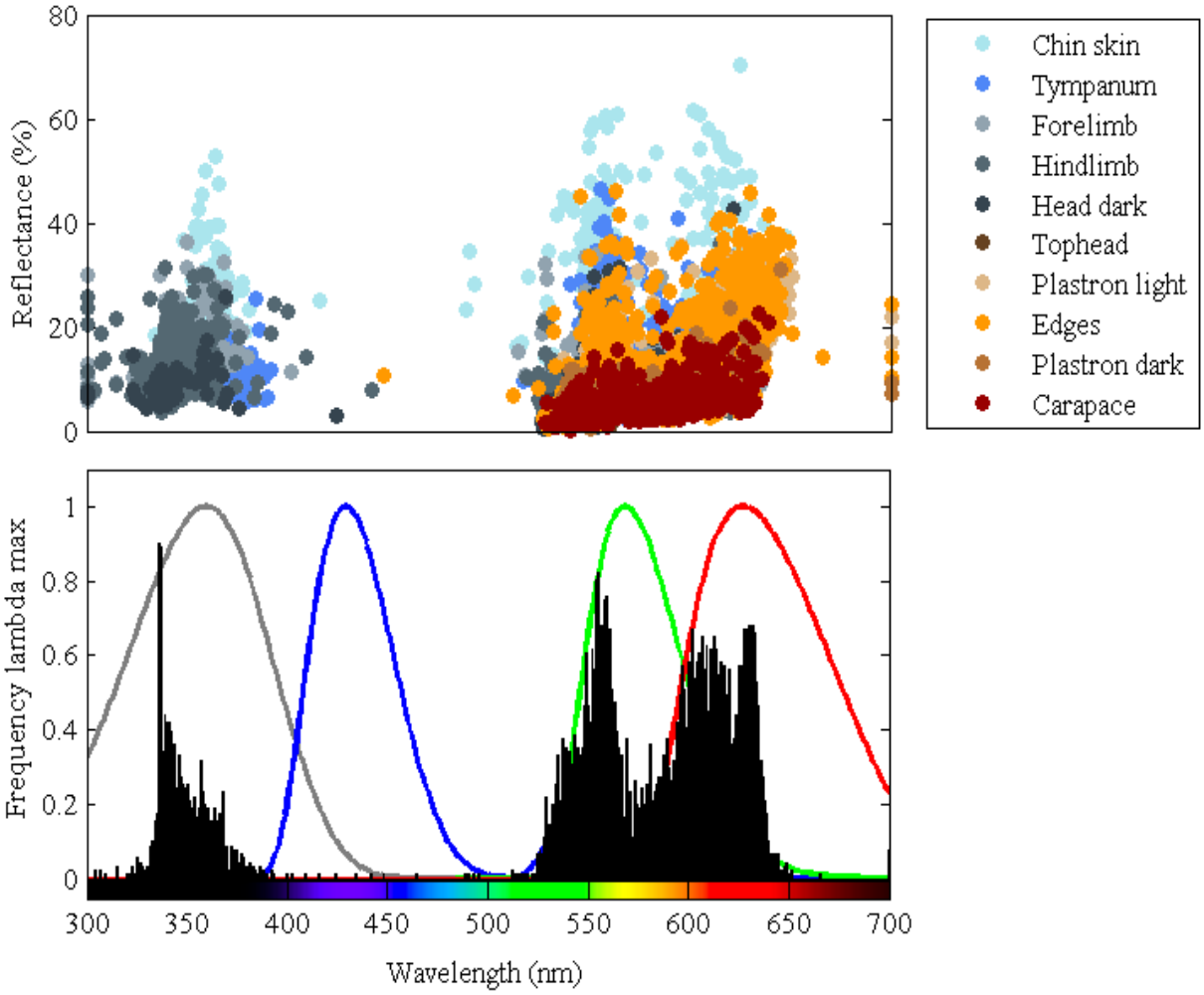

Figure 3.5: (A) Scatter plot of reflectance spectra maxima (λmax) for each patch. The maxima cluster around the UV, green and red spectral regions. (B) Frequency histogram of wavelength maxima plotted with the modeled tetrachromatic sensitivity curves of terrapin cone photoreceptors with λmax: 356 nm (UV-sensitive SWS1), 427 nm (blue-sensitive SWS2), 572 (green-sensitive MWS) and 630 nm (red-sensitive LWS).

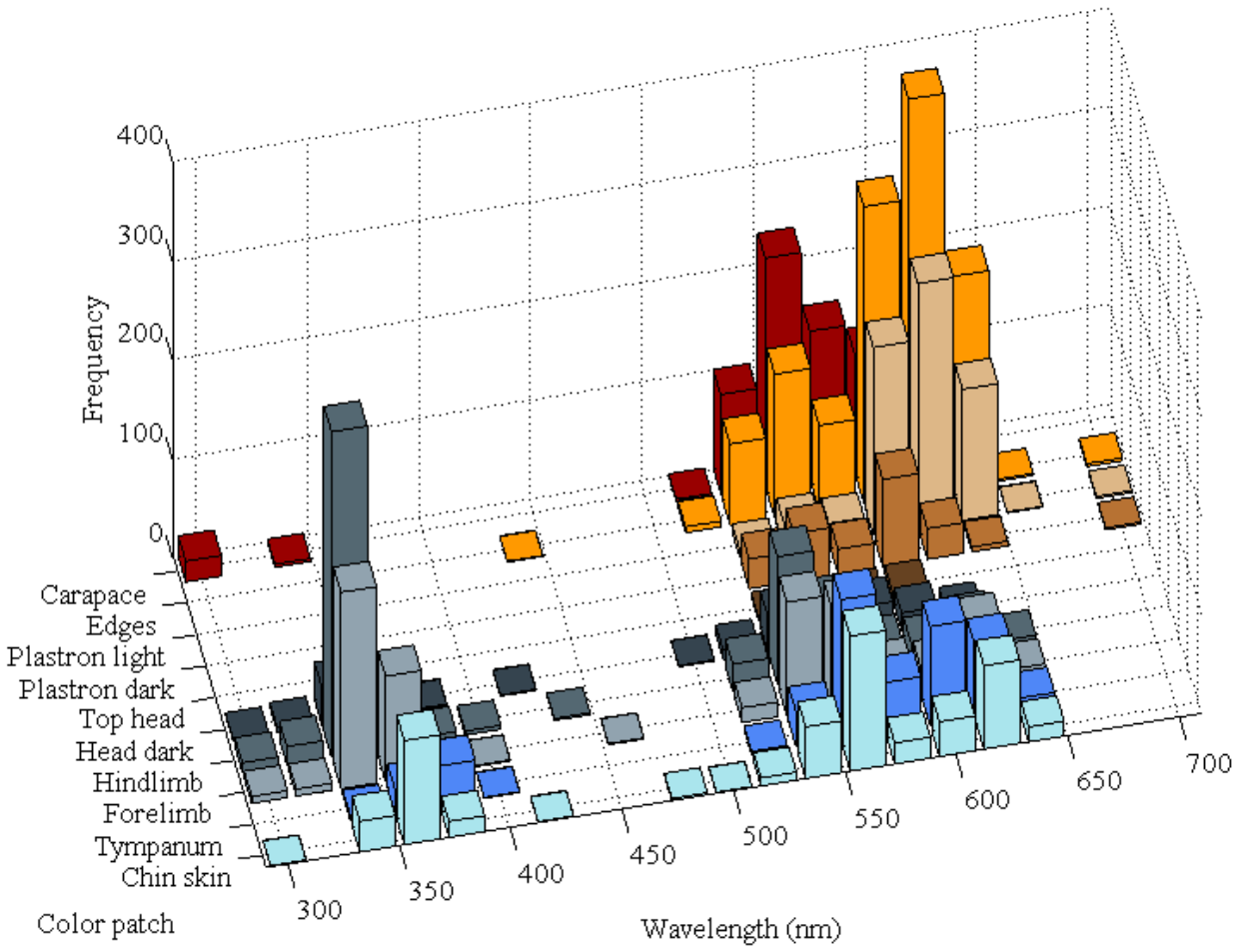

Figure 3.6: Three dimensional frequency histogram of wavelength maxima for each color patch measured on terrapins from Barnegat Bay, New Jersey (N ≈10,000). Reflectance maxima group in the UV, green and red portions of the spectrum, with each patch demonstrating more or less normal and continuous distributions around maxima in each spectral portion. Shorter bars that do not cluster near a maximum are most likely the result of low reflectance values that produced arbitrary hues.

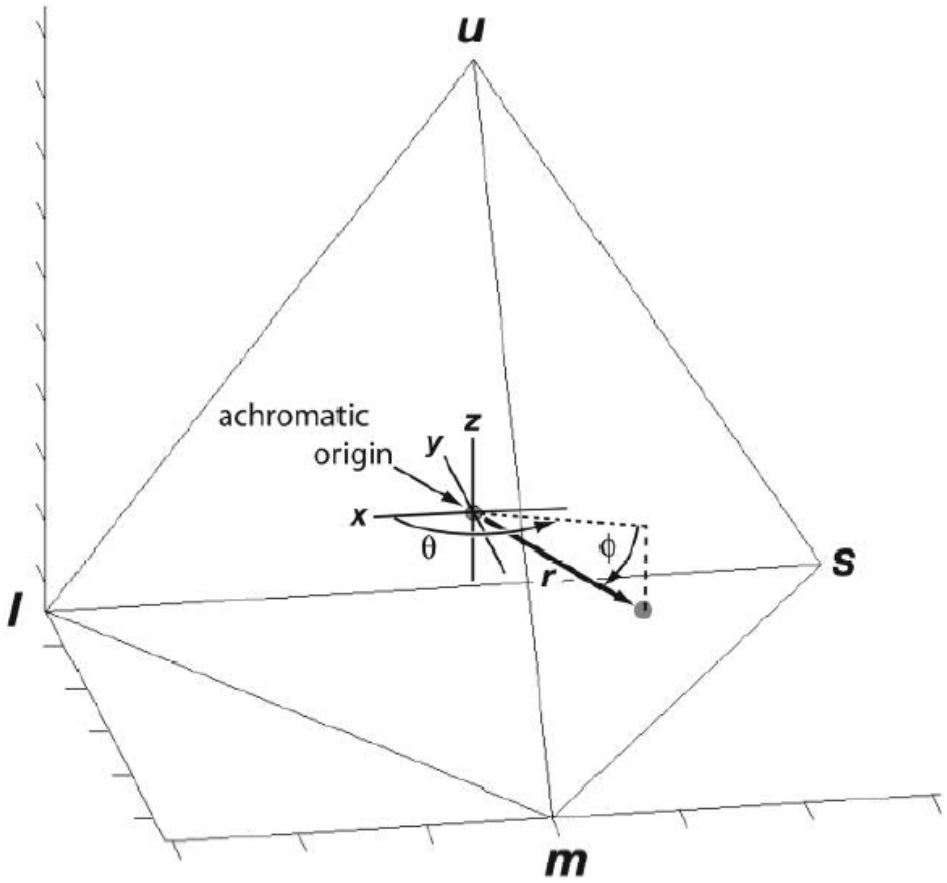

Figure 3.7: Tetrahedral color space borrowed from Stoddard and Prum (2008). Each corner in the tetrahedron represents stimulation of the one of the four cone photoreceptors. The UV-sensitive (u), the short or blue-sensitive (s), the middle or green-sensitive (m) and the long or red-sensitive (l). If a color stimulates all four cones equally, then it will fall at the achromatic (gray) origin of the tetrahedron. The color stimulus is plotted in tetrahedral color space using spherical coordinates: θ, Φ, and r which together describe hue and chroma. See Stoddard and Prum (2008) for further details.

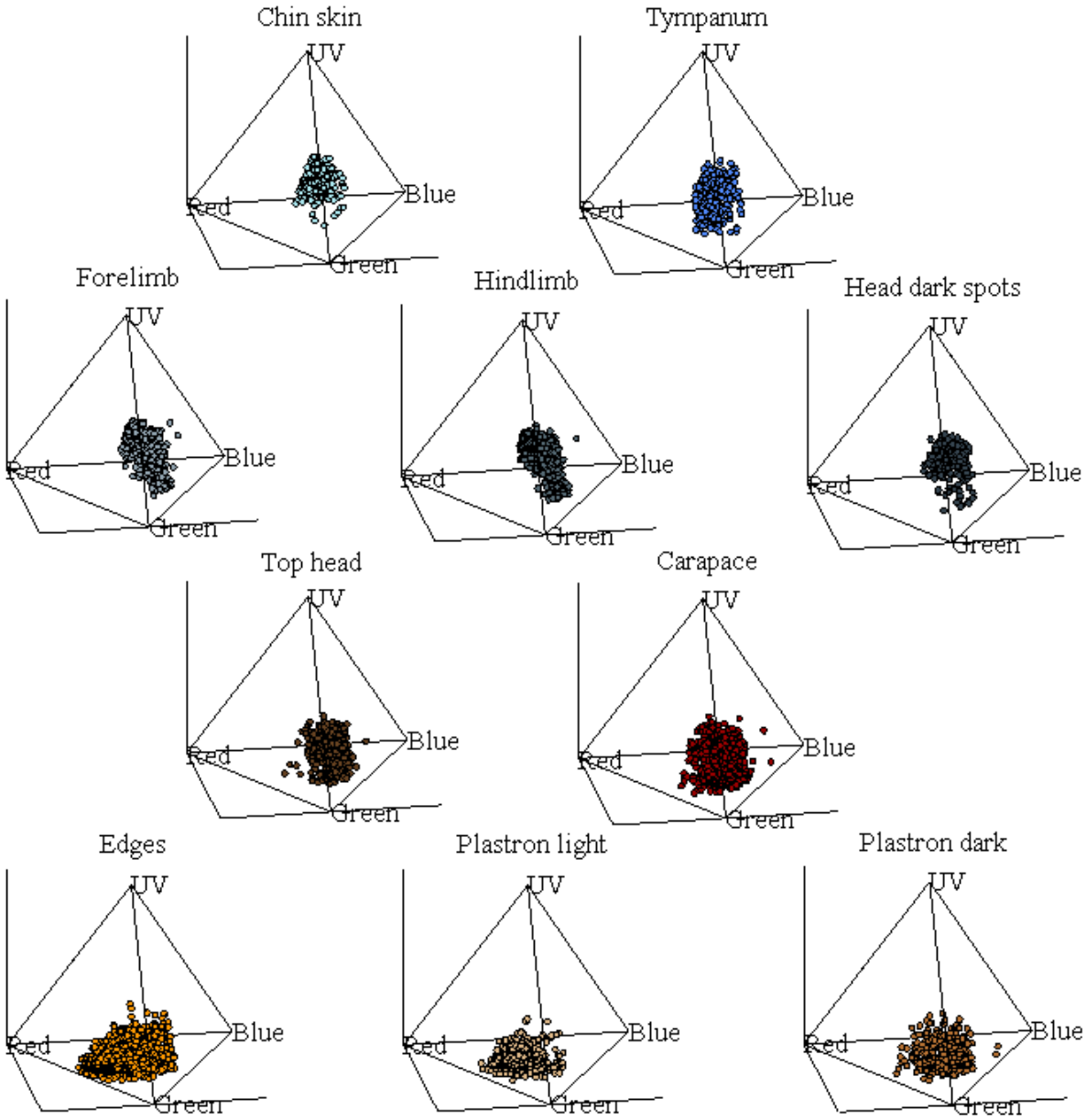

Figure 3.8: Tetrahedral color space plot of each of the 10 color patches using terrapin cone photoreceptor sensitivities.

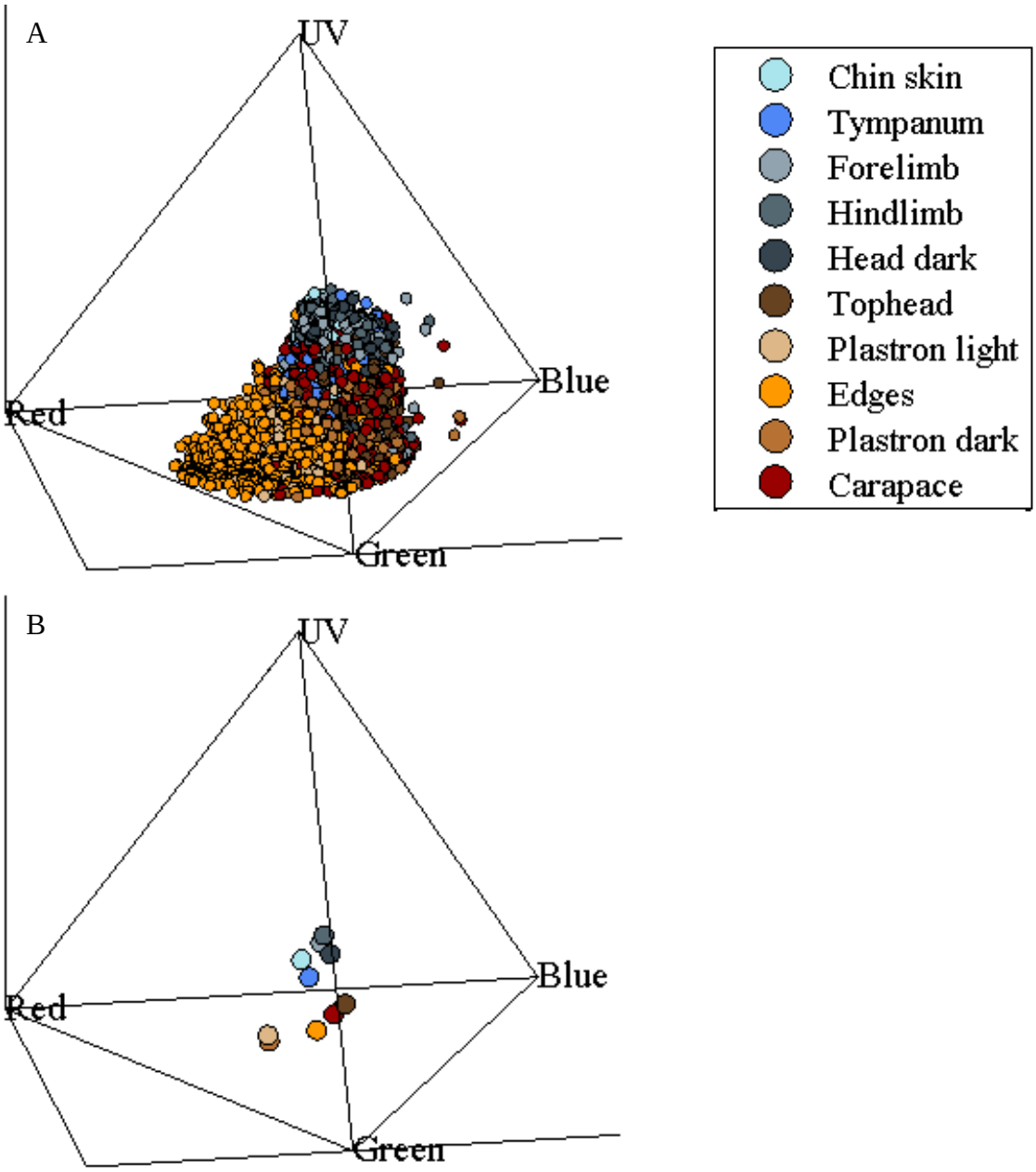

Figure 3.9: Tetrahedral color space plot of color patches using terrapin cone photoreceptor sensitivities. (A) All color patch reflectance measurements. (B) Mean color patch reflectance measurements.

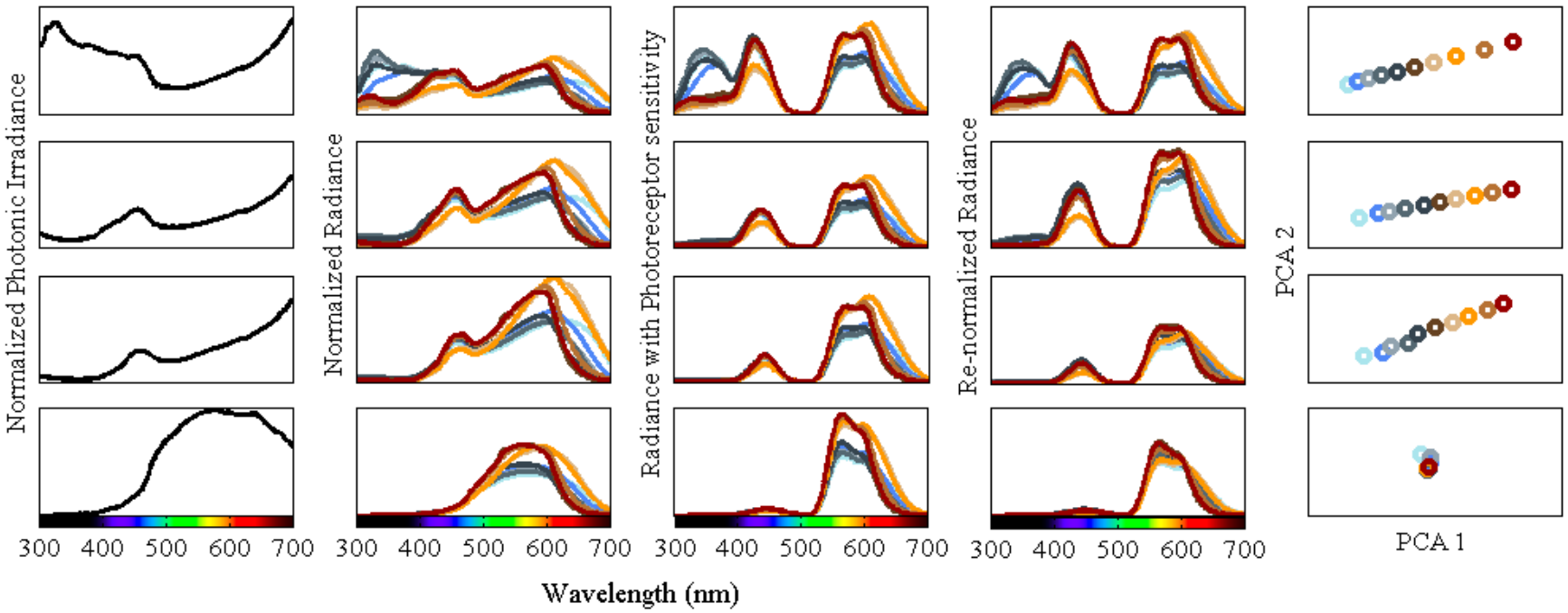

Figure 3.10: Modeled color signal reception by the terrapin given measured irradiance, measured cone photoreceptor sensitivities, and measured reflectance spectra. Column 1: Irradiance spectra measured in Barnegat Bay, NJ: (A) Surface downwelling, (B) half-meter downwelling, (C) one meter downwelling, and (D) surface upwelling. Column 2: Probable color or radiance of reflectance spectra in the corresponding irradiance row. Radiance spectra were calculated from the integral of the irradiance spectrum and mean reflectance spectrum of each color patch on the terrapin. Column 3: Probable photon capture by terrapin photoreceptors given the radiance spectra; calculated by multiplying each radiance spectrum with the additive photoreceptor sensitivities. Column 4: Re-normalized photon capture to the integral of one. Column 5: Principal component analysis of probable photon capture by the terrapin for each irradiant environment demonstrates changes in the ability to distinguish between colors.

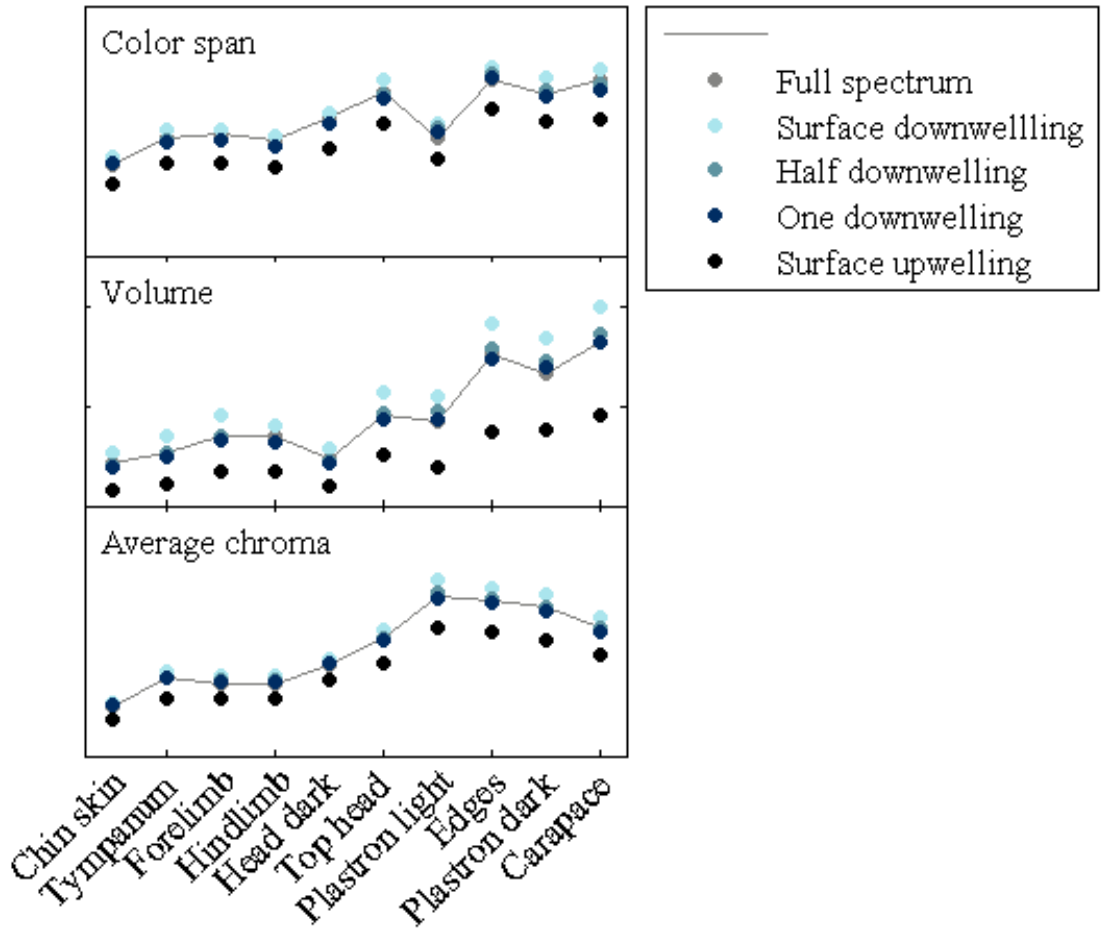

Figure 3.11: Effects of underwater irradiant environments on within-color patch differences based on Euclidean distance. The full spectrum irradiant model calculated color metrics without an irradiance spectrum; gray line denotes boundary above which spectral irradiance attenuation increased differences, and below which decreased differences. Generally, the surface downwelling spectral irradiance increased color differences while upwelling spectral irradiance would decreased differences (see irradiant spectra in Fig. 3.10). Color span was the average Euclidean distance between any two color patches in tetrahedral color space. Volume is the space occupied by the minimum convex polygon created by the color patch coordinates in tetrahedral color space. Chroma is the hue saturation for each color patch calculated in tetrahedral color space.

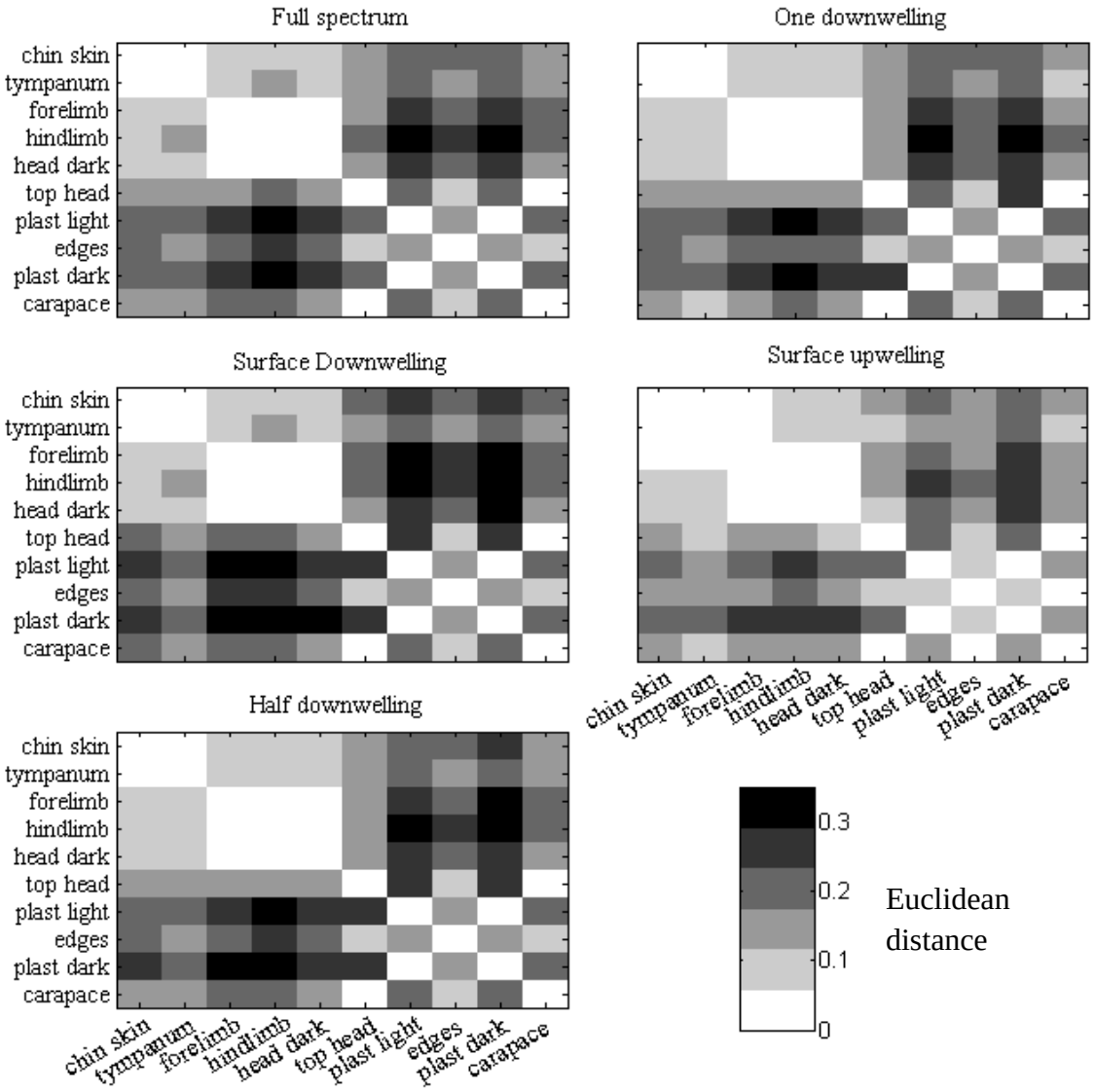

Figure 3.12: Effects of underwater spectral irradiance environments on average within-turtle differences based on Euclidean distances. Pairwise Euclidian distances, or color span, as measured in tetrahedral color space, change with the spectral irradiance environment. Color span and contrast generally decrease with increasing depth and light attenuation.

CHAPTER 4: Phenotypic factors influencing potential mate preference of female diamondback terrapins (*Malaclemys terrapin*)

Abstract

Sexual selection is generally defined as sex-biased selection through mate preference in one sex for a trait, or suite of traits, in the other. Mate preference is often exhibited by females that perceive greater fitness in males that possess the preferred trait. A common consequence of sexual selection is sexual dimorphism in the form of dichromatism, where males express more conspicuous color patterns than their female counterparts, resulting in secondary-sexual characteristics. The terrapin exhibits widely variable and conspicuous color patterns, but does not have dichromatism. However, terrapins do not have sex chromosomes and therefore cannot easily develop secondary-sexual characteristics or traits; males and females could equally express a preferred trait if sexual selection occurs in the population. To determine if some form of female mate preference could lead to maintenance of the observed polymorphic phenotypes, I assigned paternity to successful hatchlings that resulted from a successful mating. Phenotypes were recorded through digital photography and spectral reflectance of 10 distinct color patches, and used to create color statistics for the population to which phenotypes of genotype-matched fathers were compared. Comparison of color patches within and among individuals revealed potential female preference for high color contrast mediated through greater chroma (hue saturation). Color contrast was not isolated to any specific pair of color patches, suggesting a holistic assessment of potential mates by females.

Introduction

The diamondback terrapin is an estuarine turtle with a large geographic distribution ranging from Cape Cod, Massachusetts to Corpus Christi, Texas (Schoepff 1792; Gray 1844). Historical and current anthropogenic factors—over-harvesting, shoreline development, vehicular mortality, boat traffic, loss of natal nesting sites, and unintentional trapping in crab pots (Bishop 1983; Roosenburg *et al.* 1997)—are causing population declines of this once common species. Sheridan (2010) demonstrated that skewed sex ratios resulting from vehicular mortality have significant impacts on the terrapin mating system in Barnegat Bay, NJ. Multiple paternity, in which multiple fathers contribute to a clutch, is significantly lower in areas with high road mortality of nesting females, which may be indicative of non-random mating patterns in which individual females have mating preferences (Sheridan 2010). Mating preferences tend to rely on secondary sexual characteristics that, due to some physiological or ecological cost, communicates individual fitness (Zahavi 1975). Fitness may be expressed as bright coloration (e.g. many bird and fish species) and/or prowess in courtship behavior (e.g. jumping spiders and bird leks) among other sensory cues. If there is indeed non-random mating, and female terrapins have mate preferences, then on what basis are females choosing mates?

Sexual selection and female mate preference usually result in sexual dichromatism or dimorphism in which males express the preferred trait while females do not (Kodric-Brown & Brown 1984; Badyaev & Hill 2000). These differences are maintained by sex chromosomes either through direct genetic control or indirectly through hormonal and immune control (Bortolotti *et al.* 1996; Bulte *et al.* 2013).

Terrapins, like most turtles and other reptiles, do not have sex chromosomes, so any genetically controlled coloration will be equally expressed by male and female terrapins. Indeed, there is no apparent dichromatism in terrapin populations. Dimorphism is present however, with females being three times larger than males on average. This disparity in size is attributed to the interaction of two factors: (1) females need to reach a certain size to carry eggs; generally the bigger they are the more eggs they can carry, and (2) males are mature at a smaller size because there is no male-male competition, and males do not force copulation (Berry & Shine 1980). This is likely true for most species where the male is smaller than the female. In turtle species where the male is the same size or larger than the female, there is likely little sexual selection as there is little female choice. As a result of the female-biased size difference in the terrapin, females can easily disregard any male if she is not receptive to mating. In most species, reproduction is more costly to females and if given the ability to choose, females are likely to be selective of mates (Trivers 1972) and base their choice on a sensory cue (e.g. visual, olfactory).

Until recently, sensory cues in sexual selection studies have focused largely on bird and fish species, and studies involving reptiles have focused mainly on lizards. However, recent studies indicate that turtles utilize chemical, visual and acoustic signals for intraspecific communication (Galeotti *et al.* 2007; Galeotti *et al.* 2011; Ibanez *et al.* 2013; Polo-Cavia, Lopez & Martin 2013; Wang *et al.* 2013). Terrapins exhibit widely variable colors within interbreeding populations, begging the question: how is this variation maintained? Predation is likely a selective pressure against highly visible colors, so it would seem that some factor, possibly female mate preference, is an opposing selective force enforcing conspicuousness. I hypothesize that if female terrapins are

selective of mates based on color or color-pattern, then the fathers that contribute to successful offspring should have similar phenotypes and differ from the general population. A lack of dichromatism between mothers and genotype-matched males would not necessarily demonstrate a lack of sexual selection. The absence of sex chromosomes and consequent inability to have sex-linked genes (Ciofi & Swingland 1997) may result in all offspring, both male and female, expressing the preferred trait(s). Female mate preference could also lead to large-scale geographical differences in population phenotypes if preference varies across populations. Indeed, terrapins are categorized into seven subspecies based on differences in color and color-pattern.

Methods

Clutch collection and hatchery

I captured gravid females from June to mid-July, the terrapin nesting season, from 2010 to 2012 in the Edwin B. Forsythe Wildlife Refuge in Barnegat Bay, NJ. Method of capture included passive hoop and fyke nets, dip nets, and hand captures on nesting beaches (Conklin and Carvel Islands). Gravidity was determined through palpation of the body cavity under the plastron. I confirmed gravidity and determined clutch size through X-radiography using a MinXray portable x-ray system with Vetel Diagnostics © flat panel portable imaging system. Gravid females were placed in a bucket of water and induced to oviposit using an interperotineal injection of 10-30 IU/kg oxytocin (Ewert & Legler 1978; Sheridan 2010). After completion of oviposition, I released females at site of capture. Artificial nests were created in a hatchery at our field site in Waretown, NJ, the Lighthouse Center for Natural Resource Education. Clutches were buried between 16

cm and 10 cm below the surface; bottom and top of nest. I protected nests from predators using 2 in. mesh-wire fencing. Additionally, one cm mesh-wire or plastic fencing was placed around the clutch area within the predator excluder fencing to collect hatchlings upon emergence. Nests were checked regularly until hatchling emergence. If emergence was past due, I excavated the nest. I marked hatchlings with a cohort notch code by clipping small pieces from marginal scutes and stored these clippings in 1.5 ml microcentrifuge tubes at -20°C for later DNA extraction. I released hatchlings at the same site where the mother was captured.

DNA collection, extraction and amplification

I collected blood samples from the subcarapacal sinus vein and preserved them on Whatman FTA® blood cards (GE Healthcare) from all newly captured and previously un-sampled adult terrapins. I dried and stored blood cards at room temperature for later processing in our laboratory at Drexel University. I collected carapacal tissue samples from hatchlings, and tail tissue samples from adults when FTA® blood cards were not available. I stored tissue samples in labeled 1.5 ml microcentrifuge tubes in a -20°C freezer for later processing.

Following directions for FTA® blood card sample extraction, I took a 1.2 mm hole-punch from each blood card and placed it into a strip-tube for each (2) multiplexed PCR amplification. To prepare the hole-punch samples for PCR amplification, I washed the samples in ~50 µl of 70% ethanol, ~50 µl of FTA® purification reagent, and ~50 µl of TE buffer, with removal of liquid between each wash. I allowed samples to dry for 20-

30 minutes before running PCR amplification. To prepare tissue samples for PCR amplification, I washed tissue samples with ~100 µl of 1x Phosphate Buffer Saline Solution and extracted genomic DNA using the DNeasy Tissue Kit (Qiagen).

I used the 6-microsatellite loci protocol developed by Sheridan (2010) that exhibited high levels of polymorphism (Table 4.1). I used the same primers, multiplex PCR reactions, ABI 3100 capillary sequencer and internal size standard GENESCAN 500 ROX (Applied Biosystems) as Sheridan (2010). I completed fragment analysis using the genotyping software GeneMarker® 2.2.0 (SoftGenetics LLC).

Paternity assignments and phenotype assessment

I determined and assigned paternity by calculating probable paternal genotypes from known mother and hatchling genotypes using GERUD 2.0 (Jones 2005). In the cases where multiple paternal solutions were calculated, the most probable solutions based on allele frequencies were chosen for further analysis. These calculated paternal genotypes were matched to known male genotypes in the population using the multi-locus allele match function in GENALEX 6.5 (Peakall & Smouse 2006; Peakall & Smouse 2012).

To assess the potential for female mate preferences based on coloration, I compared color metrics of probable fathers to the population mean. I first quantified color by collecting spectral reflectance measurements from specific anatomical sampling points called color patches (Chapter 3). Across the population, I found 10 distinct color patches (5 skin and 5 shells): chin skin, tympanum, forelimb, hindlimb, head dark spots, top head,

carapace, plastron light, plastron dark and edges. On an individual basis, some color patches may not be present, such as no head dark spots or the presence of only one plastron hue. As a consequence, between 8 and 10 color patches were available for comparison between probable fathers and the population mean. Principal component analysis (PCA) and tetrahedral color space analysis were performed for each pairwise comparison. Due to the nature of PCA, the relative placement of the mean color patches changed depending on the interaction with the color patches of the male being compared. Each PCA required individual assessment of component differences.

Results

Clutch and hatchery data

From a total of 96 clutches obtained between the years 2010 and 2012, only 73 successfully produced hatchlings and only 47 were viable for paternity analysis (Table 4.2). Average clutch size was between 11 and 12 eggs for all three years. Clutches were viable for paternity analysis only if all six microsatellite loci were identified, more than five individual samples were obtained from a clutch, and in some cases where the mother's genotype was known. The mother's genotype was only necessary if a common maternal contribution could not be resolved due to similarity to potential paternal genotypes as calculated by GERUD 2.0 (Jones 2005).

Paternity assignments and phenotype assessment

I found 14 males in the sampled population whose genotype either matched or closely matched the highest probable paternal genotype calculated by GERUD 2.0, given allele frequencies in the population (Jones 2005). Thirteen of the 14 males were matched to clutches obtained during the 2012 field season; one, PVWX, was matched to a clutch obtained in 2007 and identified by Sheridan (2010). Clutches 27, 29 and 36 were matched with more than one father, and clutches 13 and 43 were obtained from the same mother two weeks apart in different locations (Table 4.3). Capture dates, sites and locations for mothers and genotype-matched fathers may indicate site fidelity by males and/or group fidelity. All but one recapture location of the genotype-matched fathers was at the original site of capture. Additionally, some mating pairs were captured in or around the same location and one mating pair in Clutch 36 was captured on the same day in the same trap. I visually and subjectively compared the color of genotype-matched fathers by compiling their digital images (Fig. 4.1). The top two rows are the paired males that matched a single clutch, with each column as separate clutches (e.g. ACHJOV and ABIJP in the second column were matched to the same clutch). Except for ACHJNW, all genotype-matched fathers had a bright yellow/orange plastron that contrasted against the skin. Even though ACHJNW had an overall melanistic plastron, there were some bright orange patches around the plastron edges. Subjectively, using human-vision-biased photography, there appeared to be no color or color-pattern that would suggest a shared female preference among genotype-matched fathers that would distinguish them from the library of male photographs taken in this study (personal observations). There may,

however, be color preferences that differ among females, as well as differing levels of rigidity in preference.

I compiled the color patches of all genotype-matched fathers, analyzed their individual color metrics, and compared them to the average terrapin that was determined from the average of each color patch in the population (Table 4.4 and Fig. 4.2). I found that the color patches of the genotype-matched fathers occupied a larger volume of space in the color tetrahedron, had a larger average color span, and a higher average chroma than the average terrapin. Average normalized brilliance, or brightness, of fathers did not seem to differ from the average terrapin (Fig. 4.2). To further support this, the average spectral reflectance for each color patch of genotype-matched fathers closely resembles the average spectral reflectance of the sampled terrapin population (Fig. 4.3 and 3.3). To detect any pairwise differences between color patches of genotype-matched fathers and the mean color patches found in the population, I performed PCA on the combined color patches of each father and the average terrapin (Fig. 4.4). Overall, the spread of the principal components indicated a larger difference between color patches measured on the father than color patches calculated for the average terrapin, suggesting that genotype-matched fathers have greater color contrast than the average terrapin.

Taking the mean of a color metric, or any vector array, can be misleading if the data are unevenly distributed. To account for outlier effects, I assessed the spread of values for color span, chroma, and brilliance (mean of all color patches) for both the population and the genotype-matched fathers with box plots (Fig. 4.5). The spread of the data suggested that genotype-matched fathers matched very well with median values found in the population. This suggests then, if only evaluating the mean color metric of

all combined color patches, that females may prefer the most common or frequently observed color phenotype. However, each color patch was widely variable (Fig. 3.2). To further break this down, I compared the spread of chroma values for each color patch between the population and genotype-matched fathers (Fig 4.6A). The spread of the data suggested that chroma, or hue saturation, of the shell tended to be higher than the median values in the population. This supported the idea that high color contrast between the skin and shell, aided strongly by a bright UV color component on the skin, may be involved in female color preference. To further this point, I took the mean chroma of each color patch for the population and genotype-matched father (Fig. 4.6B). The mean hue saturation for the color patches top head, plastron light, and edges were much higher than the population mean.

Discussion

Terrapin mating typically occurs in early spring from April to early May, with nesting beginning in June and ending around mid-July (Seigel 1980). Mating aggregations have been observed in several locations in Barnegat Bay, NJ where hundreds of terrapins have converged into a concentrated group (reported by locals). Aggregations have also been observed in other populations in Florida and South Carolina (Seigel 1980; Estep 2005). Where are these terrapins coming from? Recapture sites of genotype-matched fathers supports sex-biased dispersal found by Sheridan *et al.* (2010) in which gene flow in the Barnegat Bay, NJ population seems to be primarily mediated through females that have larger home ranges. This may explain why the genotype-matched fathers were repeatedly recaptured at the original site of capture (e.g. one

particular male, ACJPV, was captured every year for five years in Osprey Cove; Table 4.3). Larger female home ranges are likely attributed to greater habitat requirements—nesting sites—than those of males. In addition, greater home ranges may be attributed to mate finding behavior; females may travel farther to find their preferred male phenotype, while males will court any female that passes through their own home range. It is possible then, to hypothesize that local males will converge at the nearest aggregation site while females may travel from farther away. Indeed, it has been observed that male terrapins arrive early to an aggregation site before the arrival of females, with females leaving first (Estep 2005). Furthermore, Estep (2005) observed that the male terrapins likely aggregated near a female thoroughfare that allows access to nesting sites, thus increasing access to receptive females. In Barnegat Bay, NJ, many genotype-matched fathers were captured in Osprey Cove, which sits directly behind Conklin Island beach, a major nesting site. This behavior fits with the definition of lekking, commonly observed in bird species, where males gather at a particular site for the purpose of encountering and attracting females.

While it is well known that interbreeding terrapins vary widely in coloration and color-patterning, there is little understanding of how or why this variation exists (Hartsell 2001; Lee & Chew 2008). Animal coloration, when it functions in intra- or inter-specific communication, largely depends on the visual system of the intended observer. Terrapin coloration, while highly variable to the trichromatic human eye, is interpreted differently by the tetrachromatic visual system of the terrapin. Thus, potential comparison of male coloration by females should be evaluated using the terrapin visual model developed in previous chapters. Included in these models are the effects of spectral irradiance (ambient

light) on the radiance spectrum (object color received by the eye). In Chapter 3, surface downwelling irradiance optimized detection of color differences, suggesting that color assessment by the terrapin visual system should be near the surface of the water column. Indeed, terrapin mating aggregations, or leks, occur at the surface of the water column which potentially optimizes female detection of separate colors, or color contrast, on preferred males.

The genotype-matched fathers, on average, have greater color contrast (color span and chroma) than the average terrapin. This suggests that those males that exhibit greater color contrast are largely more successful than males that do not. Higher color contrast between the shell and skin seems to be the common trait among genotype-matched fathers, as well as a high degree of within shell contrast as compared to the mean shell color patches of the population (Fig. 4.4). The contrast on the shell (carapace and plastron) is likely dictated by the presence and concentration of carotenoid and melanin pigments. Those with darker, more intense orange patches have higher concentrations of carotenoids. Those with dark brown to black coloration have higher concentrations of melanin. The presence of these pigments increase color contrast and thus increase potential female detection. These pigments may also be an indication of genetic fitness to a female since maintenance of these pigments is partially dependent on diet (Negro *et al.* 1998).

Different color combinations, however, can yield the same color contrast, which is potentially the driving force behind the widely variable color phenotypes in the terrapin. Although color brightness did not differ between genotype-matched fathers and the average terrapin, it may aid in detection of color contrast. Thus, chromatic differences

that cause high color contrast between color patches, aided by brightness, may be the trait on which sexual selection and female mate preference occurs in the diamondback terrapin. This evidence of potential sexual selection in a terrapin population sheds new light on our current understanding of their mating system.

Table 4.1: Characteristics of the 6-microsatellite multiplex kit (reprint from Sheridan 2010, Table 4-1).

Loading and PCR Plex	Locus	GenBank Accession #	Primer Concentration	Size Range (bp)	Florescent Label
A	*Gmu*B08	AF517229	0.2	211-241	6-FAM
A	*Gmu*D121	AF517252	0.2	124-188	NED
A	*Gmu*D62	AF517241	0.25	127-175	HEX
B	*Gmu*D87	AF517244	0.2	224-276	6-FAM
B	*Gmu*D114	AF517251	0.2	88-124	NED
B	*Gmu*D90	AF517247	0.25	111-147	HEX

PCR chemistry: 20 µl PCR reactions using 5-15 ng of DNA or 1.2 mm Whatman blood card punch, 0.3175 mM dNTPs, 1x GoTaq Flexi Buffer (Promega), 3.75 mM $MgCl_2$, 0.2-0.25 mM primer, 0.5 units of GoTaq polymerase (Promega).

PCR thermocycling: 94°C for 2 min, 35 cycles of denaturation at 94°C for 45 s, annealing at 56°C for 45 s, extension at 72°C for 2 min. Final extension at 72°C for 10 min.

Table 4.2: Summary statistics of clutches obtained from captured gravid female terrapins in Barnegat Bay, New Jersey with hatchery success and relative ability to match paternal genotypes.

Year	2010	2011	2012	All years; this study
Total clutches	15	25	56	96
Total egg number	173	280	587	1040
Average clutch size	11.5 ± 0.6	11.2 ± 0.6	11.4 ± 0.5	11.4 ± 0.3
Total living hatchlings	154	205	327	686
Total tissue samples	173	224	383	780
Viable clutches	12	20	41	73
Viable clutches for paternity analysis	4	9	34	47
Paternal matches with known phenotypes	0	0	13	14*

*****One match found by Sheridan (2010) was phenotyped in this study.

Table 4.3: Capture summary of terrapin mating pairs through paternal genotype matching determined from GENALEX (Peakall & Smouse 2012) and GERUD 2.0 (Jones 2005)

Father ID	Mother ID	Clutch # (Year)	Father Capture date(s)	Father Capture site(s)	Father GPS Locations(s)	Mother Capture date(s)	Mother Capture site(s)	Mother GPS Location(s)
BCHNOV	ABCHOQ	37 (2012)	9/4/2012	GUNNING RIVER	570352 4397321	7/1/2011; 6/28/2012	CONKLIN ISLAND; OSPREY COVE	570612 4399215; 571337 4398859
ABCOPQ	ABJKNX	18 (2012)	7/9/2011	VOL SEDGE	574957 4399577	6/15/2012	OSPREY COVE	571250 4399028
ABCJKW	ABJNOP	6 (2012)	7/3/2011	HARVEY SEDGES	571470 4394414	6/10/2012	CARVEL ISLAND	571442 4393264
AJNQVX	ABJOQW	10 (2012)	8/15/2012	GUNNING RIVER	570191 4397500	6/13/2012	CARVEL ISLAND	571442 4393264
ACJPV	ABKOQV	13,43 (2012)	6/20/2008; 6/26/2009; 6/29/2010; 7/6/2011; 6/6/2012	OSPREY COVE	571398 4398802; 571412 4398809; 571414 4398817; 571408 4398811; 571410 4398806	6/15/2012; 7/1/2012	CARVEL ISLAND; CONKLIN ISLAND	571383 4393239; 570079 4399348
BCHKNQ	ABKPQX	17 (2012)	9/1/2012	GUNNING RIVER	570352 4397321	6/15/2012	OSPREY COVE	571278 4398977
ABHPVX	ACHINW	27 (2012)	8/3/2011	BIG FLAT CREEK	570708 4395334	6/21/2012	CARVEL ISLAND	571442 4393764
ACHJNW	ACHINW	27 (2012)	6/23/2012	OSPREY COVE	571272 4398838	6/21/2012	CARVEL ISLAND	571442 4393764
ABHINV	ACHIQV	29 (2012)	7/15/2011	HARVEY SEDGES	571376 4394355	6/22/2012	CARVEL ISLAND	571442 4393764
AINOQW	ACHIQV	29 (2012)	8/10/2012	BIG COVE	570340 4394492	6/22/2012	CARVEL ISLAND	571442 4393764
BCHPW	ACHIVX	31 (2012)	7/9/2010; 6/29/2012	OSPREY COVE	571343 4398856; 571337 4398859	6/22/2012	CARVEL ISLAND	571442 4393764
ABIJP	ACHJOW	36 (2012)	6/13/2010; 8/13/2011	CINCO COVE; DEFENDERS PASS	569521 4399243; 569397 4398338	6/26/2012	GUNNING RIVER	570040 4398542
ACHJOV	ACHJOW	36 (2012)	6/26/2012	GUNNING RIVER	570040 4398542	6/26/2012	GUNNING RIVER	570040 4398542
PVWX	ACHO	8 (2007)	7/6/2006; 8/22/2011; 6/29/2012	OSPREY COVE	571304 4398051; 571254 4398845; 571337 4398859	6/21/2007	OSPREY COVE	571293 4398858

Table 4.4: Summary of color space metrics of genotype-matched terrapin fathers. Each color metric accounts for all color patches on an individual. Volume was determined from the minimum convex polygon created from the coordinates of all color patches in the tetrahedron. Color span is the average Euclidean distance between all color patch coordinates from an individual. Chroma is the average distance from the achromatic origin of the tetrahedron; can be interpreted as hue saturation. Brilliance is the average brightness of the normalized spectral reflectance of all color patches on an individual. All measurements are unitless. See Fig. 4.2.

Father ID	Volume	Color span	Chroma	Brilliance
ABCJKW	0.0017	0.2013	0.2128	0.0321
ABCOPQ	0.0031	0.2049	0.1612	0.0771
ABHINV	0.0010	0.2010	0.1729	0.0651
ABHPVX	0.0026	0.2067	0.2357	0.0316
ABIJP	0.0018	0.2135	0.1823	0.0946
ACHJNW	0.0017	0.1805	0.2156	0.0543
ACHJOV	0.0106	0.2443	0.2172	0.0736
ACJPV	0.0039	0.2533	0.2295	0.0852
AINOQW	0.0029	0.1982	0.1821	0.1367
AJNQVX	0.0008	0.1855	0.1672	0.0804
BCHKNQ	0.0011	0.1633	0.1985	0.0453
BCHNOV	0.0008	0.1821	0.1896	0.0500
BCHPW	0.0015	0.1693	0.1763	0.0641
PVWX	0.0022	0.2282	0.1728	0.1095
Average terrapin	0.0002	0.1423	0.1410	0.0760

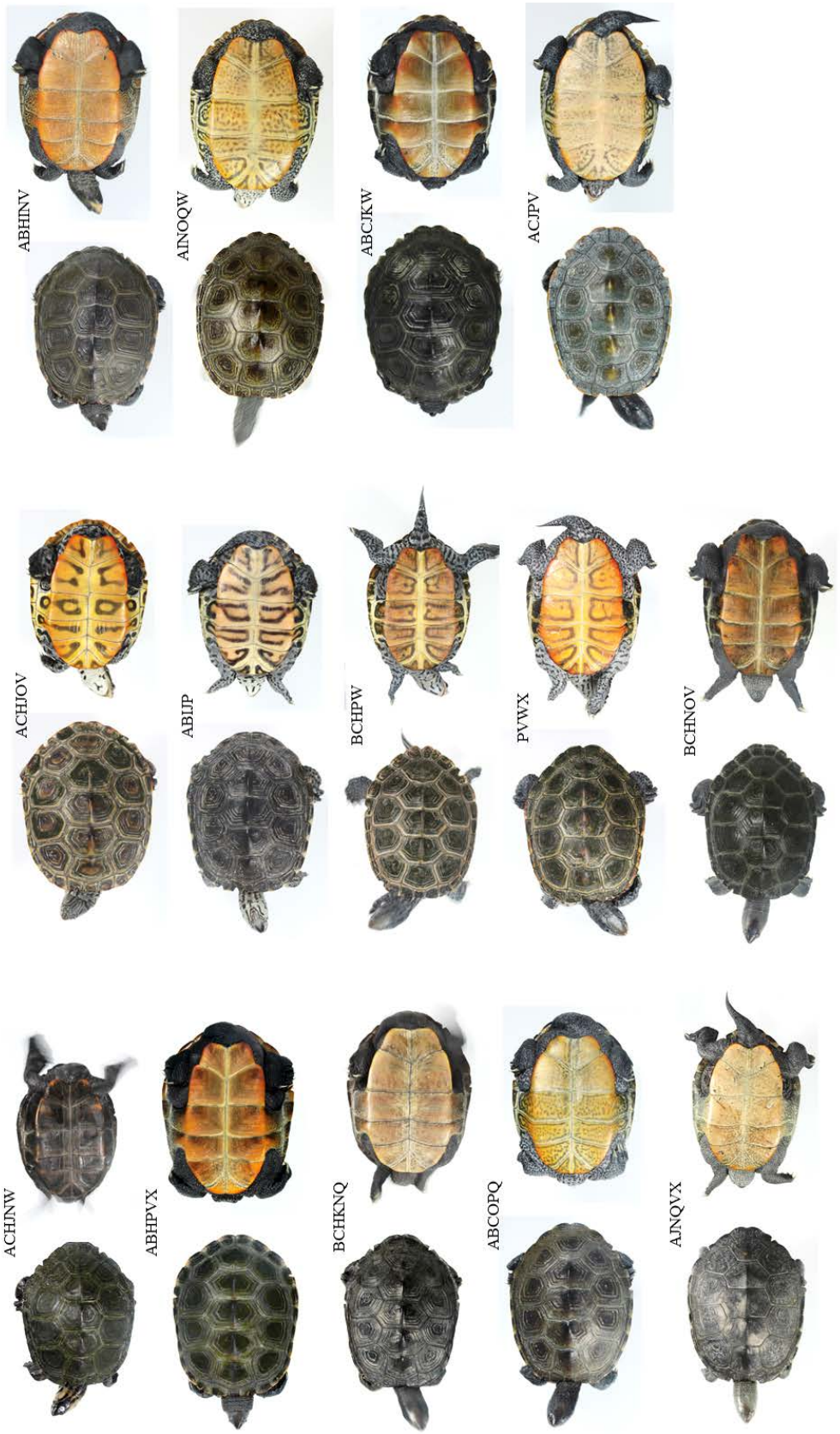

Figure 4.1: Digital photographs of the carapace and plastron of genotype-matched fathers. Each pair of photographs are labeled with the terrapin's notch code ID.

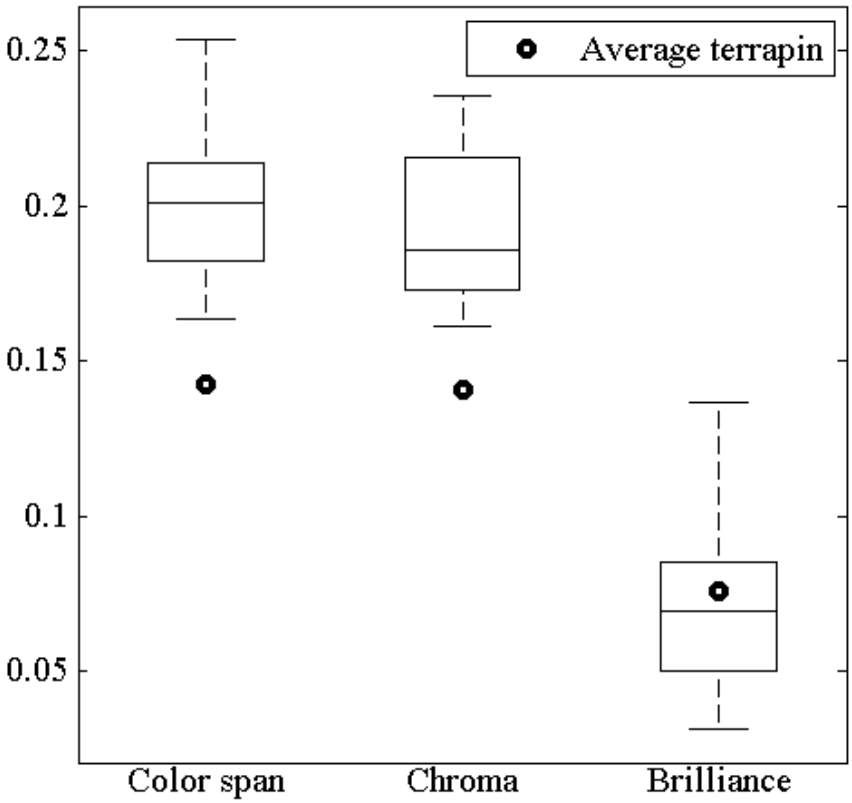

Figure 4.2: Box plot demonstrating spread of the means of color span, chroma and brilliance of genotype-matched terrapin fathers compared to the mean color span, chroma and brilliance of the average terrapin. Measurements are unitless (see Table 4.4).

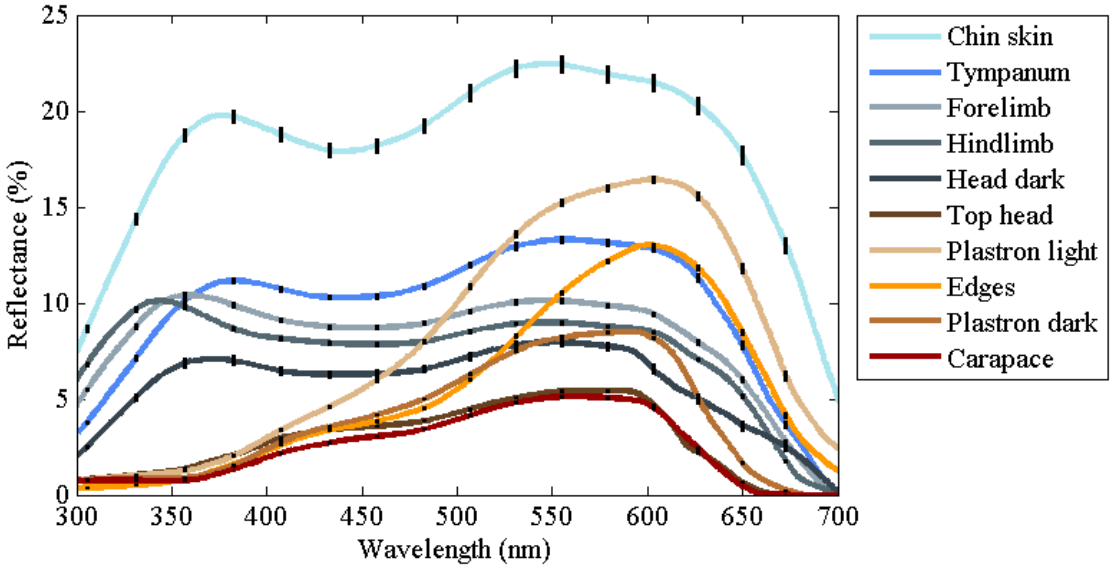

Figure 4.3: Mean reflectance spectra of genotype-matched fathers in the Barnegat Bay, NJ terrapin population. Compare to mean reflectance spectra of the sampled population in Figure 3.3A.

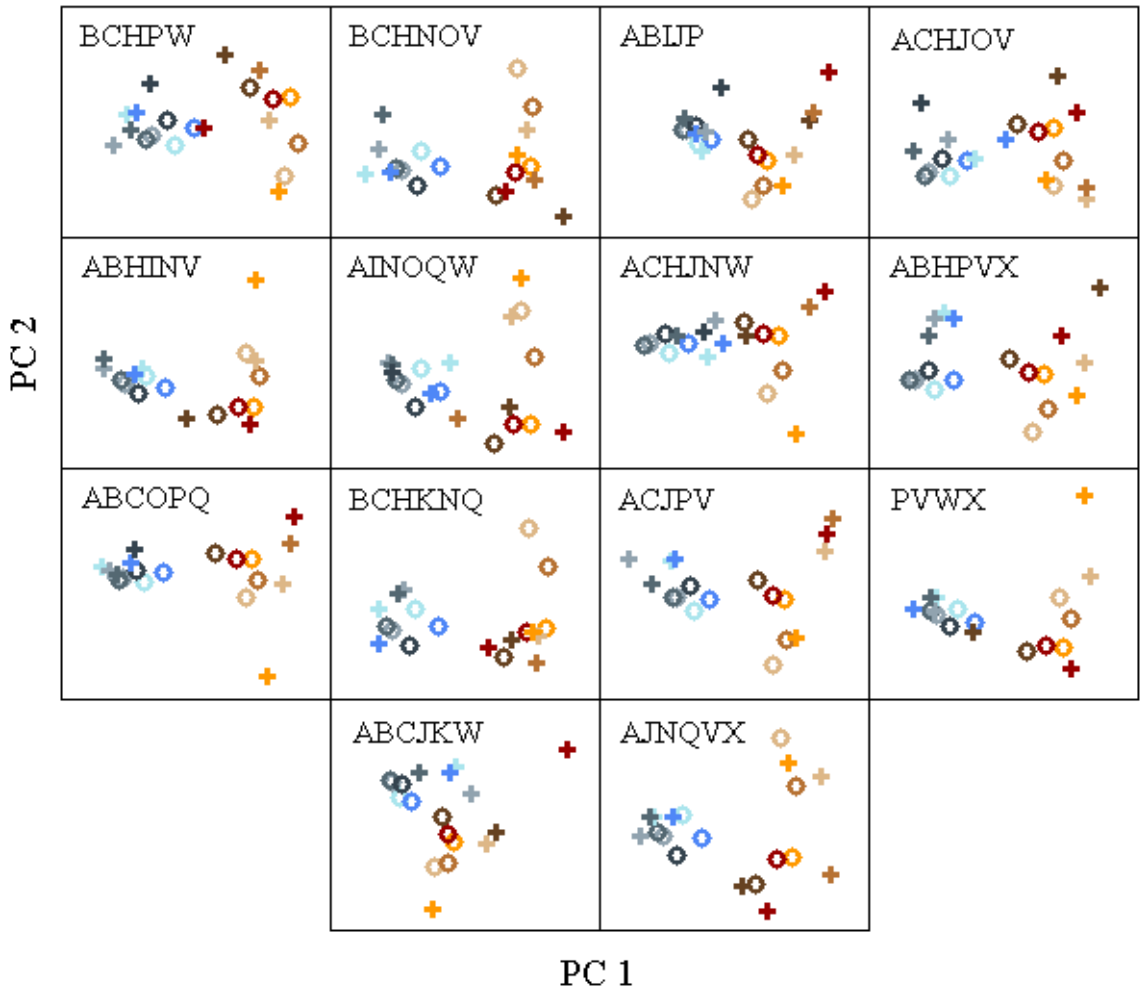

Figure 4.4: Principal component analysis (PCA) comparing color patches of genotype-matched fathers to the mean color patches in the sampled terrapin population in Barnegat Bay, NJ. Factor loadings for the x-axes (PC 1) account for 69 to 95 percent of variance. Factor loadings for the y-axes (PC 2) account for 5 to 31 percent of variance. Plus signs represent color patches measured on the individual genotype-matched father and circles represent mean color patches in the population, or the average terrapin. Cool colors are skin color patches and warm colors are shell color patches. In many cases the distance or difference between a pair of color patches on a father is greater than the distance or difference between the same pair of color patches on the average terrapin.

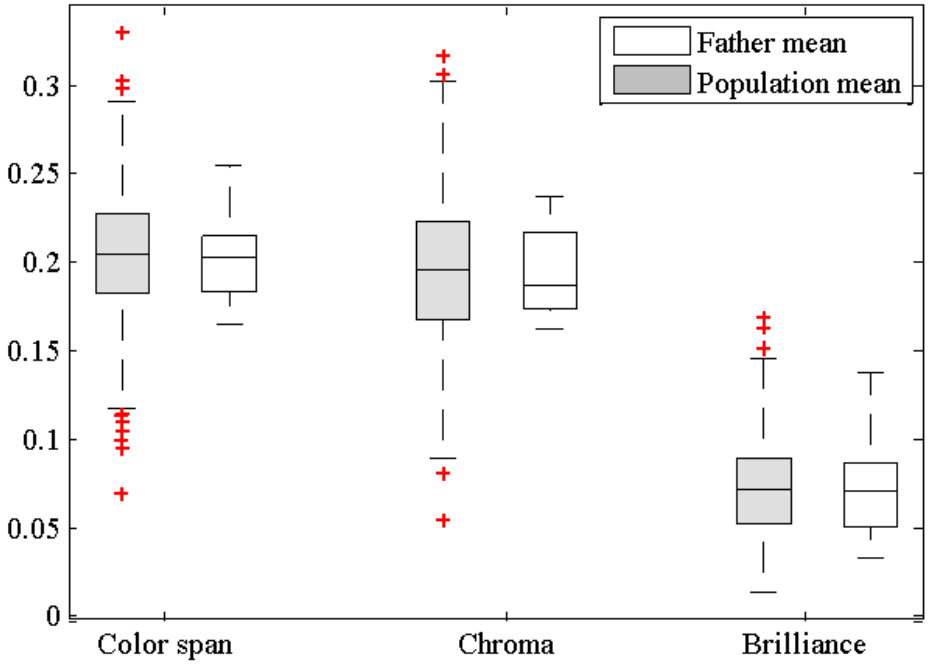

Figure 4.5: Paired box plot distributions comparing color metrics of mean color patches among individuals in the Barnegat Bay terrapin population and among genotype-matched fathers. The color span, or color patch differences as measured through Euclidean distance in tetrahedral color space, of genotype-matched fathers did not significantly differ from the color span of the mean color patches in the population. Similarly chroma, or hue saturation, of matched fathers did not significantly differ from the population. Brilliance, or brightness, was not significantly different from the population.

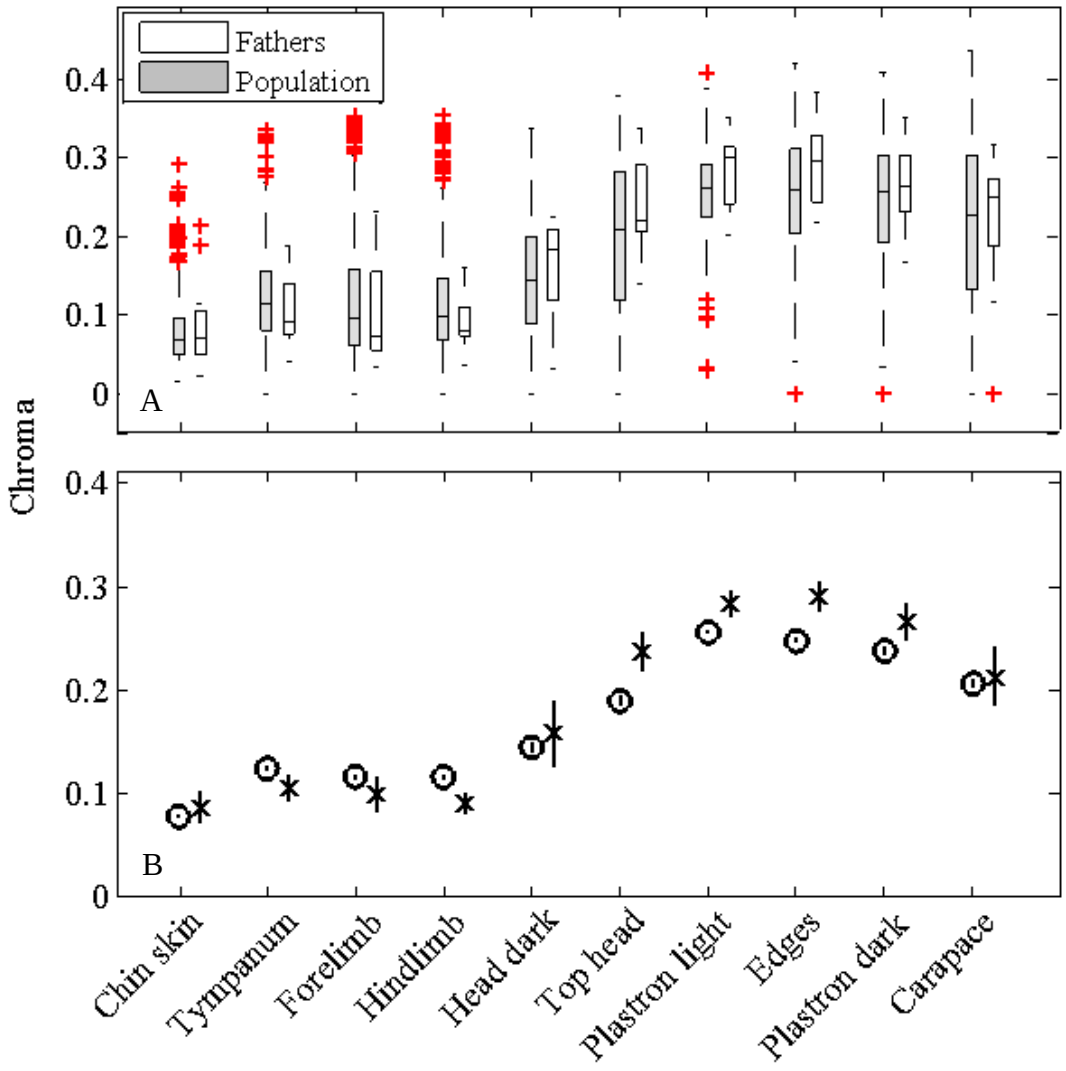

Figure 4.6: (A) Paired box plots demonstrating distributions of chroma values for each color patch among sampled individual terrapins in the Barnegat Bay, NJ population and among genotype-matched fathers. The chroma of color patches top head, plastron light and edges on genotype-matched fathers have greater hue saturation than the overall population. (B) Mean chroma of color patches with standard error of the mean (SEM). Color patches across the population represented by open circle and color patches of genotype-matched fathers represented by an 'x'. The mean chroma of color patches top head, plastron light and edges on genotype-matched fathers have greater hue saturation than the overall population.

CHAPTER 5: Conclusions and future directions

In this dissertation I examined and modeled the physiological visual ability of the diamondback terrapin (*Malaclemys terrapin*), the underwater spectral irradiance of their estuarine habitat, and male spectral reflectance in relation to potential female mate preferences. My aim was to determine whether sexual selection plays a role in the phenotypic variation observed in interbreeding terrapin populations (Hartsell 2001; Lee & Chew 2008). In order to comprehensively address this aim, I measured and integrated the three components of visual ecology: (1) the visual system (physiological visual ability), (2) the visual environment (spectral irradiance), and (3) the visual task and target (female preference for male spectral reflectance). To date, this dissertation provides the most comprehensive ecological visual model for a turtle species.

To assess the terrapin's visual system, I measured absorbance of the ocular media, oil droplets, and visual pigments (Chapter 2). Unsurprisingly, I found that the terrapin has a UVS (ultraviolet sensitive) tetrachromatic visual system like that of the closely related red-eared slider turtle (Loew & Govardovskii 2001; Ventura *et al.* 2001). It is also unsurprising when considering that UV-sensitivity is a phylogenetically ancestral trait (Heesy & Hall 2010). In addition, shallow aquatic habitats tend to have high spectral fluctuations of light, leading to complex spectral radiances, which in turn enforce complex visual systems to interpret them (Gomez & Thery 2004; Sabbah *et al.* 2013). Surprisingly, however, I found that the ocular media absorbance was unlike that of the red-eared slider turtle, and indeed unlike any other ocular media absorbance found in the published literature. Generally, the ocular media are found to transmit light equally above 400 nm and then lose transmission (increase absorbance) between 300 and 400 nm. The

steepness of this curve is species dependent and related to the sensitivity and complexity of the visual system. The terrapin however, had maximal ocular media absorbance around 500 nm with increasing transmission above *and* below. This effectively caused a gap in sensitivity between the shortwave and longwave photoreceptors, which increased the range in terrapin spectral sensitivity. I also found that ambient spectral irradiance in the water column exhibited an unusual spectral shape; downwelling light contained relatively little photonic energy around 500 nm. The spectral matching between terrapin ocular media and their spectral irradiant environment suggest terrapins are (1) well adapted to their underwater light environment, and (2) rely heavily on their visual sensory system. This further supports the notion that complex underwater light environments likely require complex visual systems in shallow aquatic organisms that depend on visual cues for survival (Sabbah *et al.* 2013).

Using the physiologically-based vision model reported in Chapter 2, I extended the model to include assessment of terrapin spectral reflectance, grouped into 10 distinct color patches, in Chapter 3. The color patches were analyzed both independent of a visual system and with the terrapin vision model. I found that percent reflectance maxima (λ_{maxes}) of the color patches matched intrinsically very well with the terrapin vision model. Nevertheless, the spectral radiances, which integrated the terrapin vision model and surface downwelling light, further increased spectral differences between color patches as potentially perceived by the terrapin. This enhanced chromatic discrimination (i.e. the ability to distinguish object colors), and the intrinsic spectral matching between color expression and potential color sensitivity in the terrapin, lends support to the idea

that terrapin color expression has evolved for optimal perception by conspecifics in dynamic estuarine light environments.

To test the hypothesis that female terrapins have mate preferences based on potential perception of color patches, I assessed and assigned paternity to hatchlings that resulted from successful mating. For males that were identified as highly probable fathers and for which I also had collected phenotypic data, I looked for correlations between these genotype-matches fathers and any variances from the population. Generally, I found that the genotype-matched fathers had higher color contrast, mostly between the skin and shell, and greater shell chroma than the average terrapin. The highest color contrast among the genotype-matched fathers was not isolated to any particular color patch pair, suggesting that females holistically assess male color patches with no particular preference for a specific hue or combination of hues. Rather, chroma (hue saturation) and hue disparity aided by brightness, contribute to overall contrast. This contrast is then enhanced by the terrapin's visual system and light environment. Color contrast has been found to be a sexually selected trait in birds (Metz & Weatherhead 1991; Endler & Thery 1996; Heindl & Winkler 2003) and lizards (Macedonia, Brandt & Clark 2002; Macedonia, Echternacht & Walguarnery 2003; Font, De Lanuza & Sampedro 2009) either between color patches within the organism or between the organism and its background environment. It is thus quite possible that female preference for within-turtle contrast, in conjunction with their uniquely expanded visual system, enforce and maintain color and color-pattern variation in interbreeding populations.

Evaluating an effective population size (the number of individuals contributing to the next generation) depends on an understanding of the mating system. These data I

have provided in this dissertation on potential female mate preference suggests a degree of non-random mating. I strongly recommend that viability assessments of terrapin populations should include consequences of non-random mating, as it may add to and exacerbate issues with skewed sex ratios, habitat fragmentation, and declining populations (Sheridan 2010). In other words, expression of mate preference in a population may decrease viability of that population if it is already experiencing external pressure on reproductive success. If there is random mating—no mate preference—then the effective population size can be small, assuming all individuals have the same chance of producing offspring. However, if there is non-random mating, the effective population size needs to be large enough to maintain enough individuals with the preferred trait. Otherwise, the presence of sexual selection in a small population increases the potential for extirpation of that population (Doherty *et al.* 2003).

The results presented in this dissertation provide a foundation for future, in-depth ecologically relevant and evolutionarily significant research questions. Indeed, this research built upon the population genetics study completed previously by Sheridan (2010), a former student in my lab. Since my results indicated potential differences in female preference and/or rigidity of preference, I recommend testing potential intra-sexual differences in female preference by conducting mate choice experiments with a number of receptive females. A larger sample size of genotype-matched fathers with phenotypes would also clarify this point. These data generated in this study could also be used to determine probable lek locations, and locations from which males and females might travel to attend a lek. In the study conducted by Sheridan (2010), genetic differences were found between the northern and southern portions of the Edwin B.

Forsythe Wildlife Refuge in Barnegat Bay, NJ. These genetic differences may be the result of separate leks; indeed, the locations of genotype-matched fathers were generally more proximate to the nesting beach on which their offspring were to be incubated than to the alternate nesting beach used in this study. A greater intensity of sampling would shed light on this potential geographic pattern, and reveal probable lek locations.

Although I did not measure the effects of turbidity and total suspended solids (TSS) on visibility in the water column, this may have an impact on perception of color contrast for finding potential mates and prey items. Human-mediated increases in turbidity and TSS may also have a significant impact on successful mating and prey finding behavior to the point where survivorship decreases. I recommend a study in which potential mates or prey items are placed in varied water conditions, and prey or mate finding behavior is measured in the terrapin.

The diamondback terrapin is an important top-down controller of marsh grasses in estuarine ecosystem habitats (Silliman & Bertness 2002). By consuming snails and crabs that feed on marsh grasses, the terrapin prevents the decimation of marsh grasses, which perform important ecosystem functions such as upland marsh stability. The balance of predator and prey populations support biological diversity, ecosystem health, and long term economic stability. This balance is threatened by the long-term and range-wide decline of terrapin populations due to several anthropogenic factors (Coker 1920; Bishop 1983; Roosenburg *et al.* 1997). The data that I have provided can be used to better understand terrapin ecology for the purpose of protecting this species from potential extirpation.

List of References

Ackleson, S.G. (2003) Light in Shallow Waters: A Brief Research Review. *Limnology and Oceanography*, **48,** 323-328.

Andersson, M. (1986) Evolution of condition-dependent sex ornaments and mating preferences: sexual selection based on viability differences. *Evolution,* **40,** 804-816.

Andersson, S. & Amundsen, T. (1997) Ultraviolet colour vision and ornamentation in bluethroats. *Proc. R. Soc. Lond. B,* **264,** 1587-1591.

Andersson, S., Ornborg, J. & Andersson, M. (1998) Ultraviolet sexual dimorphism and assortative mating in blue tits. *Proc. R. Soc. Lond. B,* **265,** 445-450.

Archer, S.N. (1999) Light and photoreception: visual pigments and photoreception. *Adaptive mechanisms in the ecology of vision* (eds S.N. Archer, M.B.A. Djamgoz, E.R. Loew, J.C. Partridge & S. Vallerga), pp. 25-41. Kluwer Academic Publishers, Boston.

Babcock, H.L. (1926) The diamond-back terrapin in Massachusetts. *Copeia*, **1926,** 101-104.

Badyaev, A.V. & Hill, G.E. (2000) Evolution of sexual dichromatism: contribution of carotenoid- versus melanin-based coloration. *Biological Journal of the Linnean Society,* **69,** 153-172.

Bels, V.L., Davenport, J. & Renous, S. (1998) Food ingestion in the estuarine turtle *Malaclemys terrapin*: comparison with the marine leatherback turtle *Dermochelys coriacea*. *J. Mar. Biol. Assoc. UK,* **78,** 953-972.

Berry, J.F. & Shine, R. (1980) Sexual size dimorphism and sexual selection in turtles (order Testudines). *Oecologia (Berl.),* **44,** 185-191.

Bishop, J.M. (1983) Incidental capture of diamondback terrapin by crab pots. *Estuaries,* **6,** 426-430.

Bortolotti, G.R., Negro, J.J., Tella, J.L., Marchant, T.A. & Bird, D.M. (1996) Sexual dichromatism in birds independent of diet, parasites and androgens. *Proceedings: Biological Sciences,* **263,** 1171-1176.

Bowmaker, J.K. (1980) Colour vision in birds and the role of oil droplets. *Trends in Neuroscience,* **3,** 196-199.

Bowmaker, J.K. & Dartnall, H.J.A. (1980) Visual pigments of rods and cones in a human retina. *J. Physiol.,* **298,** 501-511.

Bowmaker, J.K. & Hunt, D.M. (1999) Molecular biology of photoreceptor spectral sensitivity. *Adaptive mechanisms in the ecology of vision* (eds S.N. Archer, M.B.A. Djamgoz, E.R. Loew, J.C. Partridge & S. Vallerga), pp. 439-462. kluwer Academic Publishers, Boston.

Brennessel, B. (2006) *Diamonds in the marsh: A natural history of the diamondback terrapin*. University Press of New England, Hanover.

Bulte, G., Germain, R.R., O'Connor, C.M. & Blouin-Demers, G. (2013) Sexual dichromatism in the northern map turtle, *Graptemys geographica*. *Chelonian Conservation and Biology,* **12,** 187-192.

Carr, A.F. (1952) *Handbook of turtles: the turtles of the United States, Canada, and Baja California*. Cornell University Press, Ithaca, NY.

Ciofi, C. & Swingland, I.R. (1997) Environmental sex determination in reptiles. *Applied Animal Behaviour Science,* **51,** 251-265.

Coker, R.E. (1906) The natural history and cultivation of the diamond-back terrapin, with notes on other forms of turtles. *North Carolina Geological Survey Bulletin,* **14,** 1-67.

Coker, R.E. (1920) The diamond-back terrapin: past, present, and future. *Scientific Monthly,* **11,** 171-186.

Couldridge, V.C.K. & Alexander, G.J. (2002) Color patterns and species recognition in four closely related species of Lake Malawi cichlid. *Behavioral Ecology,* **13,** 59-64.

Cronin, T., Soenke, J., Marshall, J. & Warrant, E.J. (2014) *Visual Ecology*. Princeton University Press, Princeton, New Jersey.

Daw, N.W. (1973) Neurophysiology of color vision. *Physiological Reviews,* **53,** 571-611.

Doherty, P.F., Sorci, G., Royle, J.A., Hines, J.E., Nichols, J.D. & Boulinier, T. (2003)

Sexual selection affects local extinction and turnover in bird communities. *PNAS,* **100,** 5858-5862.

Dominy, N.J. & Lucas, P.W. (2001) Ecological importance of trichromatic vision to primates. *Nature,* **410,** 363-366.

Eaton, M.D. (2005) Human vision fails to distinguish widespread sexual dichromatism among sexually "monochromatic" birds. *Proceedings of the National Academy of Sciences of the United States of America,* **102,** 10942-10946.

Eaton, M.D. & Lanyon, S.M. (2003) The ubiquity of avian ultraviolet plumage reflectance. *Proceedings of the Royal Society of London Series B-Biological Sciences,* **270,** 1721-1726.

Emlen, S.T. & Oring, L.W. (1977) Ecology, sexual selection, and the evolution of mating systems. *Science,* **197,** 215-223.

Endler, J.A. (1983) Natural and sexual selection on color patterns in Poeciliid fishes. *Environmental Biology of Fishes,* **9,** 173-190.

Endler, J.A. (1990) On the measurement and classification of colour in studies of animal colour patterns. *Biological Journal of the Linnean Society,* **41,** 315-352.

Endler, J.A. & Mielke, P.W. (2005) Comparing entire colour patterns as birds see them. *Biological Journal of the Linnean Society,* **86,** 405-431.

Endler, J.A. & Thery, M. (1996) Interacting effects of lek placement, display behavior, ambient light, and color patterns in three neotropical forest-dwelling birds. *American Naturalist,* **148,** 421-452.

Estep, R.L. (2005) Seasonal movement and habitat use patterns of a diamondback terrapin (*Malaclemys terrapin*) population. Master's Thesis, College of Charleston, Charleston, South Carolina.

Ewert, M.A. & Legler, J.M. (1978) Hormonal induction of oviposition in turtles. *Herpetologica,* **34,** 314-318.

Figuerola, J., Senar, J.C. & Pascual, J. (1999) The use of a colorimeter in field studies of blue tit *Parus caeruleus* coloration. *Ardea,* **87,** 269-275.

Finneran, L.C. (1948) Diamond-back terrapin in Connecticut. *Copeia,* **1948,** 138.

Fleishman, L.J., Loew, E.R. & Whiting, M.J. (2011) High sensitivity to short wavelengths in a lizard and implications for understanding the evolution of visual systems in lizards. *Proc. R. Soc. Lond. B,* **278,** 2891-2899.

Font, E., De Lanuza, G.P.I. & Sampedro, C. (2009) Ultraviolet reflectance and cryptic sexual dichromatism in the ocellated lizard, *Lacerta (Timon) lepida* (Squamata: Lacertidae). *Biological Journal of the Linnean Society,* **97,** 766-780.

Galeotti, P., Sacchi, R., Pellitteri-Rosa, D. & Fasola, M. (2007) Olfactory discrimination of species, sex, and sexual maturity by the Hermann's Tortoise *Testudo hermanni*. *Copeia,* **2007,** 980-985.

Galeotti, P., Sacchi, R., Pellitteri-Rosa, D. & Fasola, M. (2011) The yellow cheek-patches on the Hermann's tortoise (Reptila, Chelonia): sexual dimorphism and relationship with body condition. *Ital J Zool,* **78,** 464-470.

Gomez, D. & Thery, M. (2004) Influence of ambient light on the evolution of colour signals: comparative analysis of a neotropical rainforest bird community. *Ecology Letters,* **7,** 279-284.

Govardovskii, V.I., Fyhrquist, N., Reuter, T., Kuzmin, D.G. & Donner, K. (2000) In search of the visual pigment template. *Visual Neuroscience,* **17,** 509-528.

Gray, J.E. (1844) *Catalogue of tortoises, crocodilians, and amphisbaenians in the collection of the British Museum*. British Museum of Natural History, London.

Hall, J.A., Foster, R.E., Ebner, F.F. & Hall, W.C. (1977) Visual cortex in a reptile, the turtle (*Pseudemys scripta* and *Chrysemys picta*). *Brain Research,* **130,** 197-216.

Hart, N.S. (2001) The visual ecology of avian photoreceptors. *Progress in retinal and eye research,* **20,** 675-703.

Hart, N.S. & Hunt, D.M. (2007) Avian visual pigments: characteristics, spectral tuning, and evolution. *The American Naturalist,* **169,** S7-S26.

Hart, N.S. & Vorobyev, M. (2005) Modelling oil droplet absorption spectra and spectral sensitivities of bird cone photoreceptors. *Journal of Comparative Physiology A,* **191,** 381-392.

Hartsell, T.D. (2001) Intraspecific variation in the diamondback terrapin, Malaclemys terrapin, and its ecological parameters. PhD Thesis, George Mason University.

Hastad, O. & Odeen, A. (2008) Different ranking of avian colors predicted by modeling of retinal function in humans and birds. *The American Naturalist,* **171,** 831-838.

Hay, O.P. (1892) Some observations on the turtles of the genus *Malaclemys*. *Proceedings of the national Museum,* **15,** 379-383.

Hay, W.P. (1904) A revision of *Malaclemmys,* a genus of turtles. *Bulletin of the United States Bureau of Fisheries,* **5,** 1-21.

Heesy, C.P. & Hall, M.I. (2010) The nocturnal bottleneck and the evolution of mammalian vision. *Brain Behav Evol,* **75,** 195-203.

Heindl, M. & Winkler, H. (2003) Interacting effects of ambient light and plumage color patterns in displaying wire-tailed manakins (Aves, Pipridae). *Behavioral Ecology and Sociobiology,* **53,** 153-162.

Higashi, M., Takimoto, G. & Yamamura, N. (1999) Sympatric speciation by sexual selection. *Nature,* **402,** 523-526.

Honkavaara, J., Koivula, M., Korpimaki, E., Siitari, H. & Viitala, J. (2002) Ultraviolet vision and foraging in terrestrial vertebrates. *Oikos,* **98,** 505-511.

Hunt, D.M., Carvalho, L.S., Cowing, J.A. & Davies, W.L. (2009) Evolution and spectral tuning of visual pigments in birds and mammals. *Philosophical Transactions of the Royal Society of London Series B-Biological Sciences,* **364,** 2941-2955.

Hunt, S., Bennett, A.T.D., Cuthill, I.C. & Griffiths, R. (1998) Blue tits are ultraviolet tits. *Proceedings of the Royal Society of London Series B-Biological Sciences,* **265,** 451-455.

Hunt, S., Cuthill, I.C., Bennett, A.T.D. & Griffiths, R. (1999) Preferences for ultraviolet partners in the blue tit. *Animal Behaviour,* **58,** 809-815.

Ibanez, A., Marzal, A., Lopez, P. & Martin, J. (2013) Sexually dichromatic coloration reflects size and immunocompetence in female Spanish terrapins, *Mauremys leprosa*. *Naturwissenschaften,* **100,** 1137-1147.

Ibanez, A., Polo-Cavia, N., Lopez, P. & Martin, J. (2014) Honest sexual signaling in turtles: experimental evidence of a trade-off between immune response and coloration in red-eared sliders *Trachemys scripta elegans*. *Naturwissenschaften,* **101,** 803-811.

Jacobs, G.H. (2009) Evolution of colour vision in mammals. *Phil. Trans. R. Soc. B,* **364,** 2957-2967.

Jerlov, N.G. & Nielsen, E.S. (1974) Optical aspects of oceanography. Academic Press, New York.

Johnsen, A., Delhey, K., Andersson, S. & Kempenaers, B. (2003) Plumage colour in nestling blue tits: sexual dichromatism, condition dependence and genetic effects. *Proceedings: Biological Sciences,* **270,** 1263-1270.

Jones, A.G. (2005) GERUD 2.0: a computer program for the reconstruction of parental genotypes from half-sib progeny arrays with known or unknown parents. *Molecular Ecology Notes,* **5,** 708-711.

Kelber, A., Vorobyev, M. & Osorio, D. (2003) Animal colour vision--behavioural tests and physiological concepts. *Biological Reviews,* **78,** 81-118.

Kennish, M.J., Bricker, S.B., Dennison, W.C., Glibert, P.M., Livingston, R.J., Moore, K.A., Noble, R.T., Paerl, H.W., Ramstack, J.M., Seitzinger, S., Tamasko, D.A. & Valiela, I. (2007) Barnegat Bay-Little Egg Harbor estuary: case study of a highly eutrophic coastal bay system. *Ecological Applications,* **17,** S3-S16.

Kodric-Brown, A. & Brown, J.H. (1984) Truth in advertising: the kinds of traits favored by sexual selection. *The American Naturalist,* **124,** 309-323.

Kroeger, R.H.H. & Katzir, G. (2006) Comparative anatomy and physiology of vision in aquatic tetrapods. *Sensory evolution on the threshold: adaptations in secondarily aquatic vertebrates* (eds J.G.M. Thewissen & S. Nummela), pp. 121-147. University of California Press, Berkeley.

Lee, J. & Chew, S. (2008) *Diamondback terrapins: gems of the turtle world*. Mill City Press, Inc., Minneapolis, MN.

Liebman, P.A. & Granda, A.M. (1971) Microspectrophotometric measurements of visual pigments in two species of turtle, *Pseudemys scripta* and *Chelonia mydas*. *Vision Research,* **11,** 105-114.

Lipetz, L.E. (1984) A new method for determining peak absorbance of dense pigment samples and its application to the cone oil droplets of *Emydoidea blandingii*. *Vision Research,* **24,** 597-604.

Loew, E.R. & Govardovskii, V.I. (2001) Photoreceptors and visual pigments in the red-eared turtle, *Trachemys scripta elegans*. *Visual Neuroscience*, **18,** 753-757.

Loew, E.R. & Lythgoe, J.N. (1978) The ecology of cone pigments in teleost fishes. *Vision Research*, **18,** 715-722.

Loew, E.R. & Zhang, H. (2006) Propagation of visual signals in the aquatic environment: an interactive windows-based model. *Communication in fishes* (eds F. Ladich, S.P. Collin, P. Moller & B.G. Kapoor), pp. 281-302. Science Publishers, Plymouth, England.

Losey, G.S., Cronin, T.W., Goldsmith, T.H., Hyde, D., marshall, N.J. & McFarland, W.N. (1999) The UV visual world of fishes: a review. *Journal of Fish Biology*, **54,** 921-943.

Lythgoe, J.N. (1979) *The ecology of vision*. Clarendon Press, Oxford.

Lythgoe, J.N. (1985) Aspects of photoreception in aquatic environments. *Symposia of the Society for Experimental Biology* (ed. M.S. Laverack), pp. 373-386. The Company of Biologists Limited, Cambridge, England.

Macedonia, J.M., Brandt, Y. & Clark, D.L. (2002) Sexual dichromatism and differential conspicuousness in two populations of the common collared lizard (*Crotaphytus collaris*) from Utah and New Mexico, USA. *Biological Journal of the Linnean Society*, **77,** 67-85.

Macedonia, J.M., Echternacht, A.C. & Walguarnery, J.W. (2003) Color variation, habitat light, and background contrast in *Anolis carolinensis* along a geographical transect in Florida. *Journal of Herpetology*, **37,** 467-478.

Marshall, N.J., Jennings, K., McFarland, W.N., Loew, E.R. & Losey, G.S. (2003) Visual biology of Hawaiian coral reef fishes. II. Colors of Hawaiian coral reef fish. *Copeia*, **2003,** 455-466.

McCauley, R.H. (1945) *The reptiles of Maryland and the District of Columbia*. Privately printed, Hagerstown, Maryland.

Metz, K.J. & Weatherhead, P.J. (1991) Color bands function as secondary sexual traits in male red-winged blackbirds. *Behav. Ecol. Sociobiol.,* **28,** 23-27.

Negro, J.J., Bortolotti, G.R., Tella, J.L., Fernie, K.J. & Bird, D.M. (1998) Regulation of integumentary colour and plasma carotenoids in American kestrels consistent with sexual selection theory. *Functional Ecology,* **12,** 307-312.

Osorio, D. & Vorobyev, M. (2005) Photoreceptor spectral sensitivities in terrestrial animals: adaptations for luminance and colour vision. *Proceedings of the Royal Society B,* **272,** 1745-1752.

Osorio, D. & Vorobyev, M. (2008) A review of the evolution of animal colour vision and visual communication signals. *Vision Research,* **48,** 2042-2051.

Partridge, J.C. (1989) The visual ecology of avian cone oil droplets. *Journal of Comparative Physiology A,* **165,** 415-426.

Partridge, J.C. & Cummings, M.E. (1999) Adaptations of visual pigments to the aquatic environment. *Adaptive mechanisms in the ecology of vision* (eds S.N. Archer, M.B.A. Djamgoz, E.R. Loew, J.C. Partridge & S. Vallerga), pp. 251-283. Kluwer Academic Publishers, Boston.

Peakall, R. & Smouse, P.E. (2006) GENALEX 6: genetic analysis in Excel. Population genetic software for teaching and research. *Molecular Ecology Notes,* **6,** 288-295.

Peakall, R. & Smouse, P.E. (2012) GenAlEx 6.5: genetic analysis in Excel. Population genetic software for teaching and research-an update. *Bioinformatics,* **28,** 2537-2539.

Polo-Cavia, N., Lopez, P. & Martin, J. (2013) Head coloration reflects health state in the red-eared slider *Trachemys scripta elegans*. *Behav. Ecol. Sociobiol.,* **67,** 153-162.

Rao, R.P.N. & Ballard, D.H. (1999) Predictive coding in the visual cortex: a functional interpretation of some extra-classical receptive-field effects. *Nature Neuroscience,* **2,** 79-87.

Roosenburg, W.M., Cresko, W., Modesitte, M. & Robbins, M.B. (1997) Diamondback terrapin (*Malaclemys terrapin*) mortality in crab pots. *Conservation Biology,* **5,** 1166-1172.

Rowe, J.W., Clark, D.L., Price, M. & Tucker, J.K. (2009) Reversible melanization following substrate color reversal in midland painted turtles (Chrysemys picta marginata) and red-eared sliders (Trachemys scripta elegans). *Journal of Herpetology*, **43,** 402-408.

Rowe, J.W., Clark, D.L., Ryan, C. & Tucker, J.K. (2006) Effect of substrate color on pigmentation in midland painted turtles (*Chrysemys picta marginata*) and red-eared slider turtles (*Trachemys scripta elegans*). *Journal of Herpetology,* **40,** 358-364.

Ruxton, G.D., Speed, M.P. & Kelly, D.J. (2004) What, if anything, is the adaptive function of countershading? *Animal Behaviour,* **68,** 445-451.

Sabbah, S., Troje, N.F., Gray, S.M. & Hawryshyn, C.W. (2013) High complexity of aquatic irradiance may have driven the evolution of four-dimensional colour vision in shallow-water fish. *The Journal of Experimental Biology,* **216,** 1670-1682.

Santos, S.I.C.O., Elward, B. & Lumeij, J.T. (2006) Sexual dichromatism in the blue-fronted Amazon parrot (Amazona aestiva) revealed by multiple-angle spectrometry. *Journal of Avian Medicine and Surgery,* **20,** 8-14.

Schluter, D. & McPhail, J.D. (1992) Ecological character displacement and speciation in sticklebacks. *American Naturalist,* **140,** 85-108.

Schoepff, D. (1792) Historia testudinum iconobus illustrata. pp. 136-136. Palm, Erlange, Germany.

Seigel, R.A. (1980) Courtship and mating behavior of the diamondback terrapin *Malaclemys terrapin tequesta*. *Journal of Herpetology,* **14,** 420-421.

Sheridan, C.M. (2010) Mating system and dispersal patterns in the diamondback terrapin (*Malaclemys terrapin*). Dissertation/Thesis, Drexel University.

Sheridan, C.M., Spotila, J.R., Bien, W.F. & Avery, H.W. (2010) Sex-biased dispersal and natal philopatry in the diamondback terrapin, *Malaclemys terrapin*. *Molecular Ecology,* **19,** 5497-5510.

Siddiqi, A., Cronin, T.W., Loew, E.R., Vorobyev, M. & Summers, K. (2004) Interspecific and intraspecific views of color signals in the strawberry poison frog Dendrobates pumilio. *The Journal of Experimental Biology,* **207,** 2471-2485.

Silliman, B.R. & Bertness, M.D. (2002) A trophic cascade regulates salt marsh primary production. *PNAS,* **99,** 10500-10505.

Smith, E.J., Partridge, J.C., Parsons, K.N., White, E.M., Cuthill, I.C., Bennett, A.T.D. & Church, S.C. (2002) Ultraviolet vision and mate choice in the guppy (*Poecilia reticulata*). *Behavioral Ecology,* **13,** 11-19.

Stavenga, D.G. & Wilts, B.D. (2014) Oil droplets of bird eyes: microlenses acting as spectral filters. *Philosophical Transactions of the Royal Society of London Series B-Biological Sciences,* **369**.

Stevens, M. (2007) Predator perception and the interrelation between different forms of protective coloration. *Proc. R. Soc. Lond. B,* **274,** 1457-1464.

Stoddard, M.C., Kilner, R.M. & Town, C. (2014) Pattern recognition algorithm reveals how birds evolve individual egg pattern signatures. *Nature Communications,* **ncomms5117**.

Stoddard, M.C. & Prum, R.O. (2008) Evolution of avian plumage color in a tetrahedral color space: a phylogenetic analysis of new world buntings. *American Naturalist,* **171,** 755-776.

Stuart-Fox, D.M. & Ord, T.J. (2004) Sexual selection, natural selection and the evolution of dimorphic coloration and ornamentation in agamid lizards. *Proceedings of the Royal Society of London Series B-Biological Sciences,* **271,** 2249-2255.

Tovee, M.J. (1995) Ultra-violet photoreceptors in the animal kingdom: their distribution and function. *Trends in Ecology & Evolution,* **10**.

Trivers, R.L. (1972) Parental investment and sexual selection. *Sexual selection and the descent of man, 1871-1971* (ed. B. Campbell), pp. 136-179. Aldine, Chicago, IL.

Ventura, D.F., Zana, Y., de Souza, J.M. & Devoe, R.D. (2001) Ultraviolet colour opponency in the turtle retina. *The Journal of Experimental Biology,* **204,** 2527-2534.

Vorobyev, M. (2003) Coloured oil droplets enhance colour discrimination. *Proceedings: Biological Sciences,* **270,** 1255-1261.

Vorobyev, M., Marshall, J., Osorio, D., de Ibarra, N.H. & Menzel, R. (2001) Colorful objects through animal eyes. *Color Research and Applications,* **26,** S214-217.

Walls, G.L. (1942) *The vertebrate eye and its adaptive radiation*. Cranbrook Institute of Science, Bloomfield Hills, Mich.

Wang, J.-C., Yang, C.-C., Liang, W. & Shi, H.-T. (2013) Spectra analysis reveals the sexual dichromatism of red-eared slider turtle (*Trachemys scripta*). *Zoological Research,* **34,** 475-478.

Witherington, B.E. & Salmon, M. (1992) Predation on loggerhead turtle hatchlings after entering the sea. *Journal of Herpetology,* **26,** 226-228.

Yokoyama, S. & Yokoyama, R. (1996) Adaptive evolution of photoreceptors and visual pigments in vertebrates. *Annu. Rev. Ecol. Syst.,* **27,** 543-567.

Zahavi, A. (1975) Mate selection--a selection for a handicap. *Journal of theoretical biology,* **53,** 205-214.

Vita

Abigail (Abby) Dominy

abbydominy@yahoo.com

Education

Ph.D., Environmental Science, Drexel University (Philadelphia, PA)	2015
B.Sc., Biological Sciences, Drexel University (Philadelphia, PA)	2007
B.Sc., Environmental Science, Drexel University (Philadelphia, PA)	2007

Professional Experience

Teaching Assistant, Drexel University	2009 – 2015
Research Assistant, Drexel University	2008 – 2013
Visiting Researcher, Dartmouth College	2014
Principal Investigator, Earthwatch Institute	2014

Funding and awards

Earthwatch Institute (Boston, MA) / Princeton University Teacher Prep	2014
William L. McLean III Fellowship for Ornithology and Environmental Science	2014
Travel Subsidy, Depts. of Biology and BEES, Drexel University	2012, 2013, 2014
Travel Subsidy, Office of Graduate Studies, Drexel University	2010, 2013
Travel Subsidy, Office of International Programs, Drexel University	2012